

# Determining the essentially different partitions of all Japanese convex tangrams

**Citation for published version (APA):**

Beelen, T. G. J., & Verhoeff, T. (2018). *Determining the essentially different partitions of all Japanese convex tangrams*. (07 ed.) (CASA report). Technische Universiteit Eindhoven.

**Document status and date:**

Published: 01/11/2018

**Document Version:**

Publisher's PDF, also known as Version of Record (includes final page, issue and volume numbers)

**Please check the document version of this publication:**

- A submitted manuscript is the version of the article upon submission and before peer-review. There can be important differences between the submitted version and the official published version of record. People interested in the research are advised to contact the author for the final version of the publication, or visit the DOI to the publisher's website.
- The final author version and the galley proof are versions of the publication after peer review.
- The final published version features the final layout of the paper including the volume, issue and page numbers.

[Link to publication](#)

**General rights**

Copyright and moral rights for the publications made accessible in the public portal are retained by the authors and/or other copyright owners and it is a condition of accessing publications that users recognise and abide by the legal requirements associated with these rights.

- Users may download and print one copy of any publication from the public portal for the purpose of private study or research.
- You may not further distribute the material or use it for any profit-making activity or commercial gain
- You may freely distribute the URL identifying the publication in the public portal.

If the publication is distributed under the terms of Article 25fa of the Dutch Copyright Act, indicated by the "Taverne" license above, please follow below link for the End User Agreement:

[www.tue.nl/taverne](http://www.tue.nl/taverne)

**Take down policy**

If you believe that this document breaches copyright please contact us at:

[openaccess@tue.nl](mailto:openaccess@tue.nl)

providing details and we will investigate your claim.

**EINDHOVEN UNIVERSITY OF TECHNOLOGY**  
Department of Mathematics and Computer Science

CASA-Report 18-07  
October 2018

Determining the essentially different partitions of all  
Japanese convex tangrams

by

T.G.J. Beelen, T. Verhoeff



Centre for Analysis, Scientific computing and Applications  
Department of Mathematics and Computer Science  
Eindhoven University of Technology  
P.O. Box 513  
5600 MB Eindhoven, The Netherlands  
ISSN: 0926-4507



# Determining the essentially different partitions of all Japanese convex tangrams

T.G.J. Beelen and T. Verhoeff (TU Eindhoven)

October 26, 2018

## Contents

<b>1</b>	<b>Abstract</b>	<b>3</b>
<b>2</b>	<b>General Introduction</b>	<b>4</b>
2.1	The relationships between the tans . . . . .	5
2.2	Problem formulation . . . . .	5
<b>3</b>	<b>Finding all layouts of the convex polygons with the Japanese tans</b>	<b>7</b>
<b>4</b>	<b>The <i>Square</i> tangram</b>	<b>8</b>
4.1	The case Tr1 . . . . .	8
4.2	The case Tr4 . . . . .	9
4.3	The cases Tr2, Tr3, Tr5 and Tr6 . . . . .	10
4.4	The cases Tr7 and Tr8 . . . . .	11
<b>5</b>	<b>The <i>Strip</i> tangram <i>J14</i></b>	<b>14</b>
5.1	Preliminaries . . . . .	14
5.1.1	Visualisation aspects . . . . .	15
5.2	Finding all possible layouts of strip <i>J14</i> . . . . .	18
5.2.1	The layouts of the strip with Tz1 and Tz2 . . . . .	18
5.2.2	The layouts of <i>J14</i> with Tz1 . . . . .	19
5.2.3	The layouts of <i>J14</i> with Tz2 . . . . .	19
5.2.4	The layouts of <i>J14</i> with Tz3 . . . . .	21
5.2.5	The layouts of the strip with Tz3 . . . . .	22
5.2.6	Summary of the analysis of <i>Strip-J14</i> . . . . .	27
5.2.7	Strip <i>J14</i> with its twin layouts . . . . .	29
5.3	Finding all different partitions for <i>J15</i> and <i>J16</i> by a combinatorial approach . . . . .	30

<b>6</b>	<b>An algorithm for generating all partitions of a convex shape</b>	<b>34</b>
6.1	A simple packing problem . . . . .	34
6.2	A more complicated packing problem . . . . .	37
6.2.1	The packing problem for <i>Strip J14</i> . . . . .	38
6.2.2	The packing problem for <i>Strip J16</i> . . . . .	38
<b>7</b>	<b>All different partitions of the shapes <i>J01</i> up to <i>J16</i></b>	<b>40</b>
<b>A</b>	<b>Analysis of the strips <i>J15</i> and <i>J16</i></b>	<b>49</b>
A.1	The case <i>J15</i> . . . . .	49
A.2	The case <i>J16</i> . . . . .	50
A.3	Finding all different partitions for <i>J15</i> and <i>J16</i> by backtracking . . . . .	51
A.4	The case <i>Tz1</i> . . . . .	52
A.5	The case <i>Tz2</i> . . . . .	60
A.6	The case <i>Tz3</i> . . . . .	62
A.7	The case <i>Tz4</i> . . . . .	64
A.7.1	Finding all possible fillings for LHS4 with one single tan inside . . . . .	64
A.7.2	Finding all complete fillings for LHS4 . . . . .	64
A.7.3	Finding all complete layouts of <i>J15</i> and <i>J16</i> with <i>Tz4</i> and LHS4 . . . . .	68
A.8	Finding all layouts for the strips <i>J15</i> and <i>J16</i> with <i>Tz</i> upside down . . . . .	71
A.9	Investigating the possible layouts for <i>J15</i> and <i>J16</i> with <i>Ty2</i> . . . . .	75
A.10	Investigating the possible layouts for <i>J15</i> and <i>J16</i> with <i>Ty3</i> . . . . .	77
A.10.1	The layouts with <i>Ty3</i> and <i>Tr</i> in LHS . . . . .	77
<b>B</b>	<b>Acknowledgments and References</b>	<b>83</b>

## 1 Abstract

In this report we consider the set of the 16 possible convex tangrams that can be composed with the 7 so-called “Sei Shonagon Chie no Ita” (or Japanese) tans, see [9]. The set of these Japanese tans is slightly different from the well-known set of 7 Chinese tans with which 13 (out of those 16) convex tangrams can be formed. In [4], [5] the problem of determining all essentially different partitions of the 13 “Chinese” convex tangrams was investigated and solved. In this report we will address the same problem for the “Japanese” convex tangrams. The approach to solve both problems is more or less analogous, but the “Japanese” problem is much harder than the “Chinese” one, since the number of “Japanese” solutions is much larger than the “Chinese” ones. In fact, only for a few “Japanese” tangram shapes their solutions can be found by a rigorous analysis supported by a large number of clarifying diagrams. The solutions for the remaining shapes have to be determined using a dedicated computer program. Both approaches will be discussed here and all essentially different solutions with the “Japanese” tans are presented. As far as we know all presented results are not yet published before.

*Keywords:* tangram, partition, backtracking, visualization.

## 2 General Introduction

The word “tangram” is reasonably well-known, especially in the context of trying to compose a given figurative picture using 7 geometrically shaped puzzle pieces called tans. A few typical examples of such pictures are given in Fig. 1. Furthermore, in the bilingual (German / Dutch) book “Tangram, / Das alte chinesische Formenspiel / Het oude Chinese vormenspel ” by J. Elffers [2] over 1600 examples on tangram puzzles and their solutions can be found. See also website [5] <http://www.pentoma.de/>.

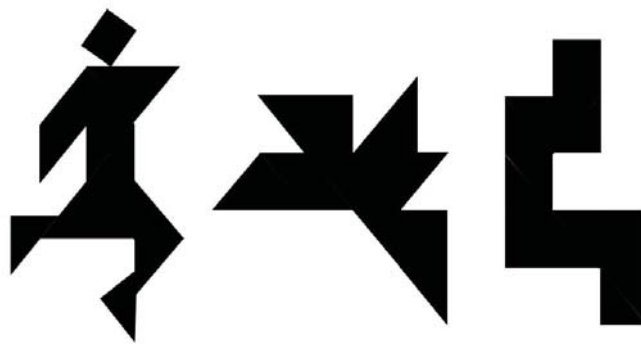


Figure 1: A few typical tangram figures.



Figure 2: The 7 individual Chinese and the 7 Japanese tangram pieces, in the top and bottom row, respectively.

It should be noticed that next to the set of Chinese tans, there also exists a less known set of Japanese tans, in shape similar to the Chinese tans. Both the sets of Chinese and Japanese tans are shown in Fig. 2. Just as in case of the Chinese tans, each Japanese piece can be decomposed into one or more of the smallest triangular pieces. See Fig. 3.

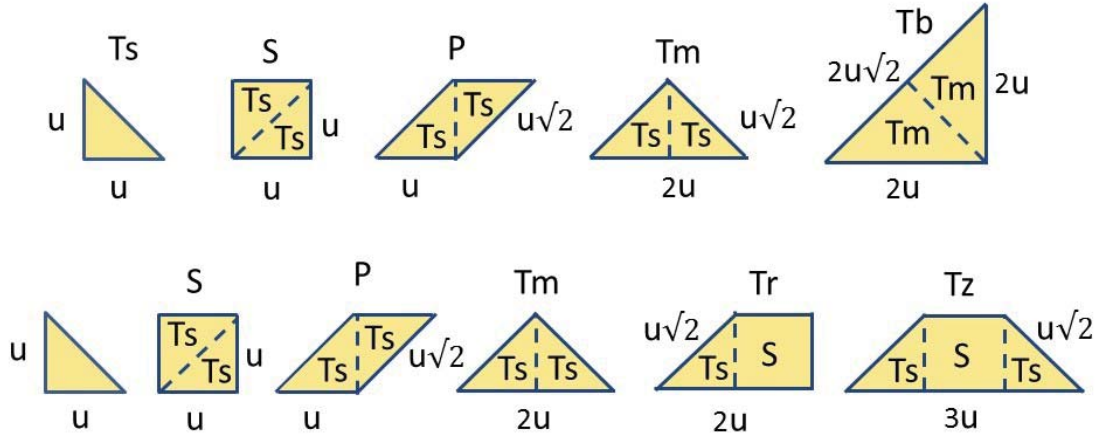


Figure 3: The composition of the Chinese (top row) and Japanese tans (bottom).

## 2.1 The relationships between the tans

Let us consider Figs. 2 and 3 in more detail. The set of Chinese tans consists of the following 7 pieces: one small triangle  $T_s$ , one square  $S$ , one parallelogram  $P$ , two medium sized triangles  $T_m$  and two big triangles  $T_b$ .

The set of Japanese tans also consists of 7 pieces: one small triangle  $T_s$ , one square  $S$ , one parallelogram  $P$ , two medium sized triangles  $T_m$  (exactly as in the Chinese set), one rectangular trapezium  $T_r$  and one isosceles trapezium  $T_z$ . Notice that the Chinese and Japanese tans  $T_s$ ,  $S$ ,  $P$  and  $T_m$  are identical.

The relationship between the areas of the tans is indicated in Fig. 3.

**Relationships between the tans :**

(1)

$$(i) S = 2 T_s, \quad P = 2 T_s;$$

$$(ii) T_m = 2 T_s, \quad T_b = 2 T_m = 4 T_s;$$

$$(iii) T_r = T_s + S = 3 T_s, \quad T_z = 2 T_s + S = T_r + T_s = 4 T_s;$$

$$(iv) \text{Tangram with all 7 Chinese tans} = 2 T_b + T_m + 2 T_s + S + P = 16 T_s;$$

$$(v) \text{Tangram with all 7 Japanese tans} = T_z + T_r + 2 T_m + T_s + S + P = 16 T_s;$$

## 2.2 Problem formulation

For convenience, let us denote the above mentioned sets of Chinese and Japanese tans by  $Tans_C$  and  $Tans_J$ , respectively. It is immediately clear that we can create a huge number of tangrams that can be composed using either the set  $Tans_C$  or  $Tans_J$ . In 1942 two Chinese mathematicians Fu Traing Wang and Chuan-Chih Hsiung published a paper [1] dealing with the problem of finding all *convex* polygons in 2D. They showed that there exist precisely 20 convex polygons, see Fig. 4. Here the numbering is conform to that in [1] as follows. The shapes marked by \* in their



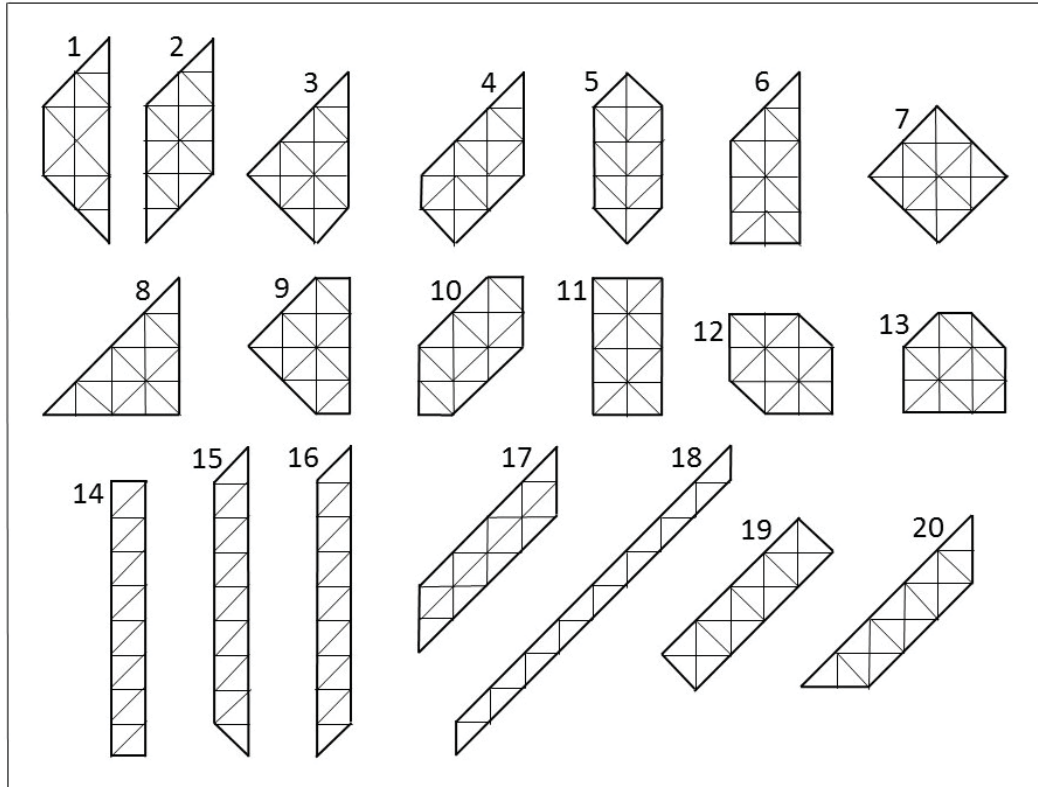


Figure 4: All 20 convex polygons.

table correspond to the numbers 14-16, while the 13 unmarked shapes as listed in their order are numbered 1-13 here. Clearly, these 13 shapes can be covered by the set  $C_{\mathcal{T}ans}$  and they will be denoted by the set  $Poly_{13}$ .

Notice that all 20 polygons can be formed by 16 rectangular isosceles triangles, as shown in Fig. 4. In 2014 it was shown by Eli Fox-Epstein and Ryunhei Uehara [9] that even 3 more (so in total 16, but not more) convex polygons can be covered by using the set  $J_{\mathcal{T}ans}$ , being the shapes 14-16 in Fig. 4. We will call the polygons 1-16 the set  $Poly_{16}$  (thus  $Poly_{16} \supset Poly_{13}$ ). Moreover, it was also shown in [9] that more coverings are possible, but then different tan sets must be used.

A mathematically interesting question on tangram covering is how many essentially different partitions for all polygons in  $Poly_{13}$  and  $Poly_{16}$  exist. In [3] this problem was extensively analyzed and solved for  $Poly_{13}$  with the set  $C_{\mathcal{T}ans}$ .

In this report we will address the covering problem for  $Poly_{16}$  with the set  $J_{\mathcal{T}ans}$ .

**Terminology** : In the rest of this report we will use the words *layout*, *partition*, *filling* and *covering* as synonyms.

### 3 Finding all layouts of the convex polygons with the Japanese tans

In this section we will give an overview of a few approaches we have chosen to solve the problem of finding all essentially different layouts with the Japanese tans (in short, to solve “The problem”). First we notice that solving this problem can be done by the well-known backtracking technique [7], [8], in a similar way as done in case of the Chinese tans (see [4]).

However, after proceeding manually as in [4] for a few “simple” tangrams it became clear that this would be a very tedious job for almost all convex shapes. So, an alternative was to carry out a backtracking algorithm by a computer. We will address this approach in section 6. In fact, we will discuss the following approaches to solve (partly or fully) “The problem”.

- (1) A systematic analysis of all possible partitions for the full square tangram, i.e. tangram 7 in Fig. 4.
- (2) A systematic analysis of all possible partitions for the rectangular strips (see shapes 14 up to 16 in Fig. 4, which will be indicated by  $J14$ ,  $J15$  and  $J16$  in the rest of this report). This analysis is done via backtracking and visualizing all possible trees. Notice that due to the length of the analyses of  $J15$  and  $J16$ , they are placed in the Appendix.
- (3) An alternative ‘combinatorial’ approach for the strips  $J14$ ,  $J15$  and  $J16$ .
- (4) A global description of an algorithm to solve a so-called packing problem. We will explain how this algorithm can be used to solve “The Problem”. Moreover, all solutions (partitions and their number) of all 16 convex shapes are included.

## 4 The *Square* tangram

We start with adding the rectangular trapezium *Tr* to the empty tangram *Square*. Since *Square* is symmetric w.r.t. both its horizontal and vertical centerline we can restrict ourselves to placing *Tr* in the lower half of *Square*. See Fig. 5. We will discuss several cases in the next sections.

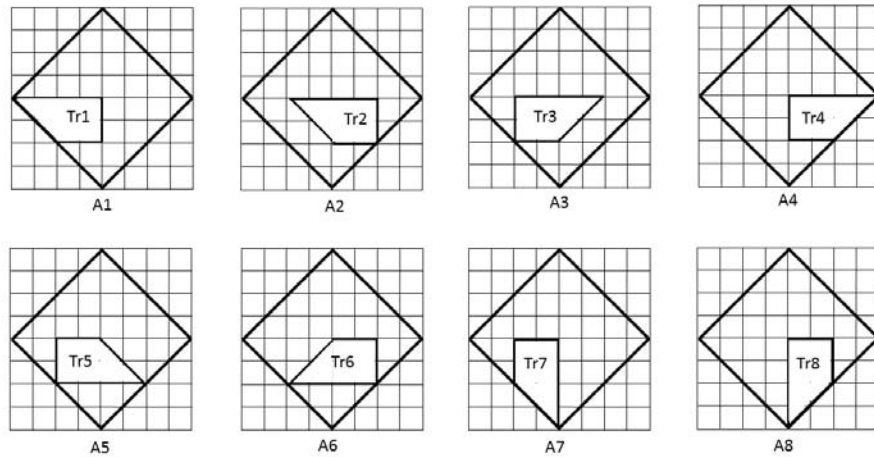


Figure 5: All possible layouts for tan *Tr* in the lower half of tangram *Square*

### 4.1 The case *Tr*1

Let us first consider the case with *Tr*1, see Fig. 5-A1. Clearly, we can add the isosceles trapezium *Tz* on 4 different positions as shown in Fig. 6. Next we can add the square *S* to these 4 layouts.

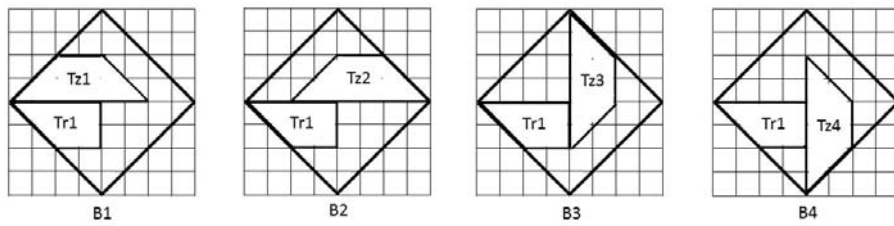


Figure 6: All possible combinations when adding *Tz* to *Tr*1 in *Square*

Clearly, we have only one possibility for *S* per layout. See Fig. 7. However, the layouts *C*3 and *C*4 are not feasible since 2 tan *Ts* are needed (but not available) for a full covering of the square.

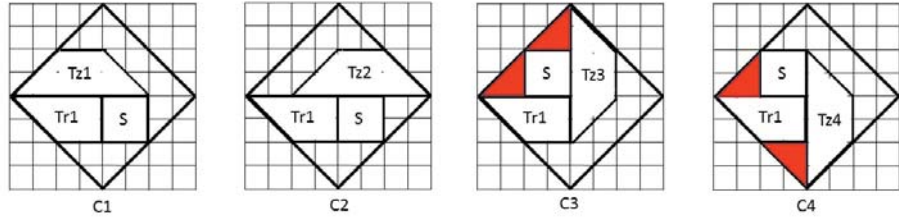


Figure 7: All possible combinations when adding S to Tr1.Tz in *Square*

So we have

**Conclusion:**

(2)

The *Square* tangram has 2 potentially feasible layouts C1 and C2 with Tr1 and Tz.

#### 4.2 The case Tr4

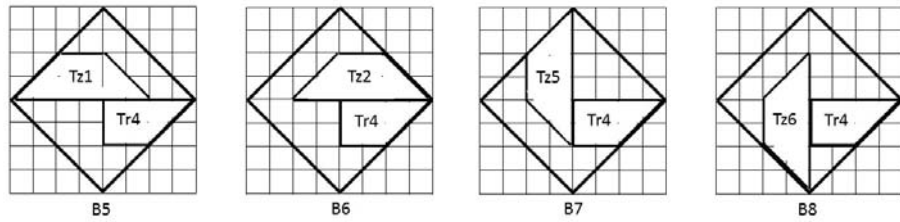


Figure 8: All possible combinations when adding Tz to Tr4 in *Square*

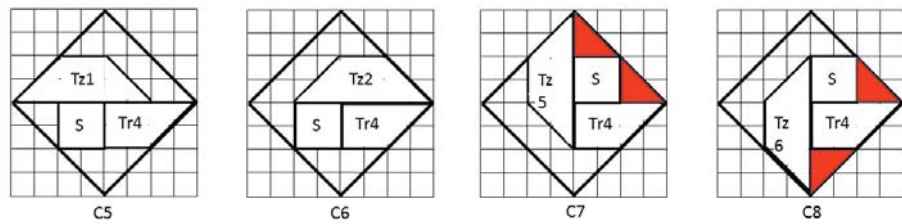


Figure 9: All possible combinations when adding S to Tr4.Tz in *Square*

In a similar way as in case Tr1 we can proceed with case Tr4. Indeed, here again we find 4 different combinations for Tr4 and Tz as shown in Fig. 8. Next we can add S to these 4 layouts, see Fig.9.

Similarly to case Tr1 the layouts C7 and C8 for Tr4 are not feasible. So we have

**Conclusion:** (3)

**The Square tangram has 2 potentially feasible layouts C5 and C6 with Tr4 and Tz.**

When comparing the potentially feasible layouts in Figs. 6 and 8 we see that the cases C1 and C6 as well as C2 and C5 are *equivalent* (by symmetry w.r.t. the vertical centerline of *Square*). Thus,

**Conclusion:** (4)

**We have to investigate the cases C1 and C2 further, but we can skip the cases C5 and C6 with Tr4.**

Before doing this, we first turn to the cases with Tr2, Tr3, Tr5 and Tr6.

### 4.3 The cases Tr2, Tr3, Tr5 and Tr6

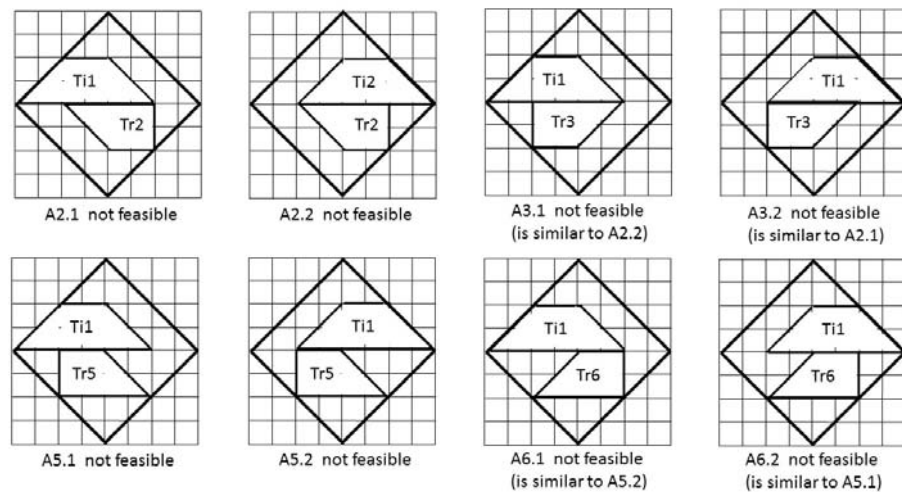


Figure 10: All possible combinations when adding Tz to Tr2, Tr3, Tr5 and Tr6 in *Square*

In Fig. 10 all possible cases with Tr2, Tr3, Tr5 and Tr6 are shown. It is easily seen that in all cases we cannot add the square tan S anymore. So, have

**Conclusion:** (5)

**The cases Tr2, Tr3, Tr5 and Tr6 are not feasible.**

Finally, we want to study the cases with Tr7 and Tr8.

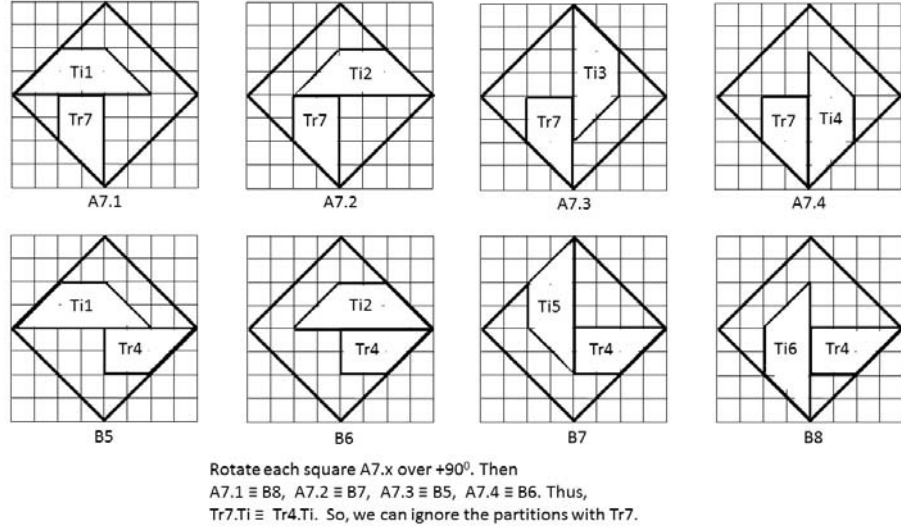


Figure 11: All possible combinations when adding Tz to Tr7 as well as to Tr4 in *Square*

#### 4.4 The cases Tr7 and Tr8

In Fig. 11 all 4 possible cases for Tr7 in *Square* are shown. Furthermore, the 4 possible cases for Tr4 are repeated here (recall Fig.8). It can easily be seen that by rotating each configuration *Square\_Tr7.Tz* over  $90^\circ$  we find one of the configurations with *Square\_Tr4.Tz*. We call such a pair *equivalent* and this will be denoted by the symbol  $\equiv$ . Specifically, in Fig. 11 we have  $A7.1 \equiv B8$ ,  $A7.2 \equiv B7$ ,  $A7.3 \equiv B6$  and  $A7.4 \equiv B5$ . Hence, we have

**Conclusion:** (6)

**We can ignore all partitions with Tr7 for further study (and continue with Tr4).**

Let us now consider case *Square\_Tr8*.

In Fig. 12 all 4 possible cases for *Square\_Tr8* are shown. Moreover, for easy comparison we also recall the 4 possible cases for Tr1 from Fig.6. It can easily be seen that by rotating each configuration *Square\_Tr8.Tz* over  $90^\circ$  we find one of the configurations with *Square\_Tr1.Tz*. Specifically, we have  $A8.1 \equiv B3$ ,  $A8.2 \equiv B4$ ,  $A8.3 \equiv B2$  and  $A8.4 \equiv B1$ . Hence, we have

**Final Conclusion:** (7)

**We can ignore all partitions with Tr8 for further study (and continue with Tr1).**

Combining all conclusions (2) up to (7) above we see that we only need to investigate the layouts C1 and C2 in Fig. 7 for yes/no feasibility.

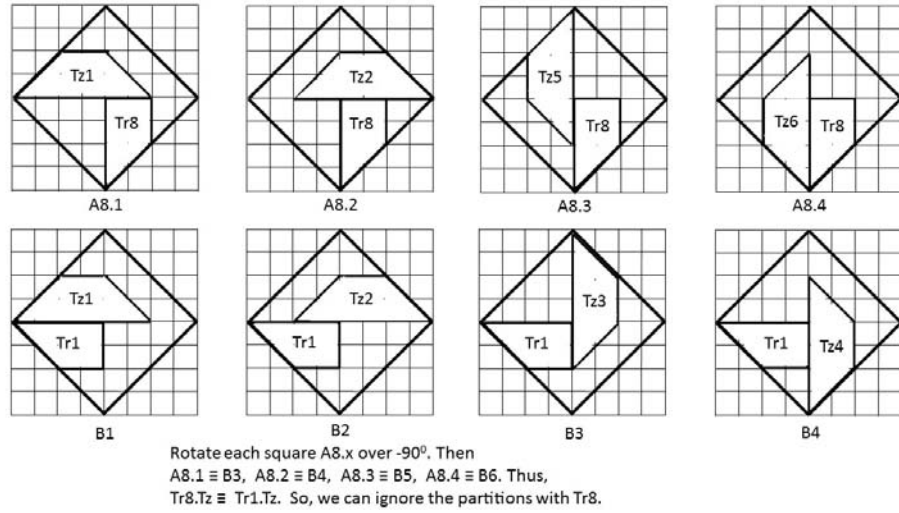


Figure 12: All possible combinations when adding Tz to Tr8 as well as to Tr1 in *Square*

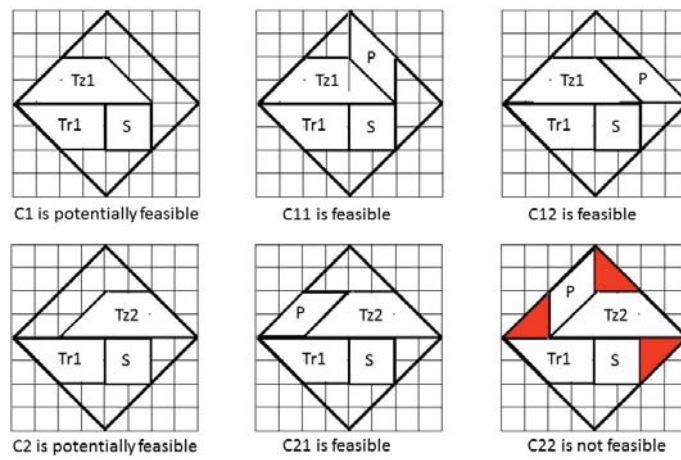


Figure 13: All possible combinations when adding P to Tr1.Tz.S in *Square*

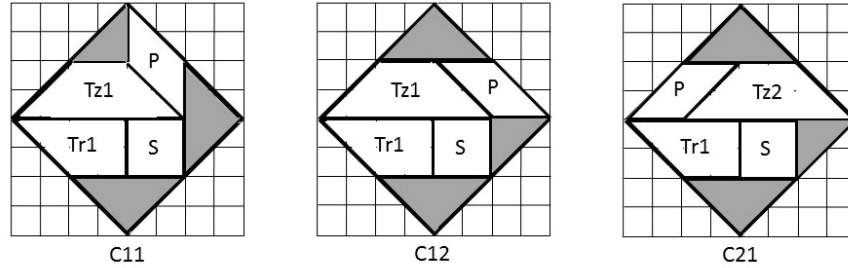


Figure 14: The 3 feasible partitions for *Square*

Therefore, we return to the layouts C1 and C2 in Fig. 7. Let us try to add parallelogram P to them, see Fig.13. Clearly, we have 2 options for adding P to *Square.Tr1.Tz1.S*, see Figs. 13-C11, C12. Clearly, after having added P we see that 3 empty regions are left in both C11 and C12, and they can be uniquely be covered by the triangles Tm1, Tm2 and Ts. Notice that the order of placing Tm1 and Tm2 is irrelevant. Thus, layout *Square.Tr1.Tz1.S* can be completed in two different ways to a full feasible covering of *Square*.

Similarly to C1 we can add P to *Square.Tr1.Tz2.S*, but now only one layout (C21) is feasible, since in the other one (C22) we cannot add both triangles Tm1 and Tm2. See Figs. 13-C21, C22. So, we have

**Final Conclusion:**

(8)

**Square  $Tr1.Tz1.S$  can be fully covered by 3 different layouts, see Fig. 14.**



## 5 The Strip tangram J14

We start by giving some preliminaries.

### 5.1 Preliminaries

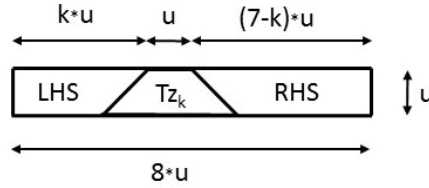


Figure 15: Trapezium  $Tz$  with its LHS and RHS parts in strip J14.

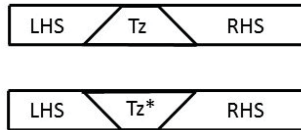


Figure 16: Equivalence of the strips with  $Tz$  and  $Tz^*$  (=  $Tz$  upside-down) in J14

Since  $Tz$  is an isosceles trapezium in a rectangular strip, we need to add tans at the left (LHS) as well as at the right hand side (RHS) of  $Tz$ . See Fig.15. Clearly, to each side of  $Tz$  we have to add a *skew*-sided tan. Notice that the subscript  $k$  in the name  $Tz_k$  refers to the length of LHS. Furthermore, notice that each strip with  $Tz$  is equivalent to the strip with  $Tz$  upside-down (due to symmetry w.r.t. the bottom edge of the strip). See Fig.16.

Let us now consider all possible positions of  $Tz$  in the strip, see Fig.17. The strips will be identified by the  $Tz$  name. It is easily seen (by reflection w.r.t. the vertical left hand edge of the strip) that the following strips are equivalent:  $Tz_4 \equiv Tz_3$ ,  $Tz_5 \equiv Tz_2$  and  $Tz_6 \equiv Tz_1$ .

Thus, we need not to generate layouts with  $Tz_4$  up to  $Tz_6$ .

So, we have

**Conclusion:**

(9)

**We only need to find all possible different layouts of the strip J15**

**with  $Tz_1$  up to  $Tz_3$  (see Fig. 17).**

Consider Fig. 15 for  $k = 1, 2, 3$ . In Figs. 18 and 19 we show all possible fillings for LHS corresponding to  $Tz_k$ . Clearly, once knowing all possible fillings for LHS and RHS we can find all different layouts of a partial strip J14 for each feasible combination of LHS and  $Tz$  (using Figs. 4 and 5) by adding step by step one tan from the set of remaining pieces. This can be done in a

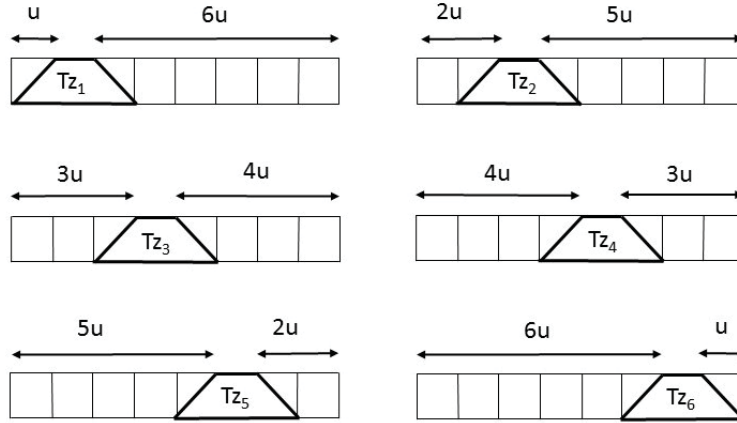


Figure 17: All possible positions of  $T_z$  in the strip.

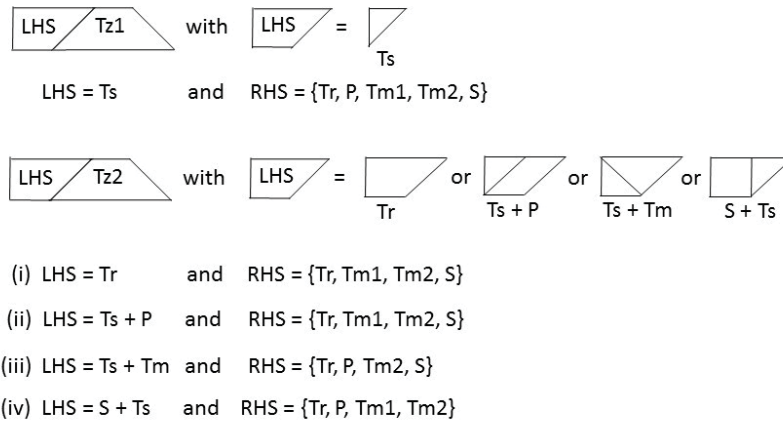


Figure 18: All fillings for LHS and  $T_{z1}$  and  $T_{z2}$  in *Strip\_J14*.

well-defined way by using the so-called backtracking procedure [7], [8]. Below we will give more details.

However, we first want to explain a few notational and visualization aspects.

### 5.1.1 Visualisation aspects

We start with a partial strip  $LHS + T_z$  and add a suitable tan (called  $T_1$  for simplicity) next to  $T_z$ . We get the (partial) strip  $LHS + T_z + RHS = LHS + T_z + T_1$ . Notice that there are 2 options for each tan to be added: either the tan fits to the strip in a unique way or the tan does not fit at all.

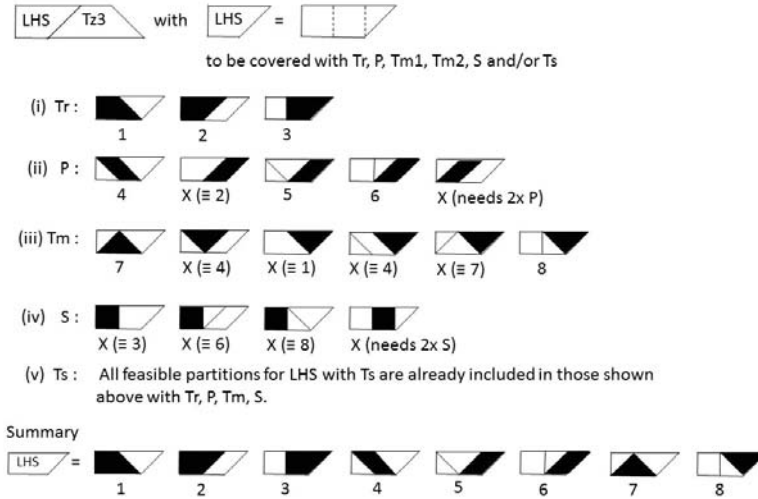


Figure 19: All fillings for LHS and Tz3 in *Strip\_J14*.

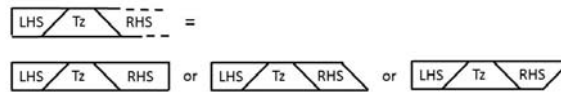


Figure 20: The 3 possible rhs-edges of a partial *Strip\_J14*.

Clearly, the rhs-edge of each partial strip is vertical, left- or right skew, see Fig. 20 and the final strip must have a vertical rhs-edge. By adding more tans  $T2, T3, \dots$  the size of the strip grows. This process can be visualized by a tree structure. It is easily seen that the tree will grow widely when showing all partial strips in full detail. However, we will show not all details but only the actual strip globally.

We will clarify this by the following representative example.

### Visualisation of the backtracking process

Consider Fig. 21 where we have a partial strip  $S0 = LHS + Tz$  with  $LHS = Ts + P$ .

Then the remaining tans are  $Tr, Tm1, Tm2$  and  $S$  and these names are listed under  $S0$ . We can extend  $S0$  with either  $Tr$  or  $Tm$ , resulting in the partial strips  $S1.1$  and  $S1.2$ , respectively.

Clearly,  $S1.1$  is fully rectangular while  $S1.2$  has a skew rhs-edge. The remaining tans for extending  $S1.1$  are  $Tm1, Tm2$  and  $S$  (these names are listed under  $S1.1$ ). However,  $S1.1$  can only be extended with  $S$ , resulting in  $S2.1$ , with  $Tm1$  and  $Tm2$  left. It is easily seen that these tans cannot be used anymore for extending  $S2.1$ . This fact is indicated by  $X$  in the figure and this branch of the tree ends here. So, adding the tans in this order does not result in a full strip.

On the other hand, when first adding one of the triangles  $Tm1$ ,  $Tm2$  (say  $Tm1$ ) to  $S0$  we find the

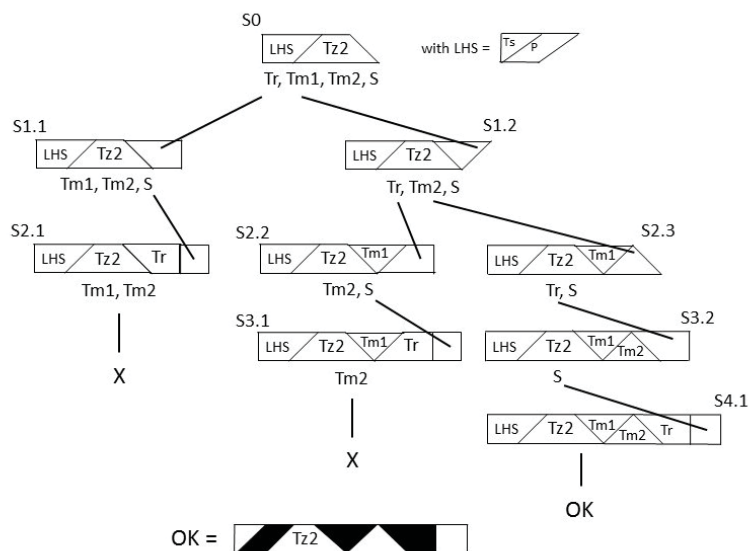


Figure 21: Example of a tree structure for finding all layouts of the strip J14.

strip  $S1.2$ , which can be extended by adding either  $Tr$  or  $Tm2$ , resulting in the strips  $S2.2$  and  $S2.3$ , respectively. Now the remaining tans for extending  $S2.2$  are  $Tm2$  and  $S$  (see below  $S2.2$ ), but only  $S$  can be added, resulting in  $S3.1$ . However,  $S3.1$  cannot be extended further, again indicated by  $X$  and this branch also ends.

Let us now consider  $S2.3$ . Here the remaining tans for extension are  $Tr$  and  $S$ . Clearly,  $S2.3$  can be extended with only  $Tr$ , giving strip  $S3.2$  and tan  $S$  is left. Finally,  $S3.2$  can be extended by  $S$ , giving a final full strip, indicated by  $OK$ . The structure of the final full strip is also given.

### Simplification of the tree visualization

It should be noticed that in fact we do not need to know the full filling details of the intermediate partial strips. Indeed, only the overall shape of each partial strip is relevant for finding a possible extension. So, we can replace the detailed scheme above by a more global scheme, as shown in Fig. 22-left. We emphasize that in this tree at each level (except top level) we have only indicated (in black) the *global* shape (and actual) size of the partial strip in the previous level. However, the newly added tan at the current level is shown with its *actual* shape and *actual* size.

Finally, we even can reduce the width of the figure a bit more by using the *same* size for all partial strips, but preserving their global shape, as shown in Fig. 22-right. In all next figures we will only use the latter compact visualization.

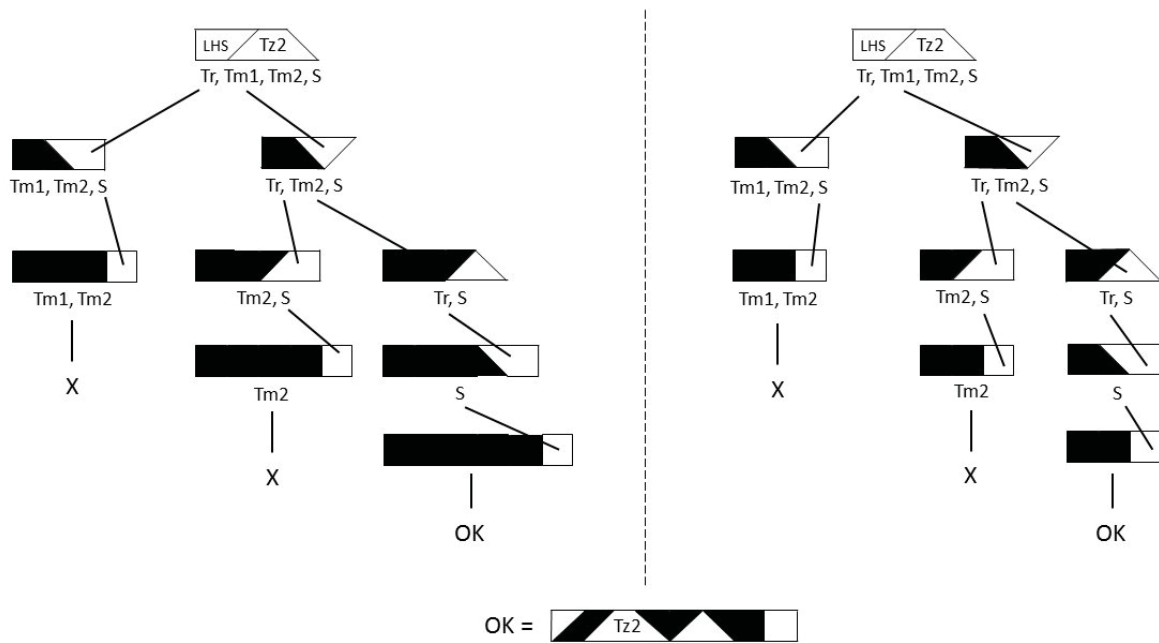


Figure 22: Two global visualizations of a tree structure for  $J14$ .

## 5.2 Finding all possible layouts of strip $J14$

### 5.2.1 The layouts of the strip with $Tz1$ and $Tz2$

As indicated in Fig. 18 we see that (i) in case of  $Tz1$  the corresponding LHS consists of one single tan, being  $Ts$ , and (ii) in case of  $Tz2$  that LHS consists of one or two tans. All layouts for  $J14$  with  $Tz1$  and  $Tz2$  are given in Figs. 23 up to 27.

### 5.2.2 The layouts of $J14$ with $Tz1$

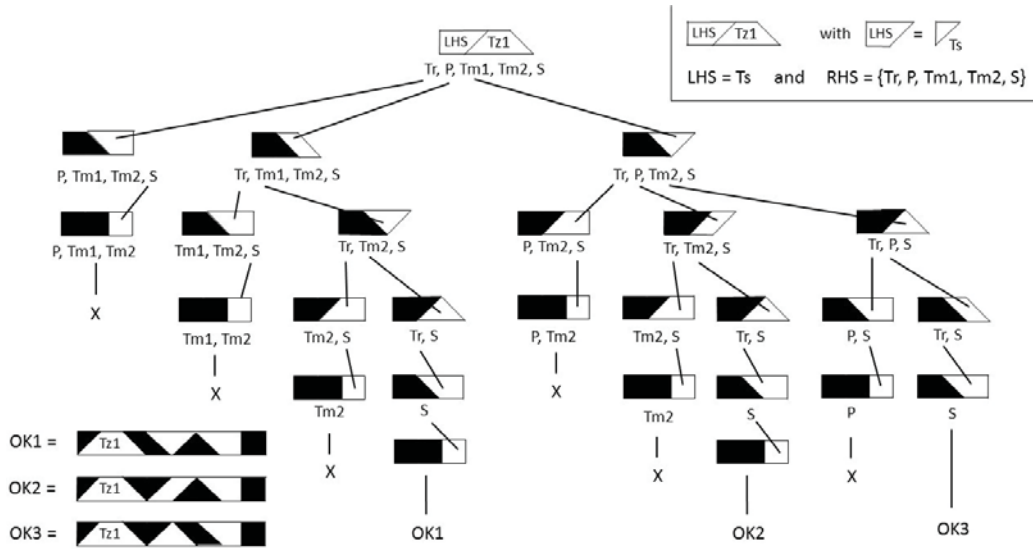


Figure 23: Visualization of Strip  $J14_{Tz1}$ .

### 5.2.3 The layouts of $J14$ with $Tz2$

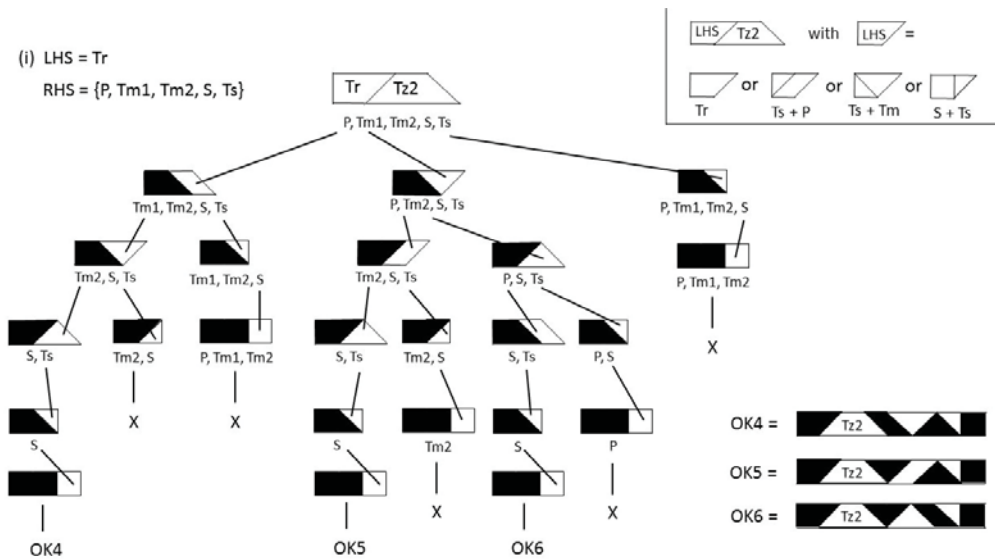


Figure 24: Visualization of Strip  $J14_{Tz2.1}$ .

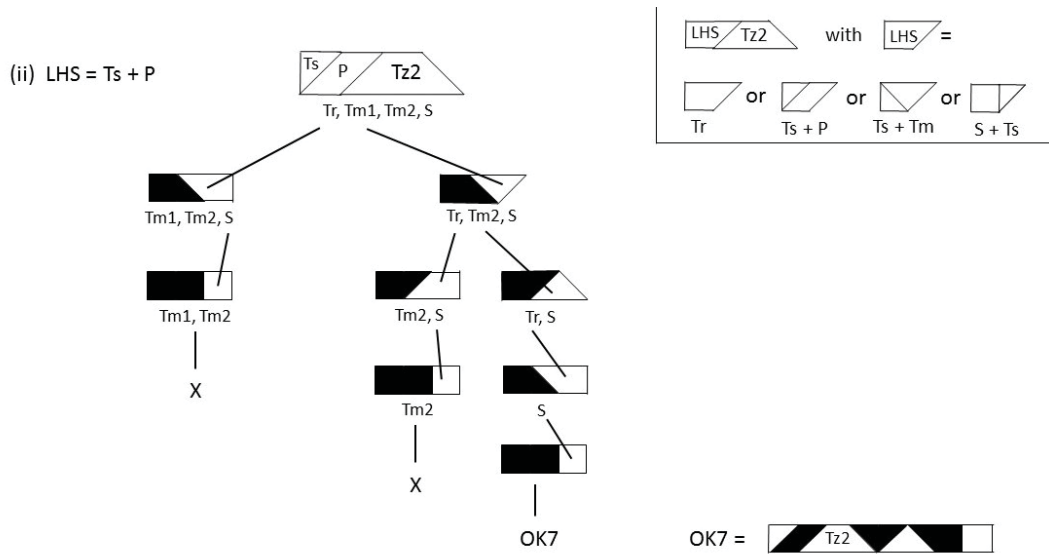


Figure 25: Visualization of Strip  $J14.Tz2.2$ .

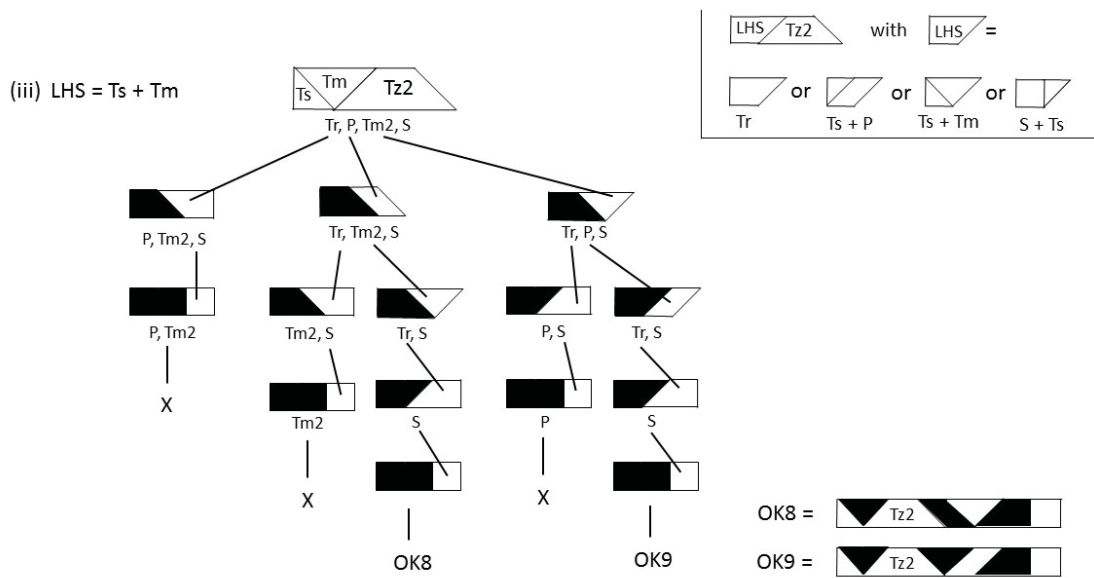


Figure 26: Visualization of Strip  $J14.Tz2.3$ .

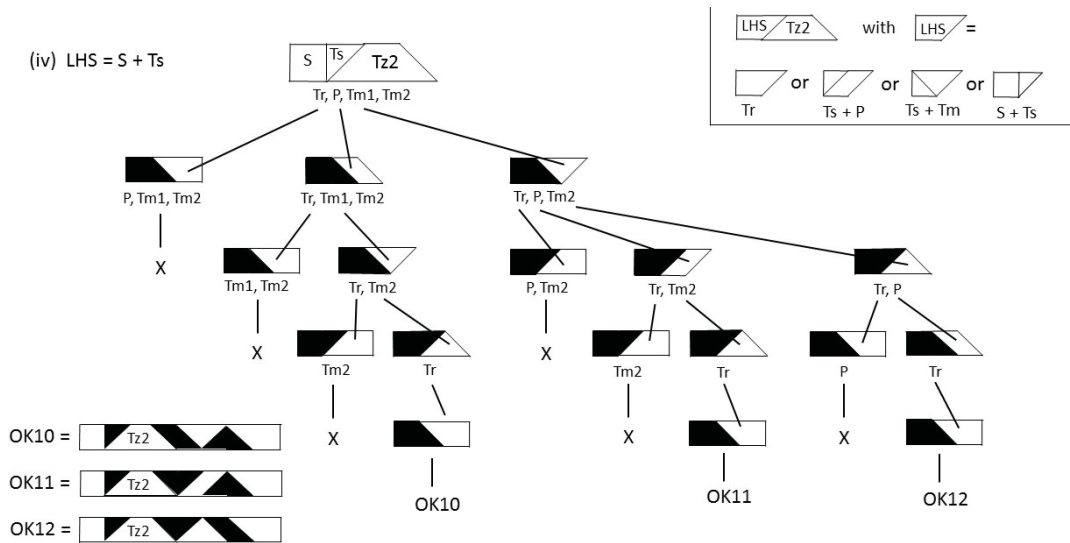


Figure 27: Visualization of Strip  $J14\_Tz2.4$ .

### 5.2.4 The layouts of $J14$ with $Tz3$

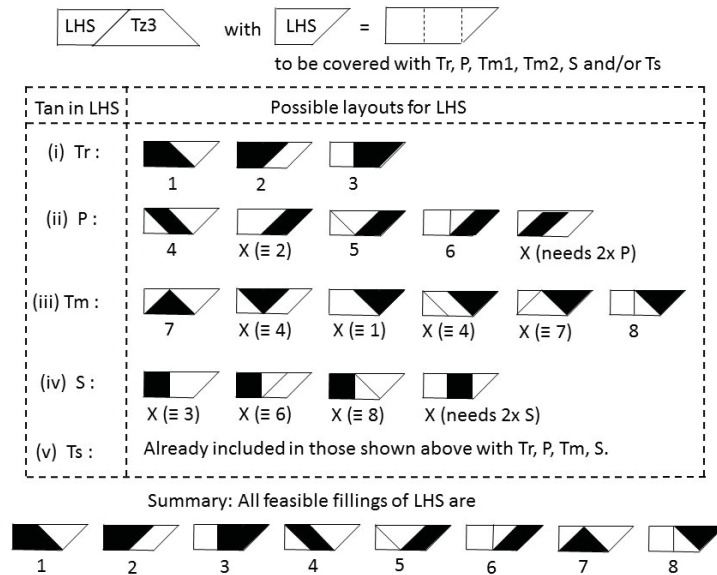


Figure 28: Investigation of the LHS partitions of Strip  $J14\_Tz3$ .



### 5.2.5 The layouts of the strip with Tz3

As indicated in Fig. 28 we see that in case of Tz3 the corresponding LHS consists of 2 or 3 tans, resulting in 8 feasible fillings. Notice that the left-edge of LHS is vertical, to be realized by one of the 3 tans Tr, S and Ts. Further, RHS has a skew left edge and a vertical right edge. The latter must also be realized by one of the 3 tans Tr, S and Ts. So, when fixing one of these 3 for realizing the vertical edge of LHS, at most 2 of them are left for building RHS.

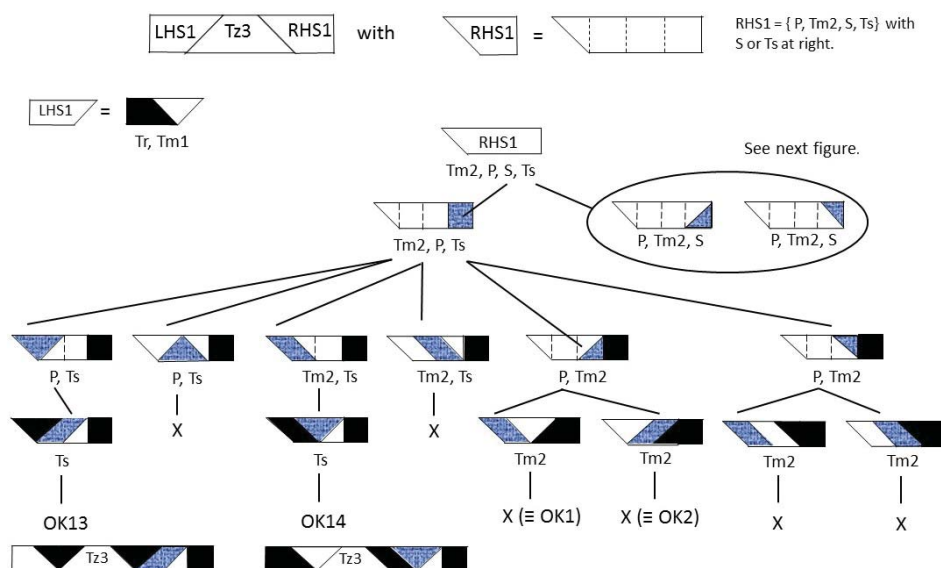


Figure 29: Investigation of Strip  $J14\_Tz31$ , part (i).

In Figs. 29 and 30 we show the partial fillings of RHS ending at right with S or Ts.

Clearly, Fig. 29 is self-explaining.

Fig. 30 shows the fillings of RHS ending at right with Ts. Next, after having added S in the 4 RHS-strips we still need to add P and Tm. However, for a full filling of all these 4 sub-strips we need an additional tan Ts, but this is not available. Thus, this branch of the tree does not end with a feasible filling of RHS.

Figs. 31 and 32 are also self-explaining.

In Fig. 33 we show the partial fillings of RHS4 ending at right with Tr or S. In Fig. 34 we consider the case where LHS5 consists of the same tans (Ts, P and Tm1) as in the previous figure. Consequently, RHS5 is identical to RHS4 since the same tans for RHS5 are available as for RHS4. However, since LHS5 has a partition being different from that of LHS4, we find with LHS5, Tz3 and RHS5 a different partition of the whole strip which is different from that in the previous case with LHS4, Tz3 and RHS4.

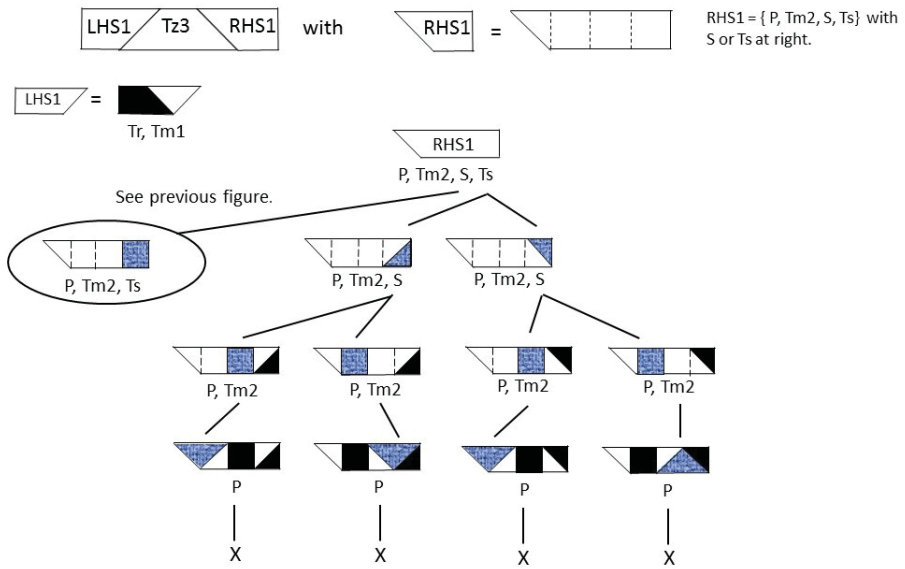


Figure 30: Investigation of Strip  $J14.Tz31$ , part (ii).

In Fig. 35 we consider the case LHS6 with  $Tr$ ,  $Tm1$  and  $Tm2$ . Since both triangles do not have a vertical edge we have to place  $Tr$  at right, resulting in 2 layouts. Clearly, only one feasible partition can be made with  $Tm1$  and  $Tm2$ .

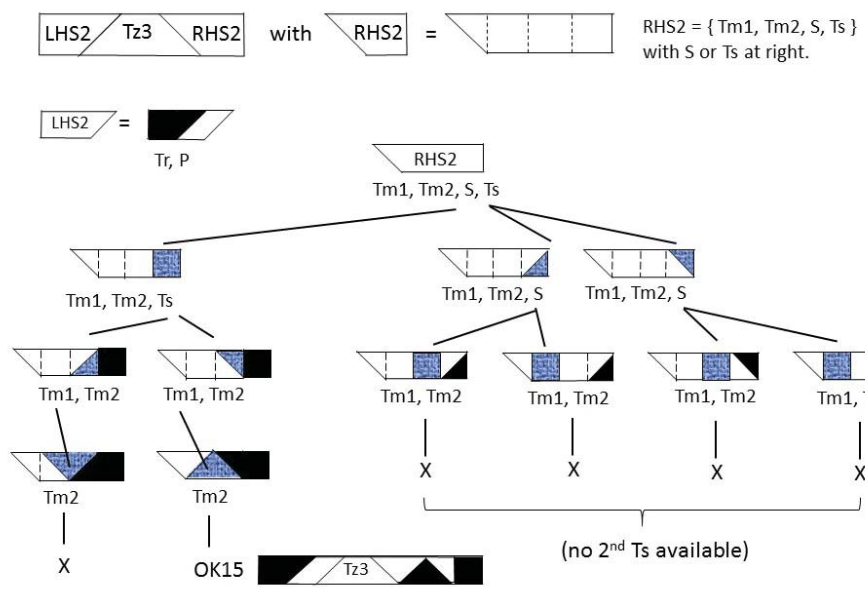


Figure 31: Investigation of Strip  $J14.Tz32$ .

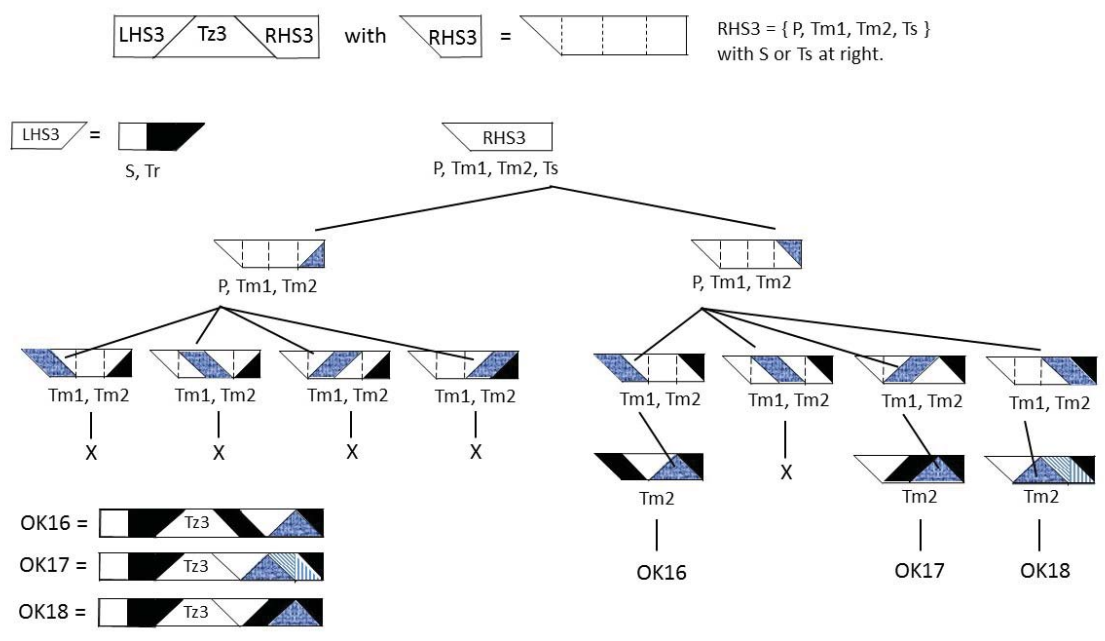


Figure 32: Investigation of Strip  $J14.Tz33$ .

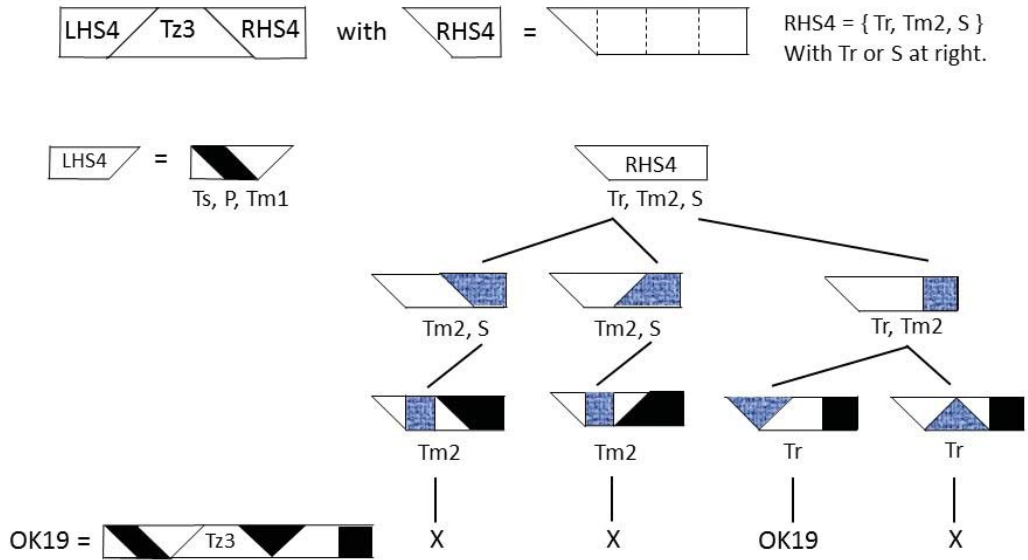


Figure 33: Investigation of Strip  $J14.Tz3.4$ .



This case is identical to RHS-4, since here the same tans are available for covering as in RHS4. So, RHS5 = RHS4. However, since LHS-4 is different from LHS-5, we do have a new different partition of the whole strip. It is labeled as OK20.

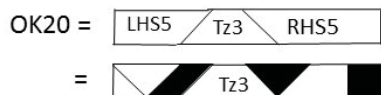


Figure 34: Investigation of Strip  $J14.Tz3.5$ .

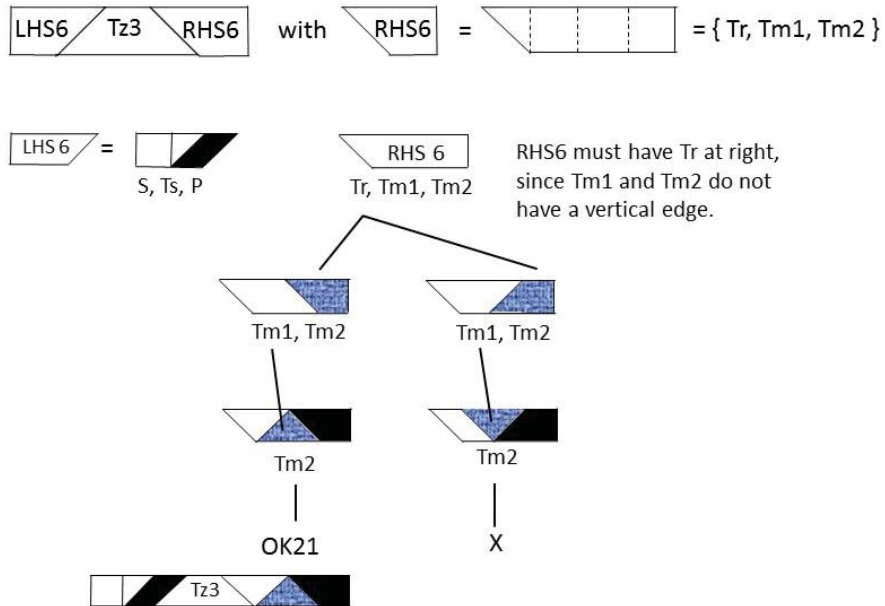


Figure 35: Investigation of the Strip  $J14.Tz3.6$ .

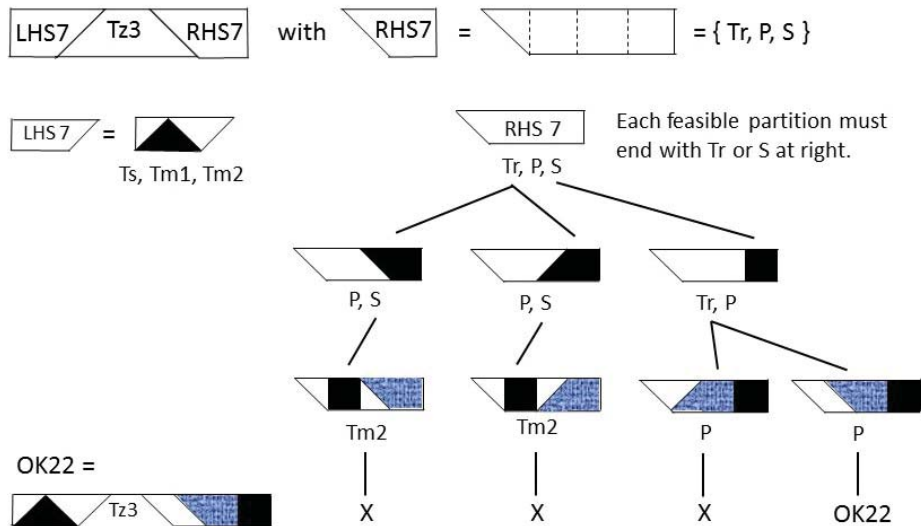


Figure 36: Investigation of the Strip  $J14.Tz3.7$ .

In Fig. 36 we consider case LHS7 consisting of Ts, Tm1 and Tm2. Hence, RHS7 must contain Tr, P and S. Both Tr and S have a vertical edge, so these tans must be placed at right, resulting in 3 partial fillings for RHS. Next we can add S and Tr to these layouts. Notice that after having added S, two tans of type Ts are required for a full filling, but these are not available. Similarly, after having added Tr we find one layout where only Tm can be added while only P is present. The other layout we have to add P and in this case this is possible, resulting in a feasible layout (denoted by OK22).

Next we have to study the strip with LHS8 with S, Ts and Tm1. Then RHS8 must contain Tr, P and Tm2. Clearly, Tr must be placed at right of RHS8 since P and Tm2 do not have a vertical edge. This gives two options where we can add P, resulting in 4 partial strips. Finally, herein Tm has to be included. This is only possible in two strips. Hence, this case with LHS8 and RHS8 results in 2 feasible partitions for the whole strip. See Fig. 37.

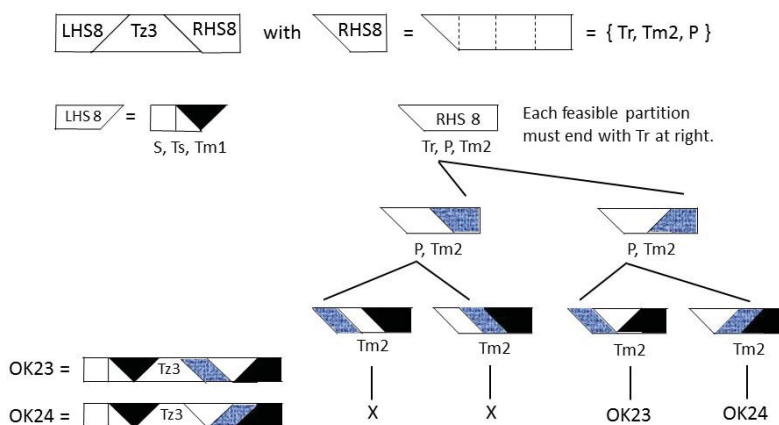


Figure 37: Investigation of the Strip  $J14_{Tz3.8}$ .

### 5.2.6 Summary of the analysis of *Strip J14*

The investigations above for finding all possible partitions of *Strip J14* with the 7 given tans can be summarized by the following steps:

1. Determine all feasible positions and orientations of the isosceles trapezium Tz in strip *J14*, see Fig. 17;
2. Determine all possible partitions for the LHS in the strip, see Figs. 18, 19 and 28;
3. For each of the LHS-partitions: determine all possible layouts for the right hand side (RHS) in the strip using the backtracking principle and being visualized by a tree structure, see Figs. 21 up to 37.

In this way we find all possible partitions of the complete strip *J14*, giving in total 24 different solutions. They are shown in Fig. 38. Moreover, these 24 solutions have also been found by our

computer program (see Fig. 39 and section 6).

For convenience, the equivalence between the partitions (“handmade” and “computer generated”) in both figures is given in Table 1 after Fig. 39. Notice that sometimes we have to apply a horizontal or vertical reflection to a particular partition in Fig. 38 to find the same picture in Fig. 39.

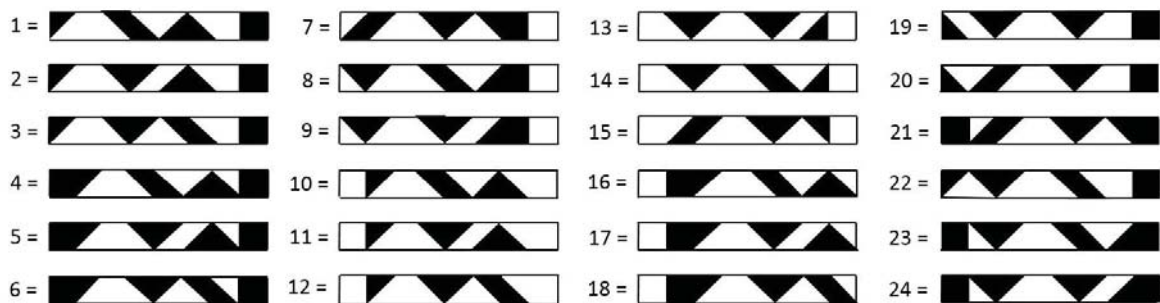


Figure 38: Strip  $J14$  with all its 24 different partitions (“handmade”).

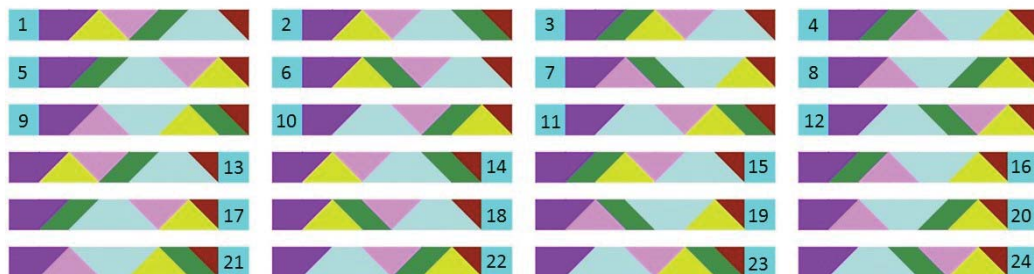


Figure 39: Strip  $J14$  with the 24 partitions (“computer generated”).

Table 1: Correspondence between the handmade and computer generated solutions for Strip  $J14$ .

<i>Handmade (part1)</i>	1	2	3	4	5	6	7	8	9	10	11	12
<i>Computer generated</i>	1	6	3	24	22	23	2	7	4	13	18	15
<i>Handmade (part2)</i>	13	14	15	16	17	18	19	20	21	22	23	24
<i>Computer generated</i>	21	20	17	12	10	11	9	8	14	5	19	16

### 5.2.7 Strip $J_{14}$ with its twin layouts

Let us consider the 24 solutions in Fig.38 in more detail. We can divide each of the strips into the tan  $S$  and a 7S-wide substrip  $L$ . Notice that  $S$  is either at the left or at the right side of the full strip. We will denote the 24 full strips by  $F_1$  up to  $F_{24}$  and their substrips by  $L_1$  up to  $L_{24}$ . Thus, we have either  $F_k = L_k + S$  or  $F_k = S + L_k$  for  $k = 1, \dots, 24$ . The strips  $L_k + S$  and  $S + L_k$  will be called twins and their twin-relationship will be indicated by  $L_k + S \Leftrightarrow S + L_k$ . It is easily seen from Fig. 38 that we have the following twins, shown in Fig. 40.

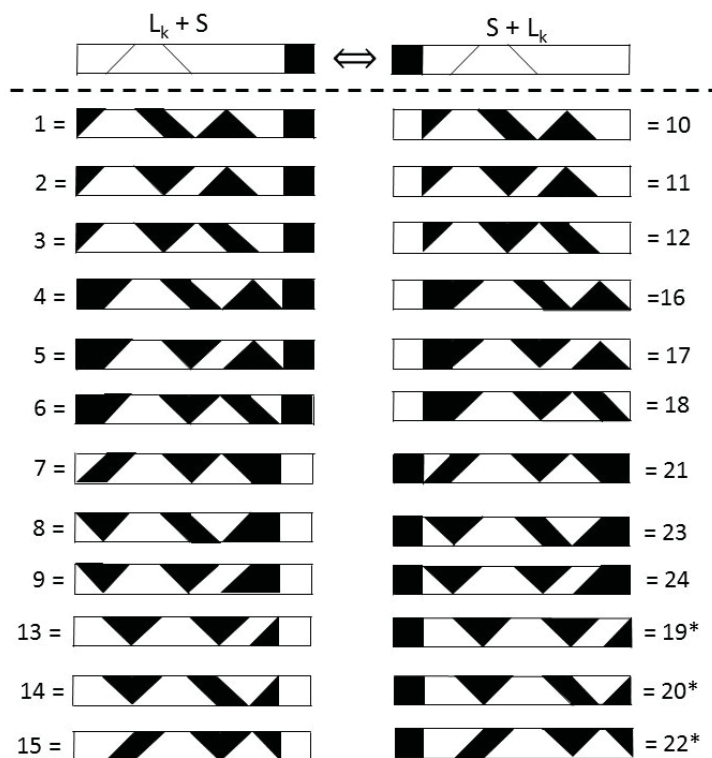


Figure 40: Strip  $J_{14}$  with its 12 twin layouts.

The strips 19\*, 20\* and 22\* are the horizontally flipped strips 19, 20, and 21 in Fig. 38.



### 5.3 Finding all different partitions for $J15$ and $J16$ by a combinatorial approach

We start with considering the structure of all feasible partitions found for the 12 twin pairs in Fig. 40. Notice that inside each of the 24 partitions there are 6 joint edges for each pair of adjacent tans. In particular, precisely 5 of these joint edges are skew, and only one joint (with  $S$ ) is vertical. We can cut  $J14$  along each of these cutting edges, resulting in 2 separate sub-strips. Next we can reverse the order of these sub-strings and glue them together. Apparently, the latter can be done in two ways (i.e., in original or in upside-down orientation) when the cutting edge is skew. We will discuss the possible situations for all strips. This is done by using one representative strip. To this end, we can take the first strip  $J14-1$  in Fig.38.

The cutting edges will be denoted by  $C1$  up to  $C6$ , with  $C6$  being vertical. See Fig. 41.

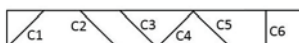


Figure 41: The cuttings edges of strip  $J14-1$ .



Figure 42: Vertical cutting and pasting of strip  $J14-1$  gives strip  $J14-10$  .

Let us first consider the case with a vertical cutting edge (i.e. the cutting along vertical edge  $C6$  of tan  $S$  inside the strip  $J14-1$ ). This is illustrated in Fig. 42-Left. We obtain the tan  $S$  and a sub-strip of width  $7S$ . After glueing  $S$  in front of the sub-string we get strip  $J14-10$ , see Fig. 42-Right. It is easily seen that carrying out this process for all strips in the lhs column of Fig. 40 results in the creation of all corresponding twin strips in its rhs column.

Next we consider the case with a skew cutting edge ( $C1$  up to  $C5$ ). The process of “cut and paste” (in two ways) is visualized by the two (representative) examples  $J14-C1$  and  $J14-C2$  in Fig. 43. Then we obtain two new strips, one having the shape of  $J15$ , and the other one that of  $J16$ .

Recalling Fig. 40 we know that  $J14-1$  and  $J14-10$  are twins. We can apply the cut-and-paste process also to twin  $J14-10$ . Now it can easily be seen from the examples  $J14-10-C1$  and  $J14-10-C2$  in Fig. 43 that cutting along a skew edge of two strips being twins results in the same strips of type  $J15$  and  $J16$ . Clearly, we can draw the following

**Conclusion:** (10)  
**The cut-and-paste process applied to each of the twin pair strips of type  $J14$  in Fig. 40 results in a pair of strips of type  $J15$  and  $J16$ .**

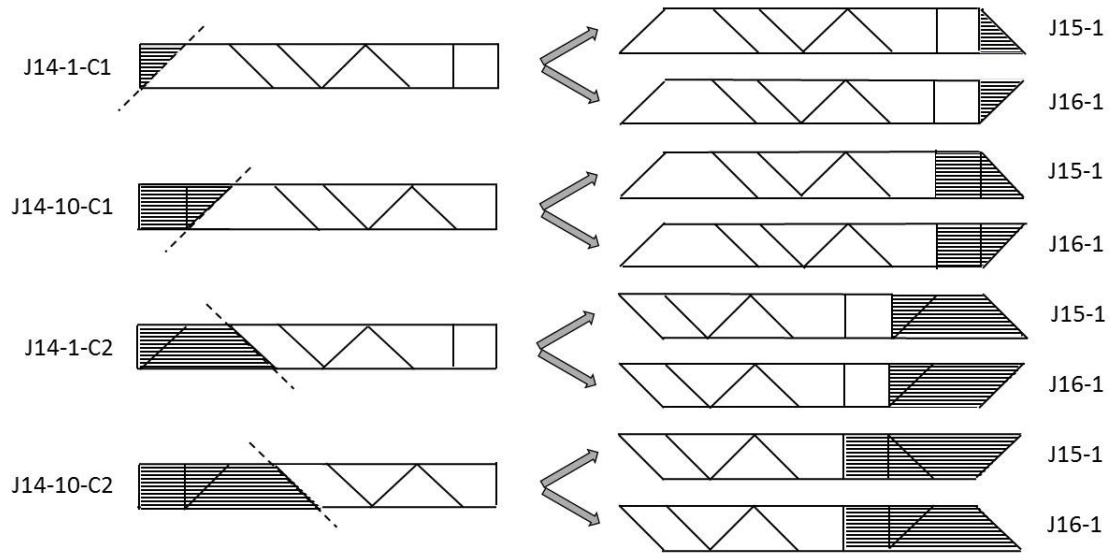


Figure 43: Cutting and pasting the twin strips  $J14$ .

Consequently, we can find precisely 60 different partitions for all  $J15$  as well as  $J16$ -strips, since we have 12 twin pairs of  $J14$ -strips and 5 different skew cutting edges per  $J14$ -strip.

These 60 layouts for both  $J15$  and  $J16$  are shown in the next figures. These layouts are arranged in the following way.

We have 12 groups of layouts, each group is headed by a  $J14$ -layout shown in the lhs column of Fig. 40. These 12 “header”-layouts are labeled by an alphabetical character, ranging from  $A$  to  $L$ . In each group 5 twin pairs consisting of a  $J15$ -layout and its dual  $J16$ -layout are given.

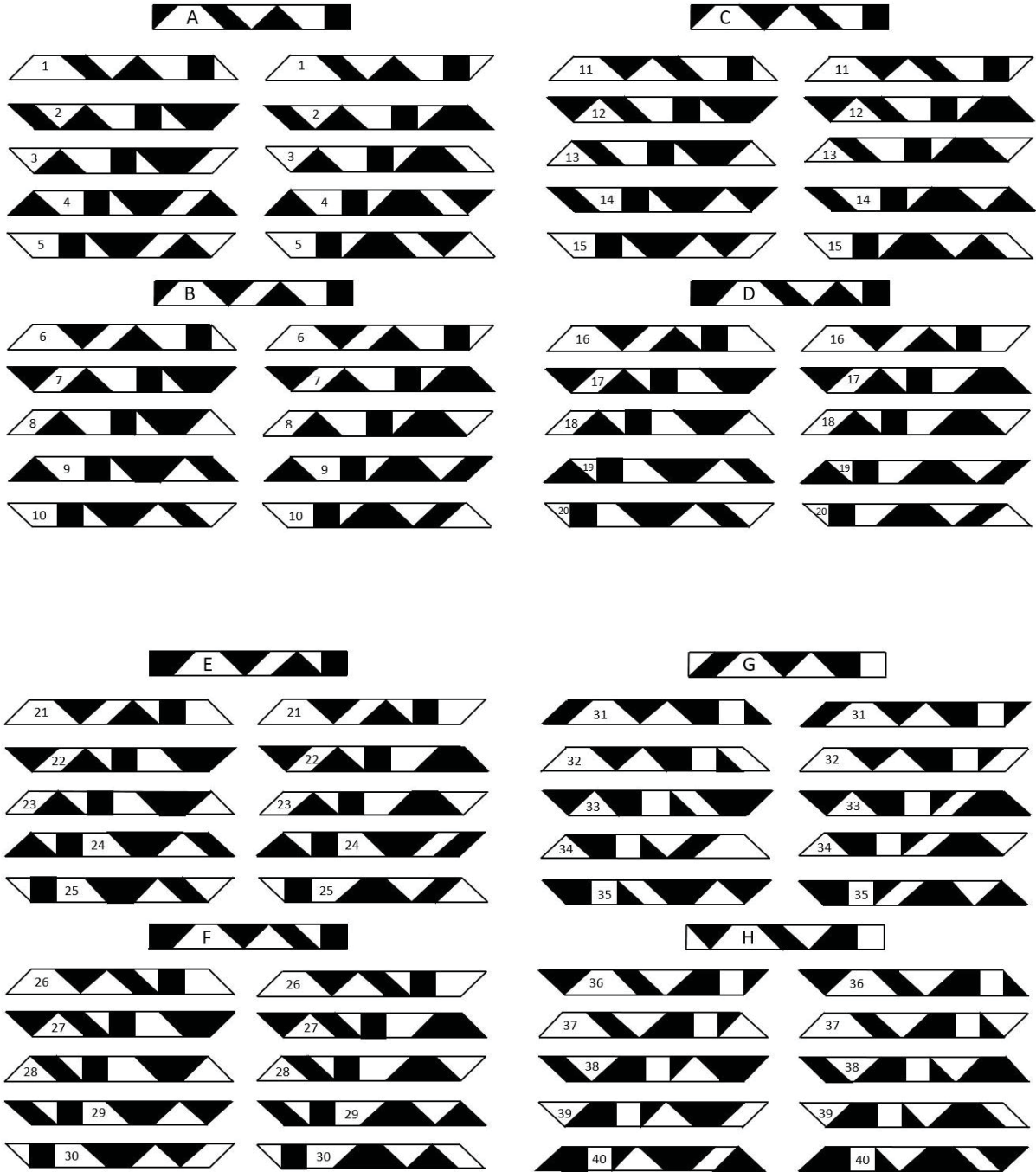


Figure 44: The solutions 1-40 (out of 60) of the strips J15 and J16.

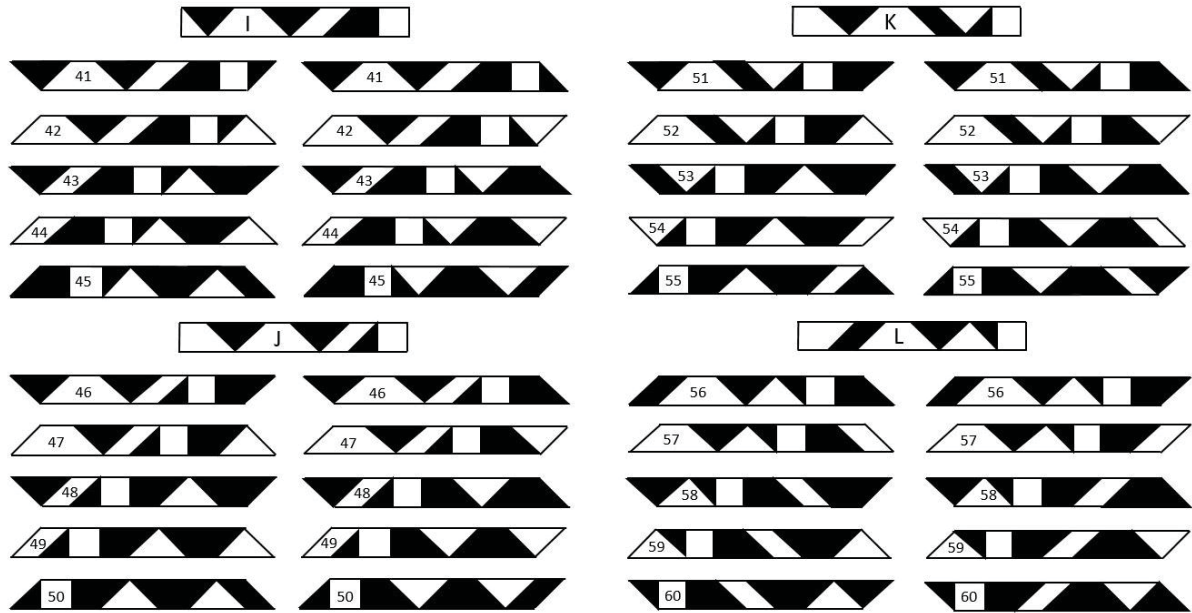


Figure 45: The solutions 41-60 (out of 60) of the strips *J15* and *J16*.

## 6 An algorithm for generating all partitions of a convex shape

Here we will (globally) explain how the problem of finding all partitions of a convex shape can be solved by a technique used for solving a *packing* problem, see [6]. This will be discussed below. We will first start with a simple packing problem.

### 6.1 A simple packing problem

Let be given a set of simple puzzle pieces and a rectangular box. The problem is to put all pieces in the box, without overlap. For an example, see the *Simple Puzzle* in Fig. 46 with a *box* with  $2 \times 3$  unit *cells* and the 3 *pieces*  $A$ ,  $B$  and  $C$ .

We introduce the notions *Aspect* and *Embedding*:

*Aspect*: the cell in the box, the type of a piece.

*Embedding*: the placement of a piece in the box can be encoded by a set of *aspects*.

In our example we have  $Aspects = \{0, 1, \dots, 5, A, B, C\}$  and the *Embeddings* are given by Fig. 47. Note that a solution to such a packing puzzle consists of a set of embeddings constituting a partition of the set of aspects; that is, the embeddings in a solution are pairwise disjoint.



Figure 46: The box with  $2 \times 3$  cells and the 3 puzzle pieces  $A$ ,  $B$  and  $C$ .

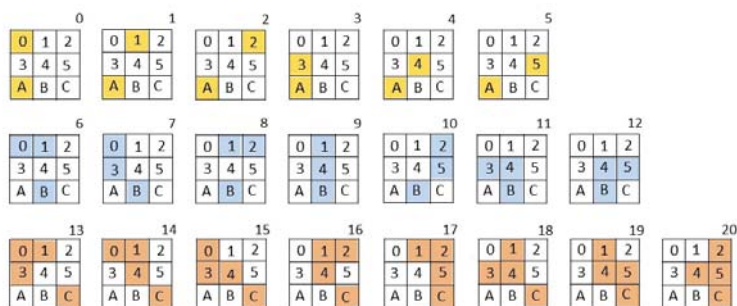


Figure 47: The Aspects and Embeddings of a simple puzzle.

It is important (for performance) that we eliminate symmetries (if any). This can be done by *restricting* the embeddings. We will illustrate this by an example. To this end, consider the previous example, where we will restrict piece  $C$  to be the *horizontally mirrored* letter L. We call

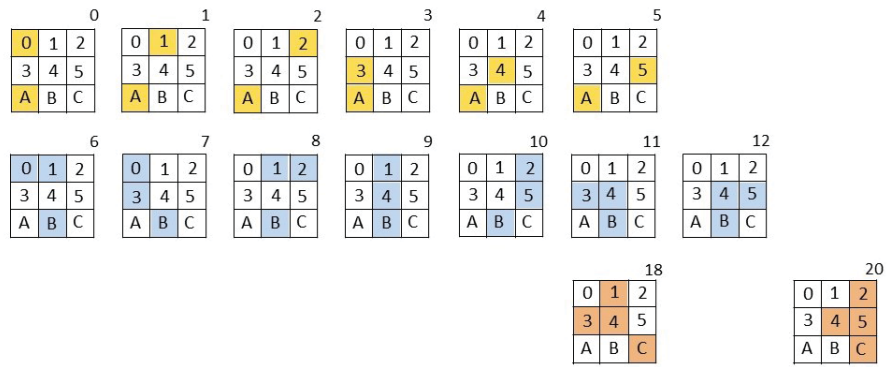


Figure 48: Eliminating symmetries by restricting embeddings.

this example *Simple L-restricted Puzzle*. This results in the embeddings in Fig. 48. It can easily be seen that the following 3 sets of embeddings  $E_1, E_2, E_3$  solve this puzzle, where

$$E_1 = \{0, 10, 18\}, E_2 = \{1, 7, 20\} \text{ and } E_3 = \{3, 6, 20\}.$$

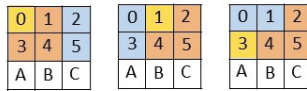


Figure 49: The 3 embeddings that solve the *Simple L-restricted Puzzle*.

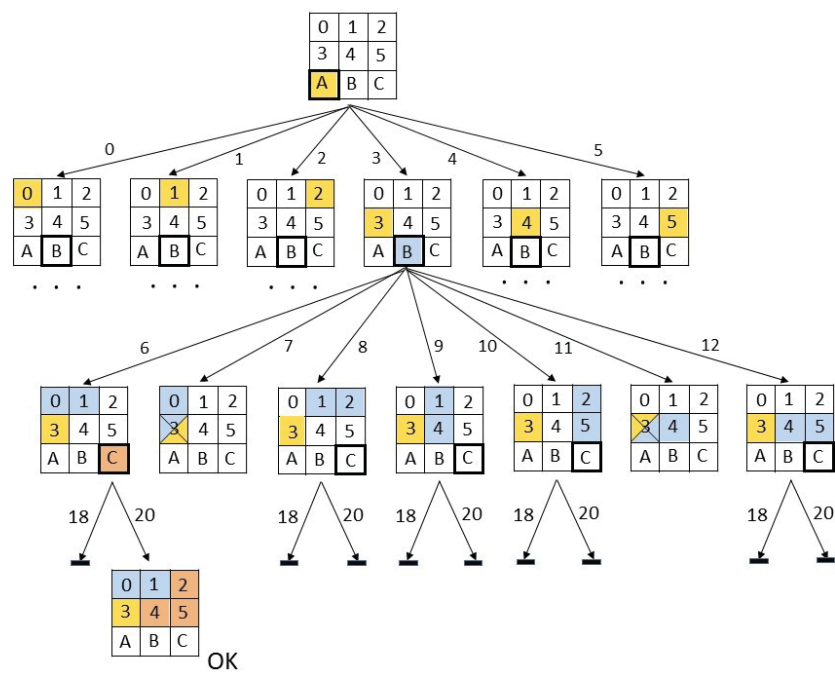


Figure 50: The backtracking tree for solving the *Simple L-restricted Puzzle*, with the embeddings  $\{3, 6, 20\}$  as solution.

Clearly, when dealing with a more complex puzzle we in general cannot easily find its solution(s) by hand. Then we might try to solve the puzzle using a computer and a dedicated solving procedure such as *backtracking*, see [7], [8]. Recall that the *search tree* is an important concept for the backtracking method. This is a graphical representation of all possible cases to be studied for finding a solution. In Fig. 50 we show (a part of) the search tree corresponding to the *Simple L-restricted Puzzle*.

## 6.2 A more complicated packing problem

Now we want to consider a more complicated packing problem which is related to the problem of finding all partitions of each of the convex shapes using the Japanese set of tans.

Recalling Conclusion (v) in (2) and Fig. 2 in section 2 we know that each convex shape formed by the 7 Japanese tans consists of 16 isosceles rectangular triangles  $Ts$ . Next we can split each  $Ts$  into two smaller triangles  $ts$ , i.e.,  $ts = Ts/2$ . So, the complete set of tans can be built up with 32 triangles  $ts$ , see Fig. 51. Now consider a rectangular box with 8 square cells, each of them being

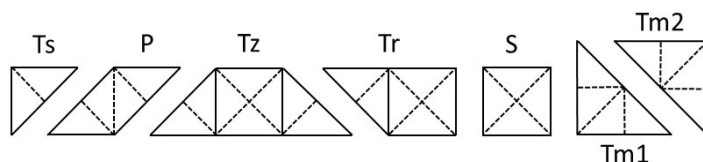


Figure 51: Subdividing all Japanese tans into triangles  $ts$ , with  $ts = Ts/2$ .

divided into 4 isosceles rectangular triangles  $ts$ . See Fig. 52.

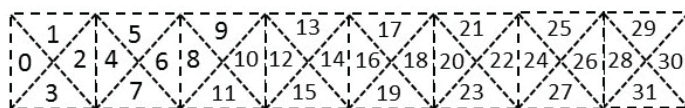


Figure 52: Box with 8 cells, each being subdivided into 4 triangles  $ts$ .

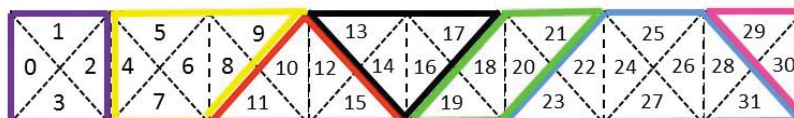


Figure 53: The box in Fig. 52 being fully covered by a partition of the strip  $J14$ .

This suggests that the 7 tans can fully fill this box. Indeed, a possible filling is given in Fig. 53.



### 6.2.1 The packing problem for Strip J14

Notice that in fact Fig. 53 shows a partition of strip J14, see also Fig. ??.

The situation in Fig. 53 is similar to that for the *Simple L-restricted Puzzle*. So, similar to Fig. 50 for this puzzle we can also use the backtracing algorithm to find all different partitions of J14.

### 6.2.2 The packing problem for Strip J16

Next, let us consider the parallelogram-shaped strip J16 (recall Fig. ??).

It is easily seen that the partition of J14 in Fig. 53 can be transformed to a partition of J16 by moving the triangle {29, 30} at the most right side to the most left side. Of course, this partition of J16 fits (partially) in a *larger* 1x9 rectangular box. See Fig. 54.

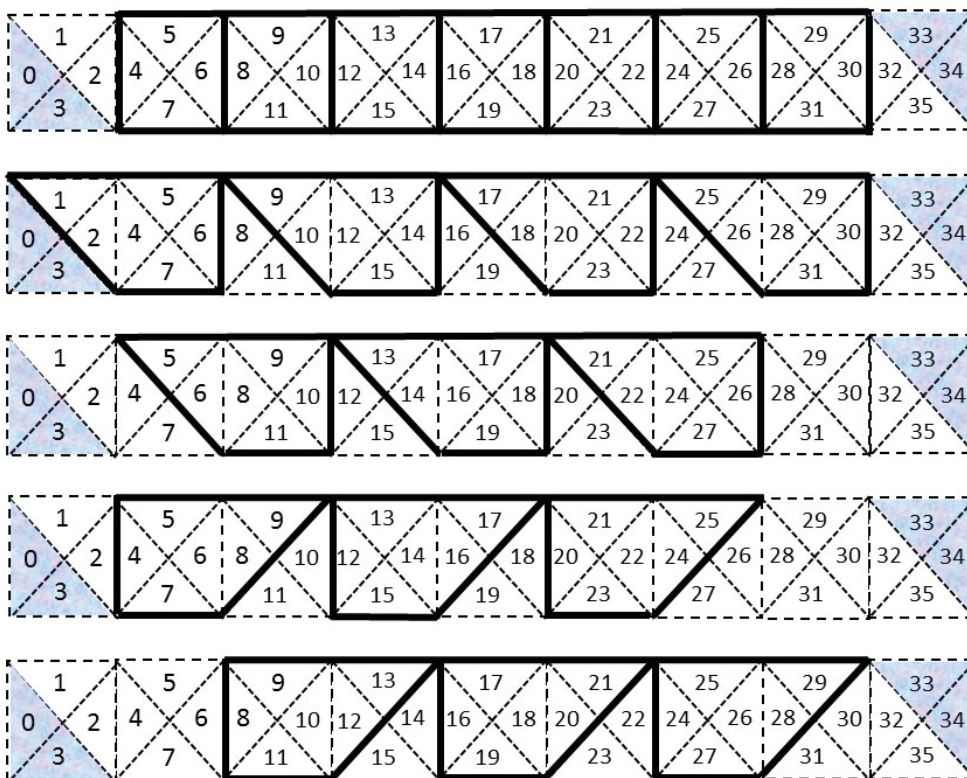


Figure 54: The enlarged box being (partially) covered by a partition of the strip J16.

Just as for the example *Simple L-restricted Puzzle* we can now establish the embeddings for each individual tan in the box in Fig. 54. Notice that in order to find all essentially different partitions we have to take into account all possible orientations of each tan when establishing the embeddings. We will illustrate this for two tans (*S* and *Tr*) only. The remaining tans can be described in a similar way.

Using Fig. 54 we find the following embeddings:

- $S$  in row 1:  $\{4, 5, 6, 7\}, \{8, 9, 10, 11\}, \dots, \{28, 29, 30, 31\}$
- $Tr$  in row 2:  $\{1, 2, 4, 5, 6, 7\}, \{9, 10, 12, 13, 14, 15\}, \{17, 18, 20, 21, 22, 23\}, \{25, 26, 28, 29, 30, 31\}$
- $Tr$  in row 3:  $\{5, 6, 8, 9, 10, 11\}, \{13, 14, 16, 17, 18, 19\}, \{21, 22, 24, 25, 26, 27\}$
- $Tr$  in row 4:  $\{4, 5, 6, 7, 8, 9\}, \{12, 13, 14, 15, 16, 17\}, \{20, 21, 22, 23, 24, 25\}$
- $Tr$  in row 5:  $\{8, 9, 10, 11, 12, 13\}, \{16, 17, 18, 19, 20, 21\}, \{24, 25, 26, 27, 28, 29\}$ .

Once having established all embeddings for all tans, we determine all possible partitions of the strip  $J16$  by using a backtracking algorithm, completely similar to example *Simple L-restricted Puzzle*.

**Remarks :**

- The establishment of the embeddings and the backtracking can be automatically generated by a dedicated computer program.
- Clearly, we can use the approach described above for *all* 16 convex polygons in Fig. ??-Right that can be formed by the set of the Japanese tans. Of course, we need a box of  $m \times n$  square cells for the polygons  $J1$  up to  $J13$ , with  $m$  and  $n$  such that the polygon under study fits in this box.
- In case we have two tans with the same shape but with different colour, then interchanging them in a layout gives a different partition, in contrast to the monochromatic case. This situation needs special attention when using a computer program for finding all different partitions.

In the next section we show all possible partitions of the mentioned 16 convex polygons.

7 All different partitions of the shapes  $J01$  up to  $J16$

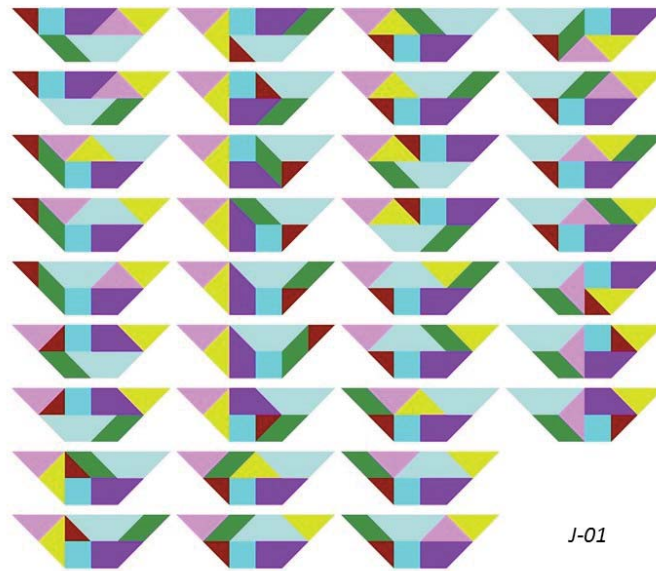


Figure 55: All 34 different layouts of shape  $J01$ .

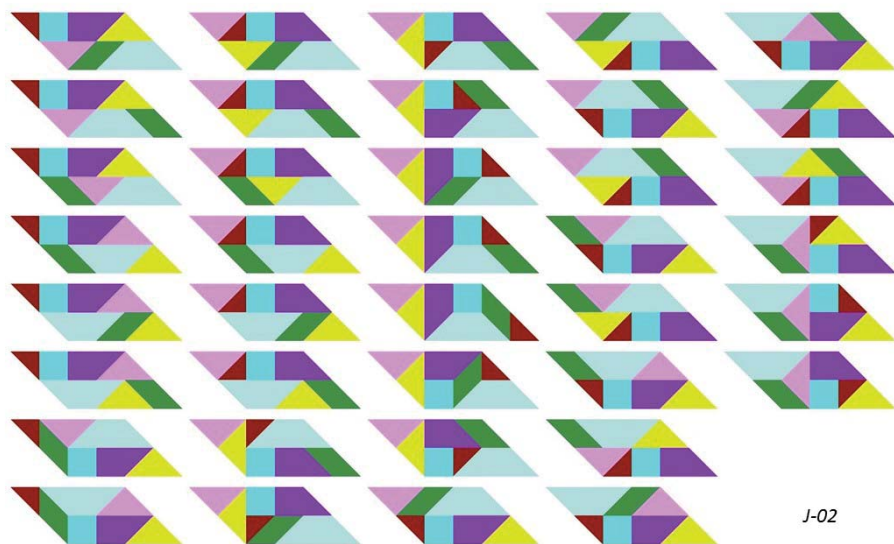


Figure 56: All 38 different layouts of shape  $J02$ .

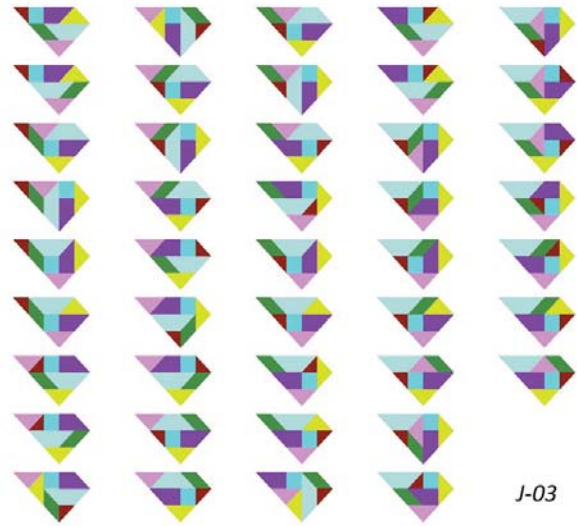


Figure 57: All 43 different layouts of shape *J03*.

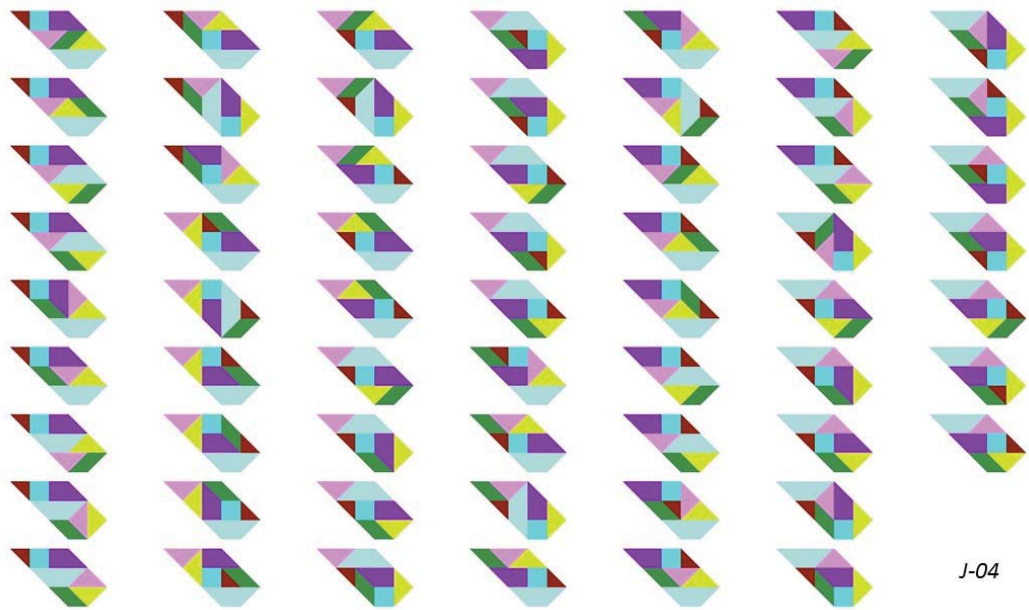


Figure 58: All 61 different layouts of shape *J04*.

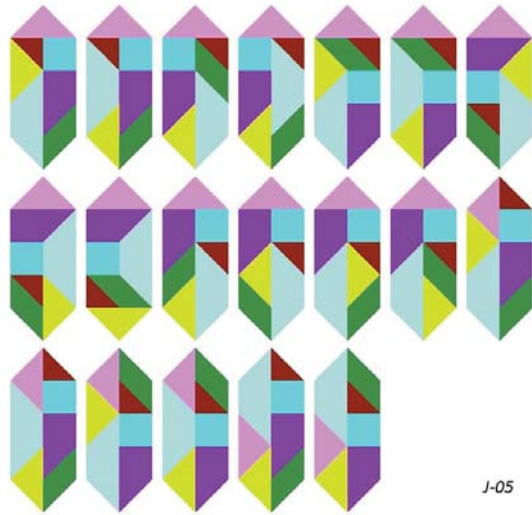


Figure 59: All 19 different layouts of shape *J05*.

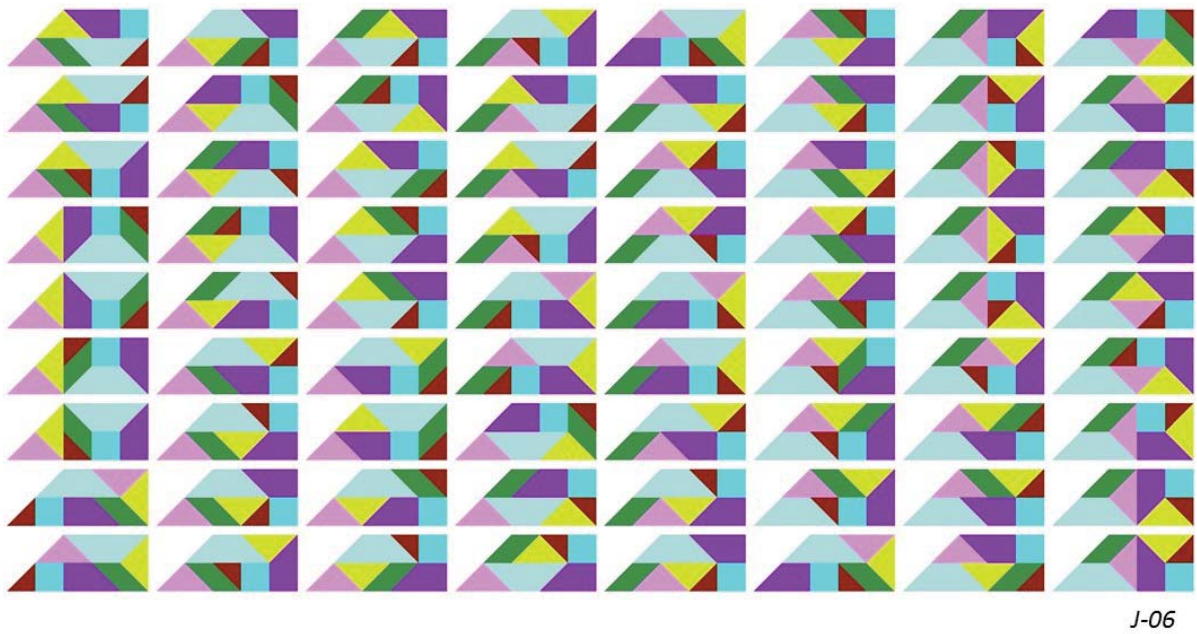


Figure 60: All 72 different layouts of shape *J06*.



Figure 61: All 3 different layouts of shape *J07*.

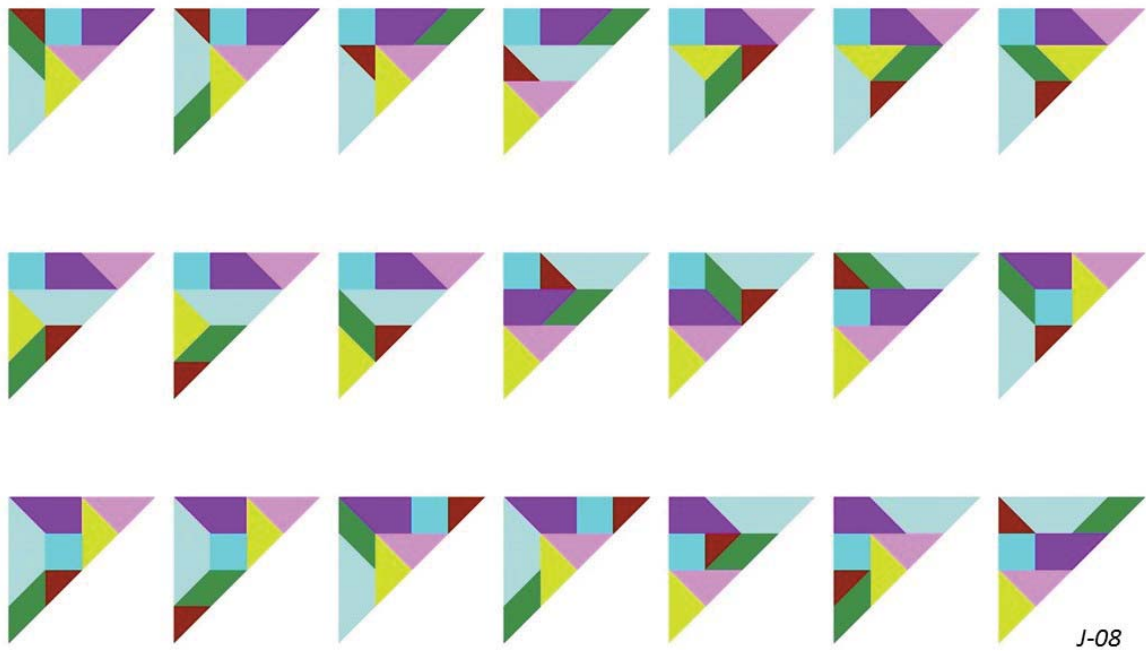


Figure 62: All 21 different layouts of shape *J08*.

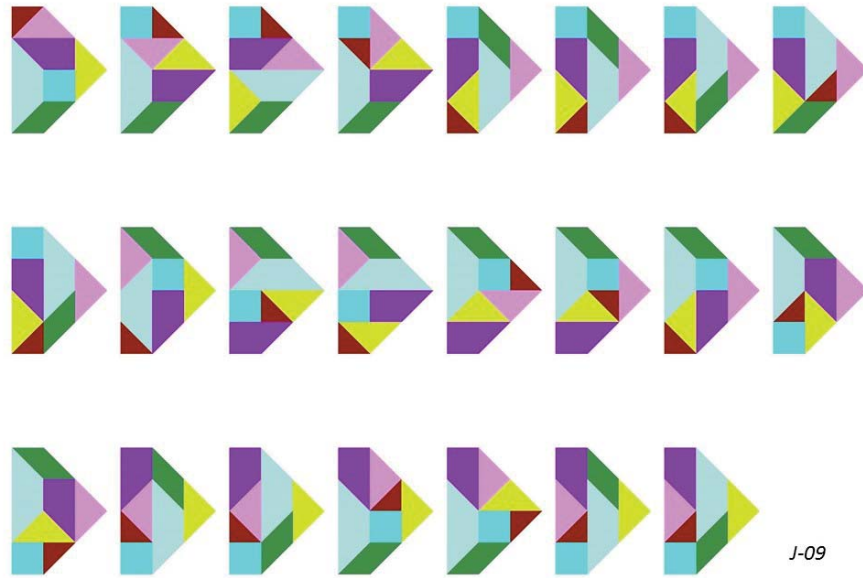


Figure 63: All 23 different layouts of shape *J09*.

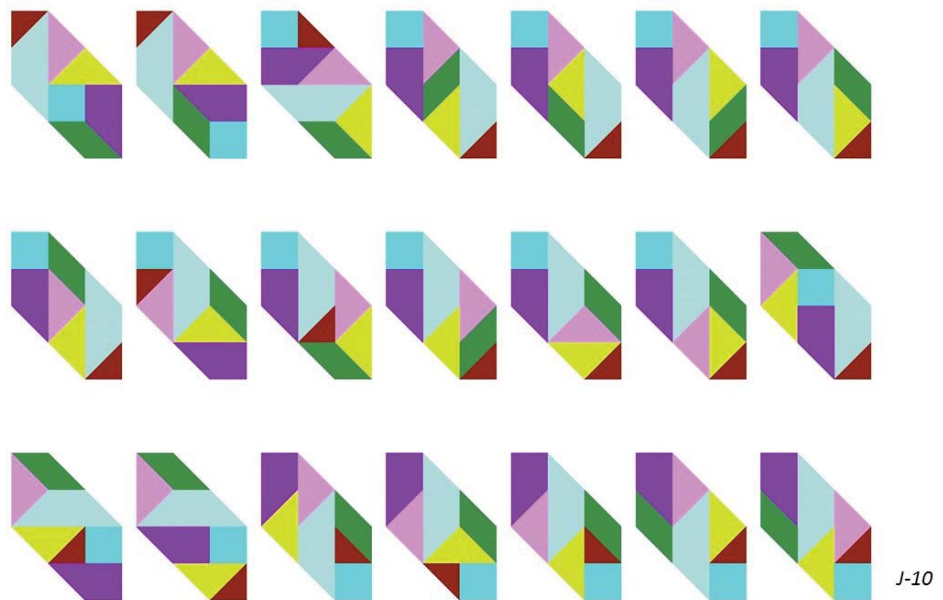


Figure 64: All 21 different layouts of shape *J10*.

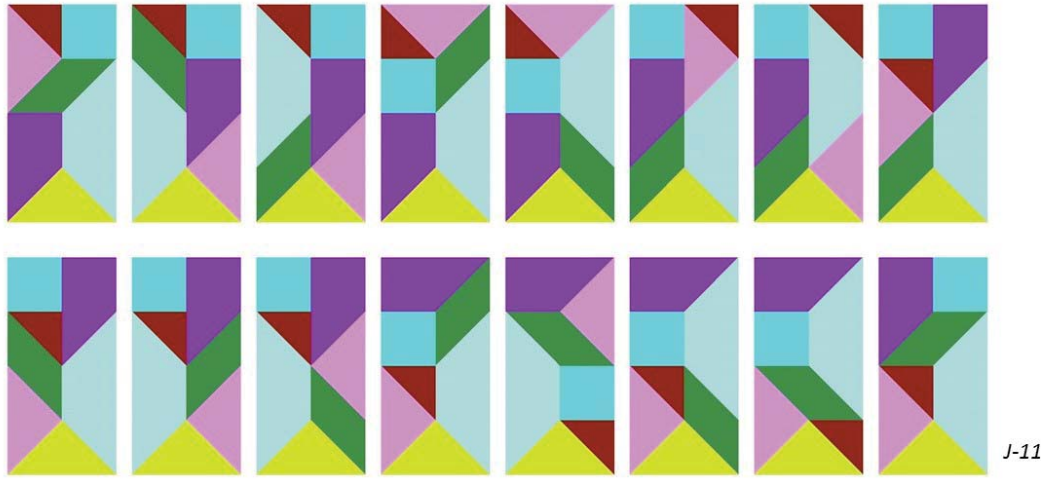


Figure 65: All 16 different layouts of shape  $J11$ .

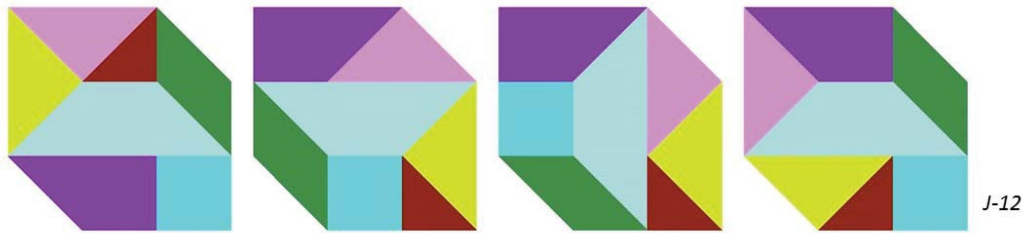


Figure 66: All 4 different layouts of shape  $J12$ .



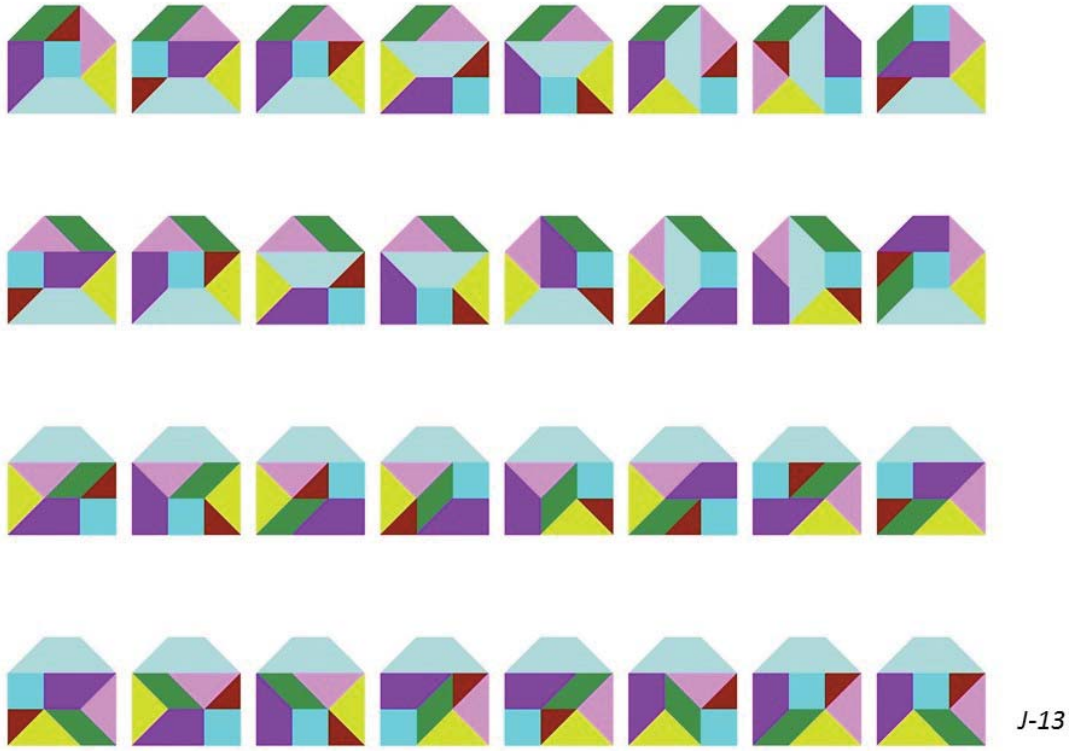


Figure 67: All 32 different layouts of shape *J13*.

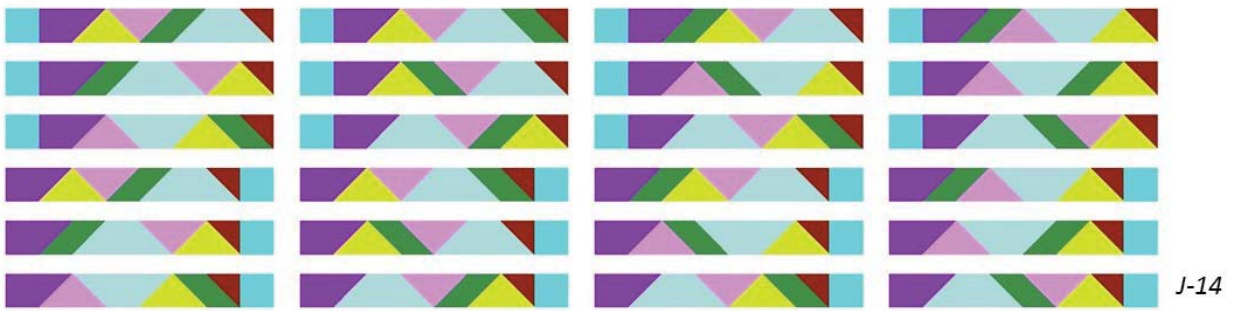


Figure 68: All 24 different layouts of shape *J14*.

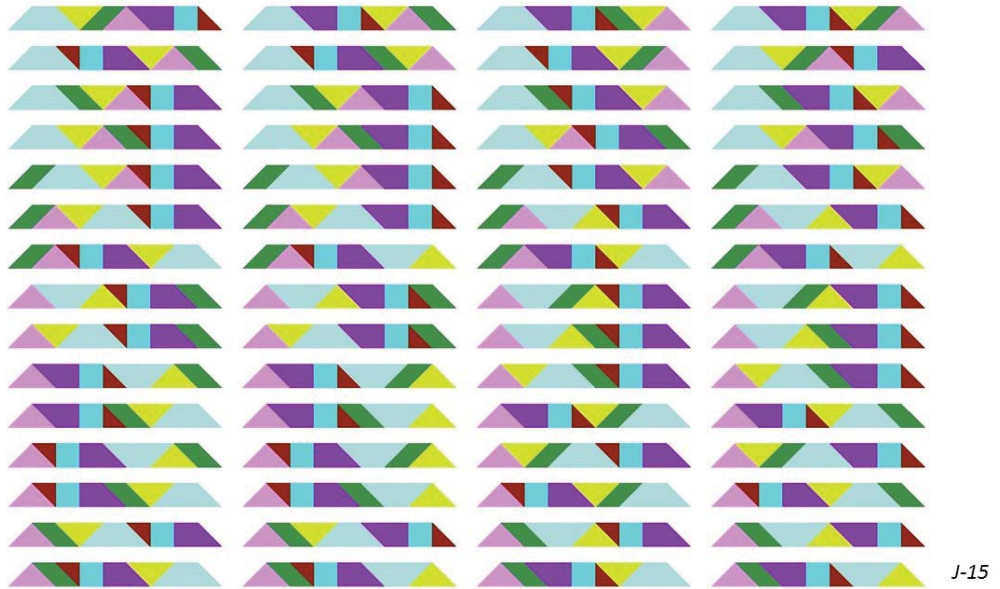


Figure 69: All 60 different layouts of shape *J15*.

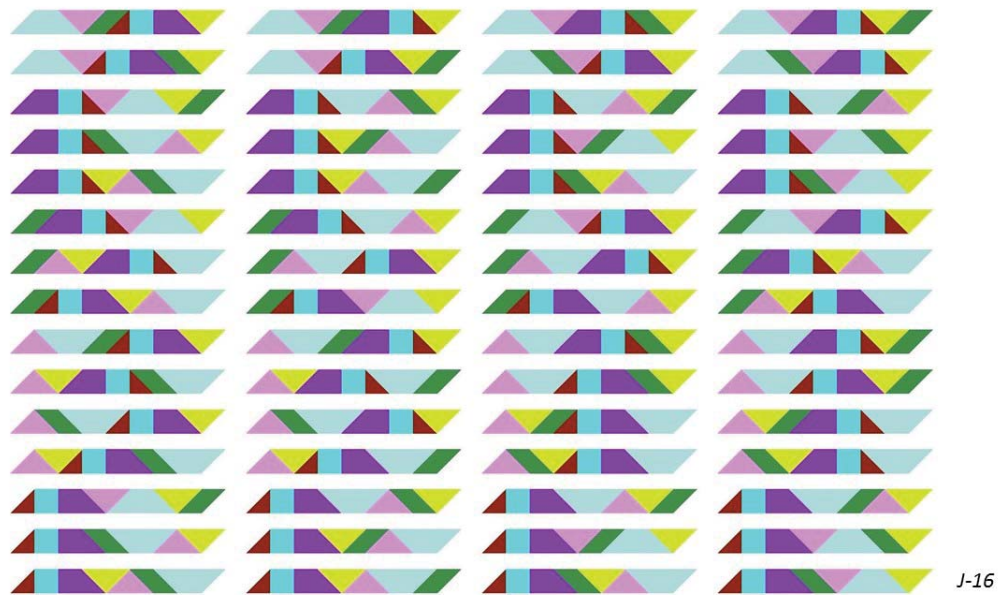


Figure 70: All 60 different layouts of shape *J16*.

Table 2: Summary: Number of different partitions per shape.

<i>Shape</i>	1	2	3	4	5	6	7	8	9	10	11	12	13	14	15	16
<i># partitions</i>	34	38	43	61	19	72	3	21	23	21	16	4	32	24	60	60

## A Analysis of the strips $J15$ and $J16$



Figure 71: The shape of the strips  $J15$  and  $J16$ .

In the paper [9] by Fox-Epstein and Uehara it was shown that besides the rectangular strip  $J14$  there are two more strips (we will call them  $J15$  and  $J16$ ) that can be built with the Japanese tans, see Fig. 71. It is easily seen that for finding all partitions of these two strips we can proceed in a similar way as for  $J14$  in section 5.

### A.1 The case $J15$

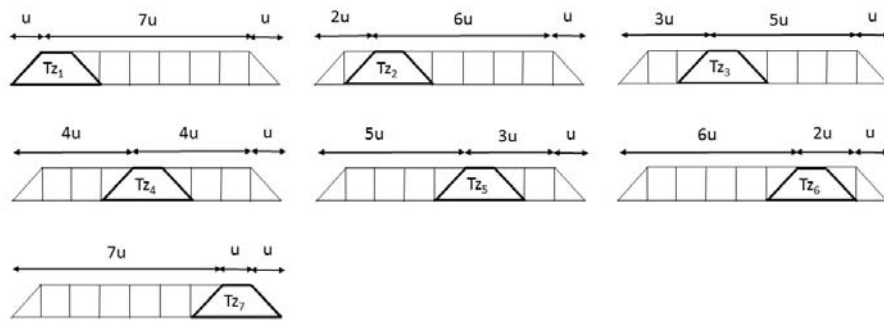


Figure 72: All possible positions of  $T_z$  in strip  $J15$

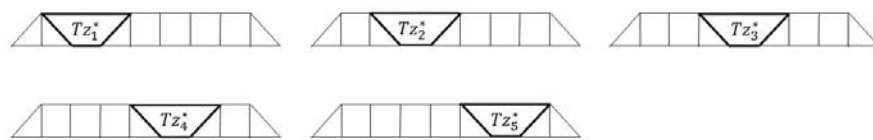


Figure 73: All possible positions of  $T_{z^*}$  in strip  $J15$

Analogously to Fig. 17 in section 5 we show all possible positions of  $T_z$  in strip  $J15$  in Fig. 72. It is easily seen (by horizontal reflection) that the following strips are equivalent:  $T_{z5} \equiv T_{z3}$ ,  $T_{z6} \equiv$

$T_{z_2}$  and  $T_{z_7} \equiv T_{z_1}$ . Thus, we need not to generate layouts with  $T_{z_5}$  up to  $T_{z_7}$  for  $J15$ . In Fig. 73 all possible positions for  $T_z$  upside down (denoted by  $T_z^*$ ) are shown. Then we see that  $T_{z_5}^* \equiv T_{z_1}^*$  and  $T_{z_4}^* \equiv T_{z_2}^*$ .

**Conclusion:** (11)

**We only need to find all possible different layouts of the strip J15 with  $T_{z_1}$  up to  $T_{z_4}$  (see Fig. 72) and with  $T_{z_1}^*$  up to  $T_{z_3}^*$  (see Fig. 73).**

## A.2 The case J16

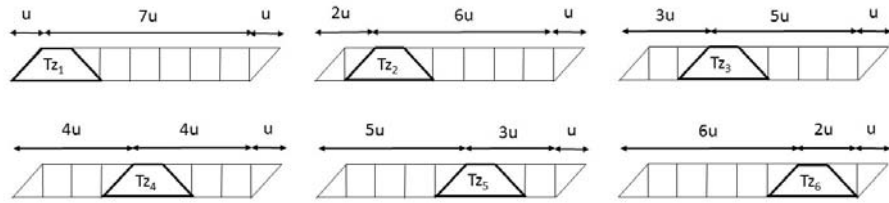


Figure 74: All possible positions of  $T_z$  in strip  $J16$

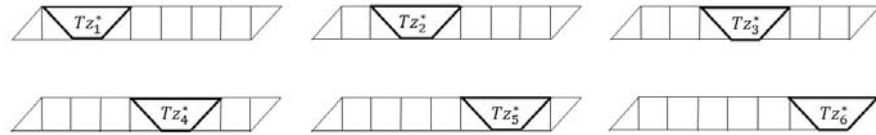


Figure 75: All possible positions of  $T_z^*$  in strip  $J16$

In this section we show all possible positions of  $T_z$  and  $T_z^*$  for  $J16$ , see Figs. 74 and 75. It should be noticed that there are some differences between the strips  $J15$  and  $J16$ . In Fig. 76 we show all possible positions for  $T_z^*$ . Moreover, the equivalence between these layouts and those with  $T_z$  are indicated. Notice that this equivalence is established by first carrying out a vertical flip and next a horizontal flip. Thus, we need not to investigate any fillings of  $J16$  with  $T_z^*$  (i.e.  $T_z$  upside down).

**Conclusion:** (12)

**For  $J16$ : we do not need to consider any layout of the strip with  $T_z^*$ , since each layout with  $T_z^*$  is equivalent to precisely one layout with  $T_z$  (see Fig. 76).**

**Consequently, we only have to find all different layouts for  $J16$  with  $T_{z_1}$  up to  $T_{z_6}$ .**

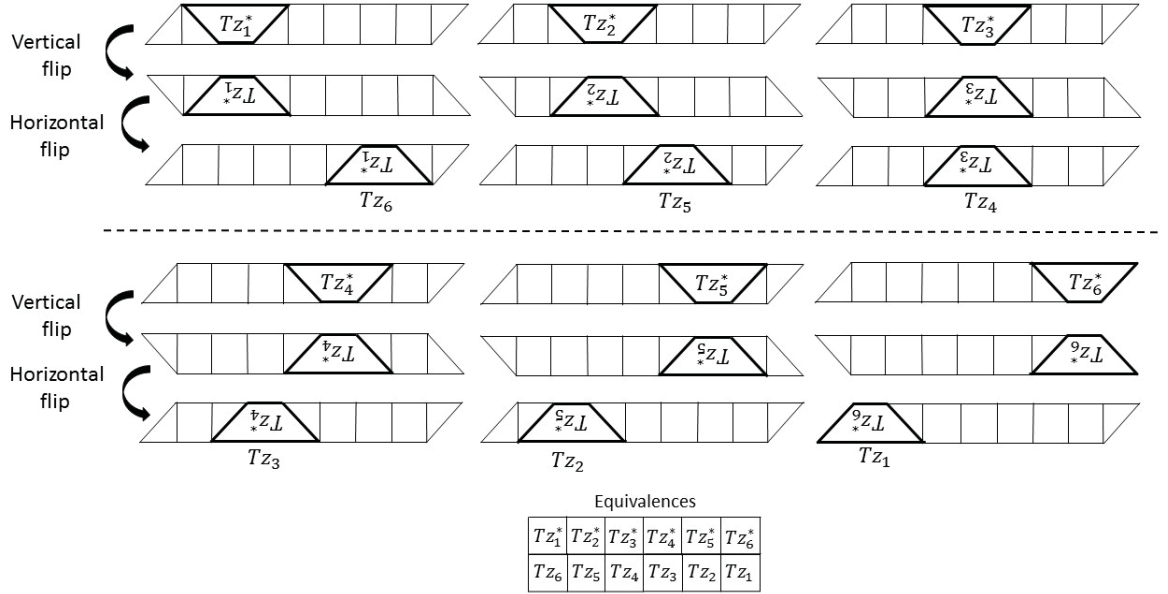


Figure 76: The equivalent layouts of  $J16$  with  $Tz$  upside down.

### A.3 Finding all different partitions for $J15$ and $J16$ by backtracking

We will demonstrate this below. Then it turns out that when using the backtracking procedure for finding the partitions for one of the two strips we also find all partitions for the other strip. So, we can say that all feasible partitions of both strip are dual.

#### A.4 The case $Tz1$

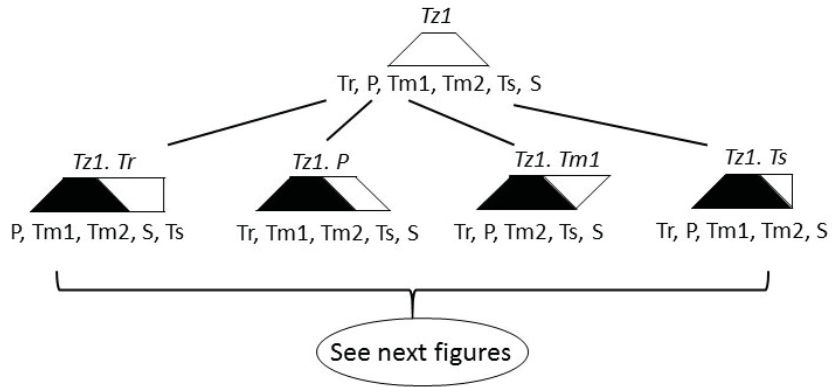


Figure 77: The tree  $Tz1$ . See also Figs. 78, 80, 83 and 90.

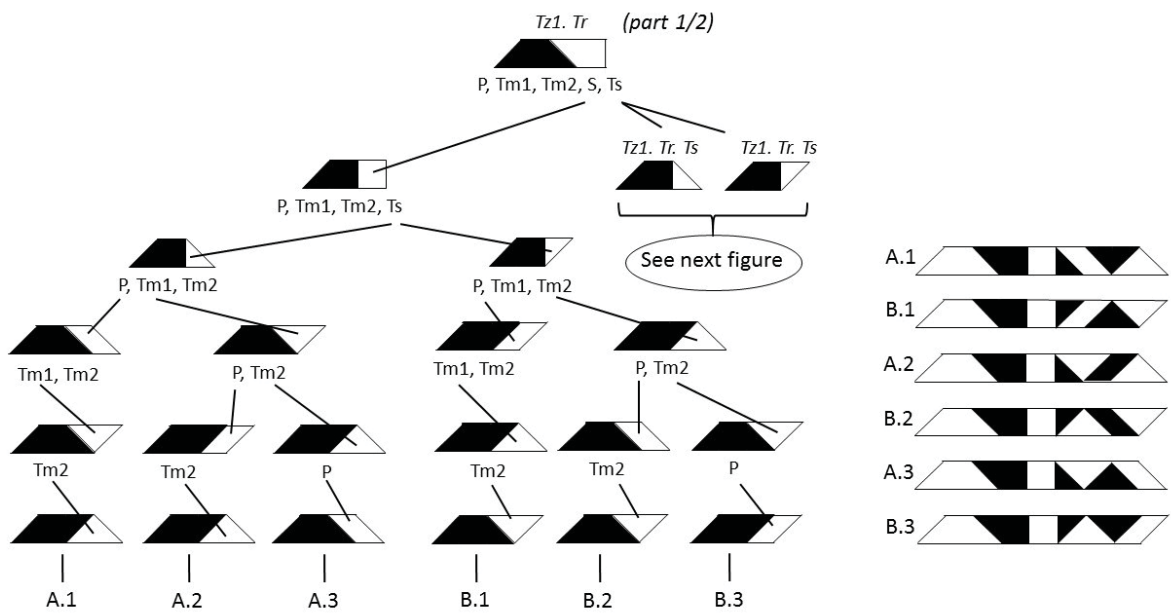


Figure 78: The tree  $Tz1.Tr$  (part 1/2). See also Fig. 79

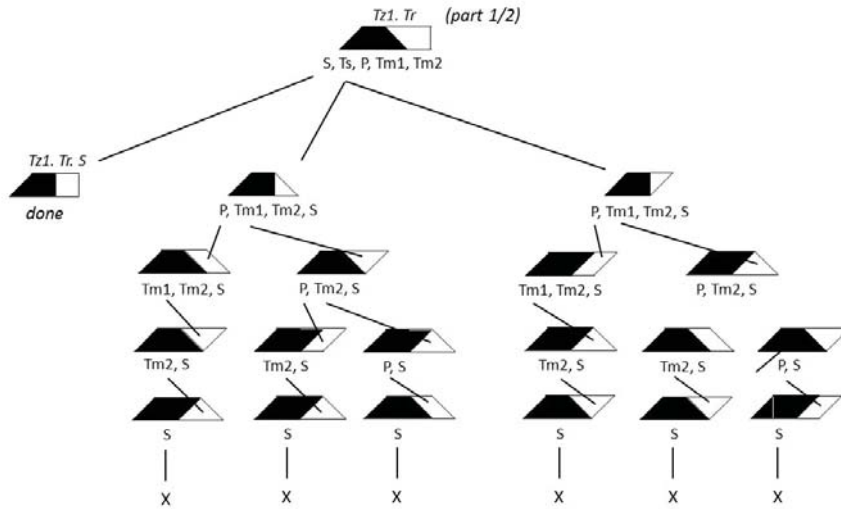


Figure 79: The tree  $Tz1.Tr$  (part 2/2).

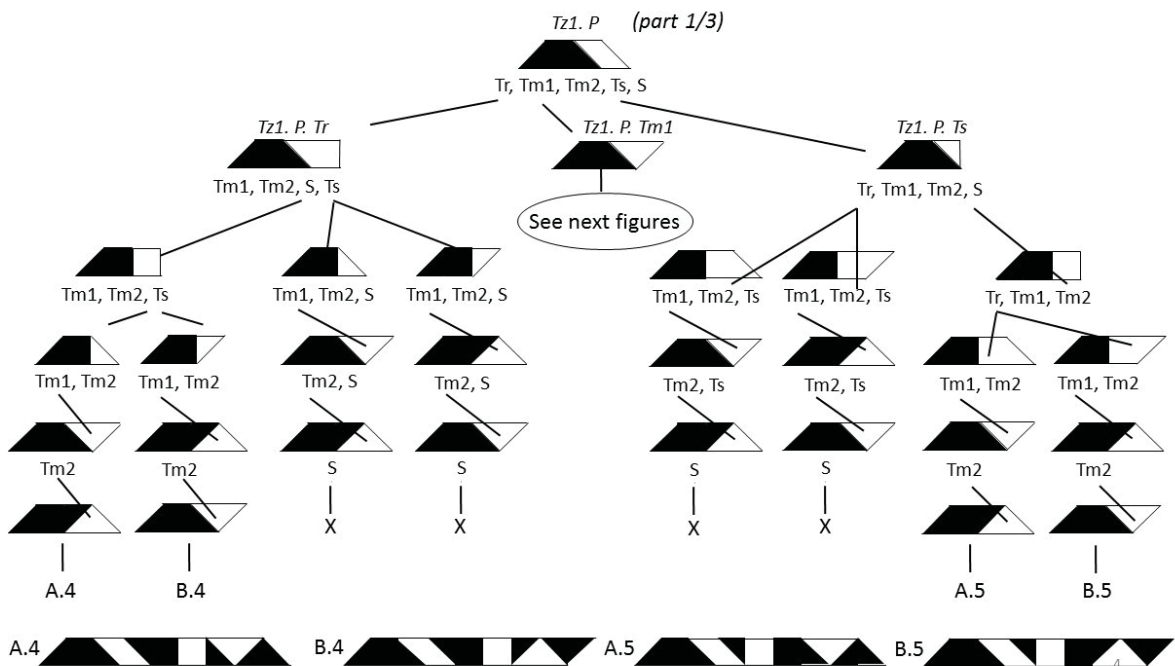


Figure 80: The tree  $Tz1.P$ . See also Figs. 81 and 82 .



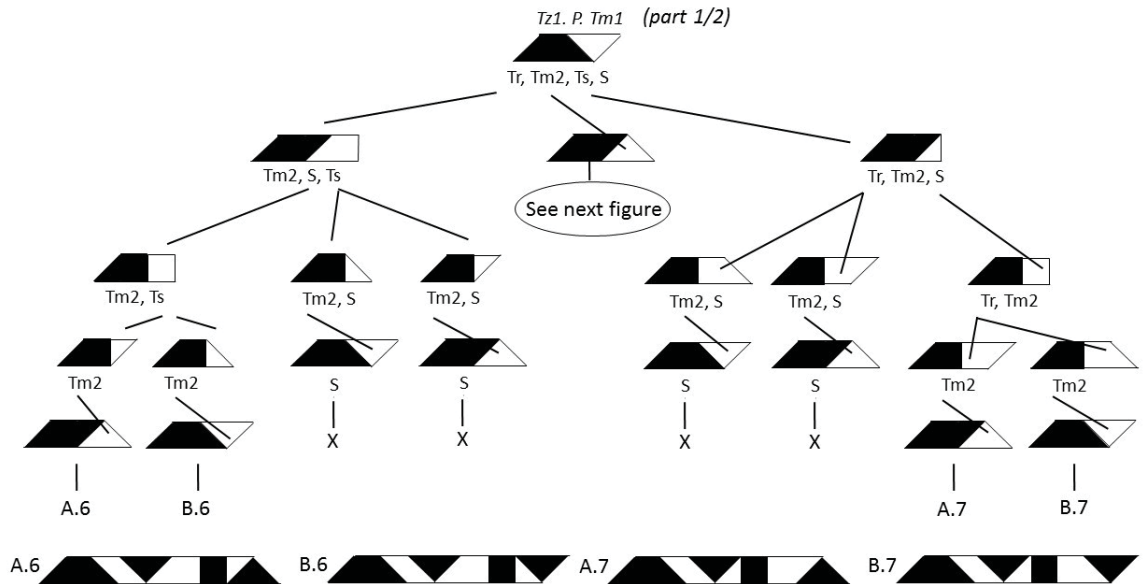


Figure 81: The tree *Tz1.P.Tm1 (part 1/2)*. See also Fig. 82.

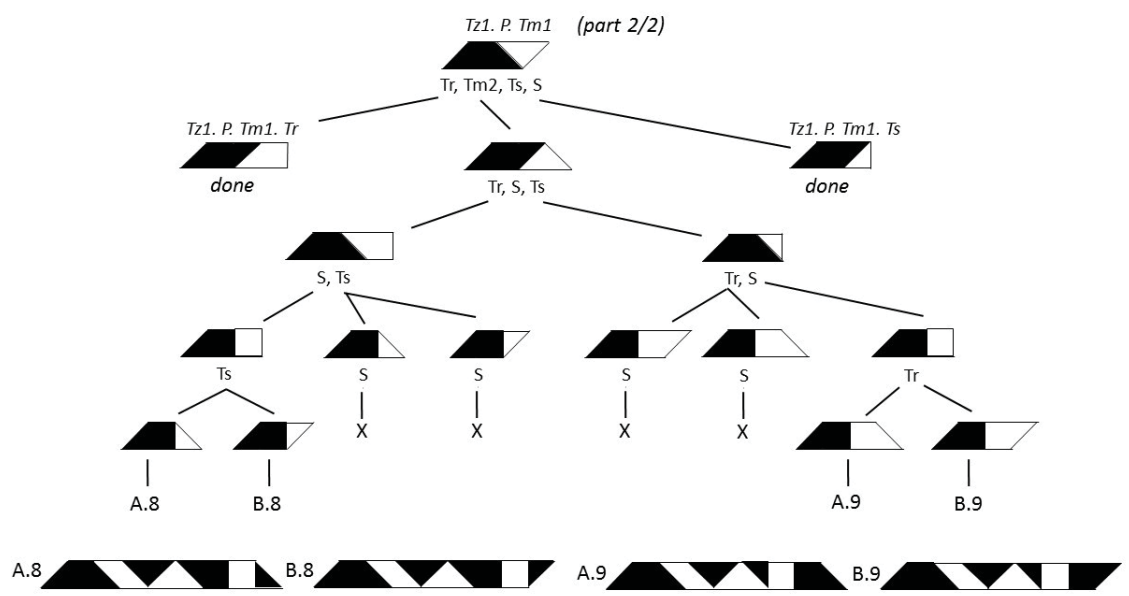


Figure 82: The tree *Tz1.P.Tm1 (part 2/2)*.

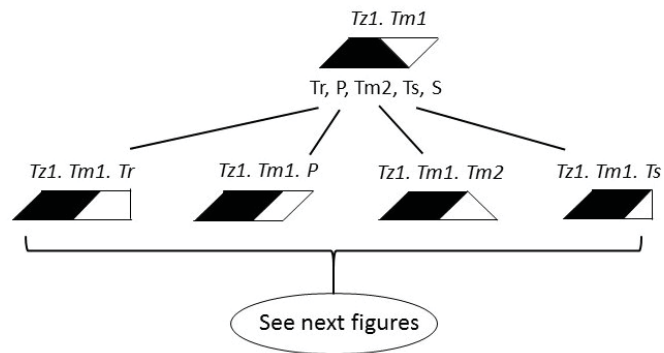


Figure 83: The tree  $Tz1.Tm1$ . See also Figs. 84, 85, 86, 87, 88 and 89.

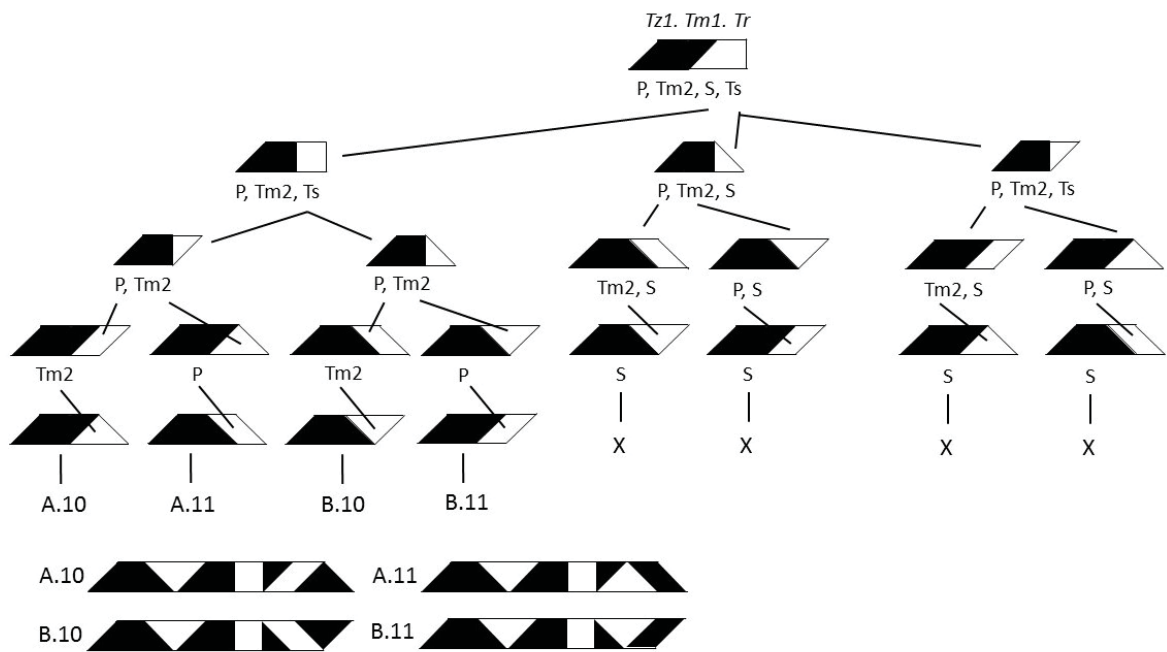


Figure 84: The tree  $Tz1.Tm1.Tr$ .

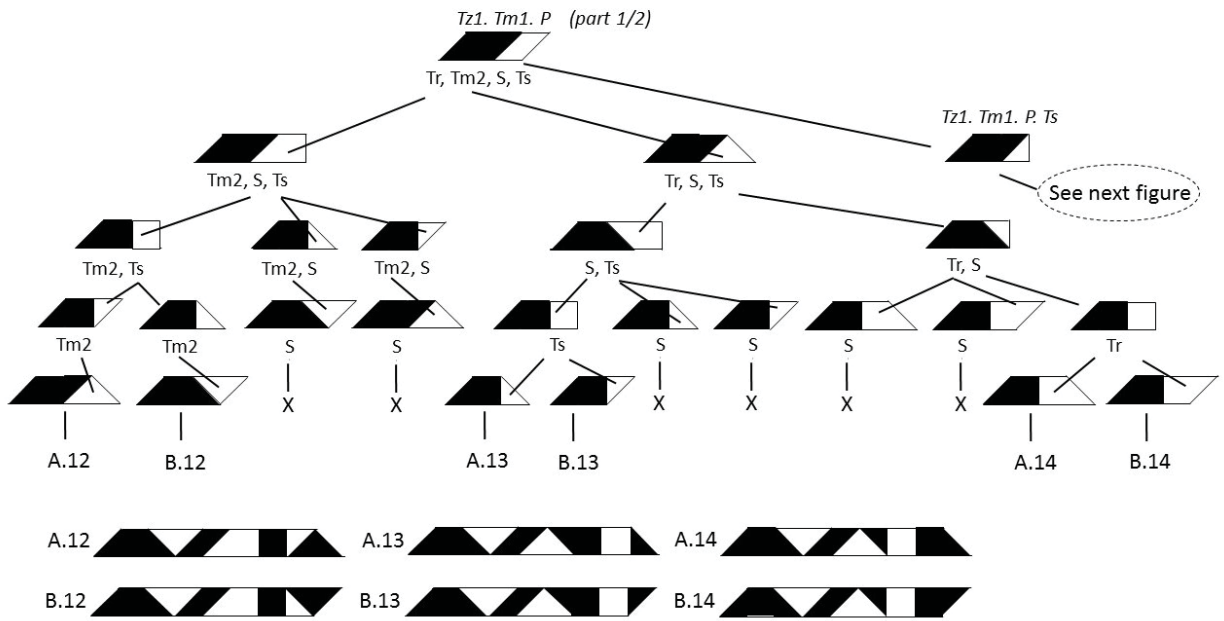


Figure 85: The tree  $Tz1.Tm1.P$  (part 1/2). See also Fig. 86.

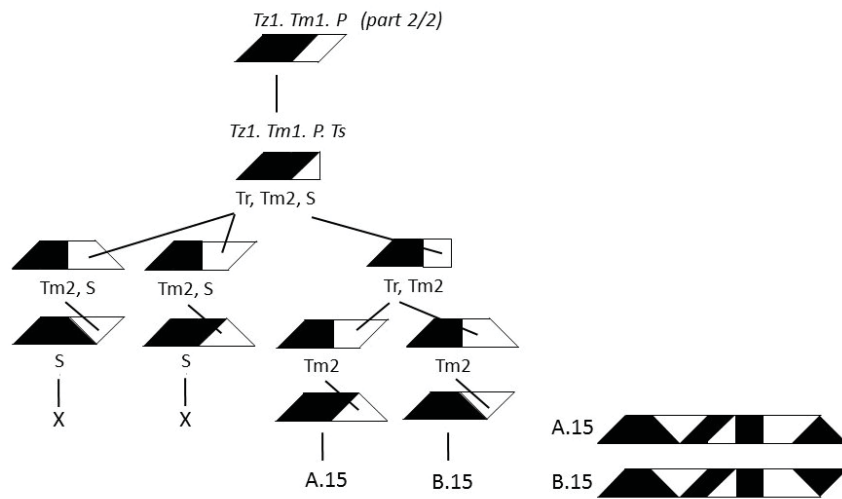


Figure 86: The tree  $Tz1.Tm1.P$  (part 2/2).

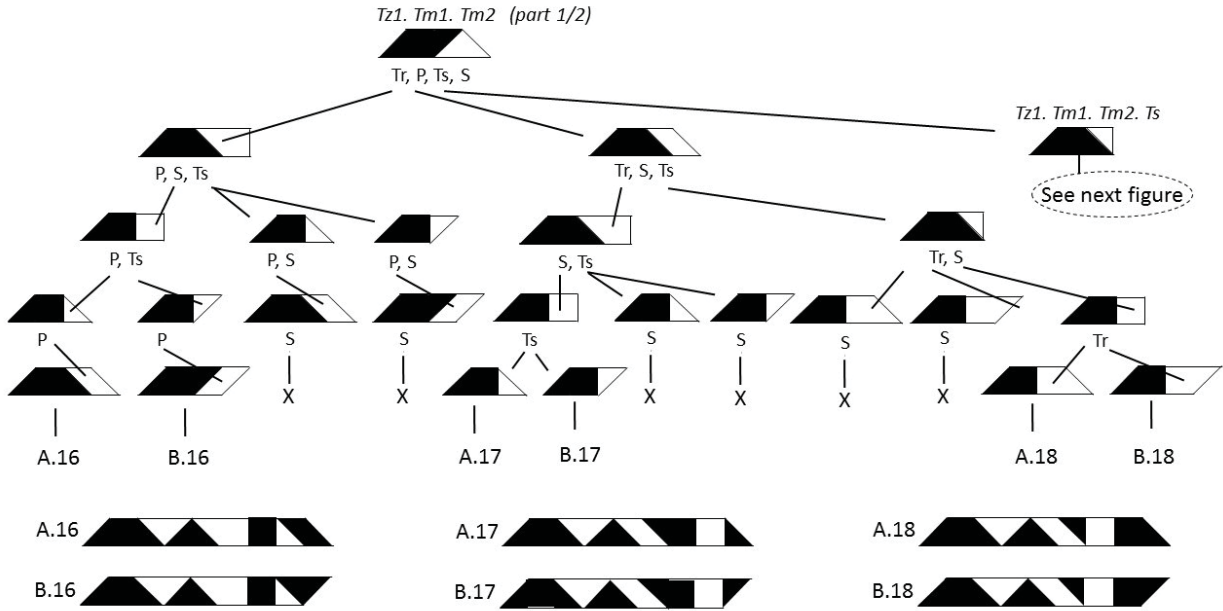


Figure 87: The  $Tz1.Tm1.Tm2$  (part 1/2). See also Fig. 88.

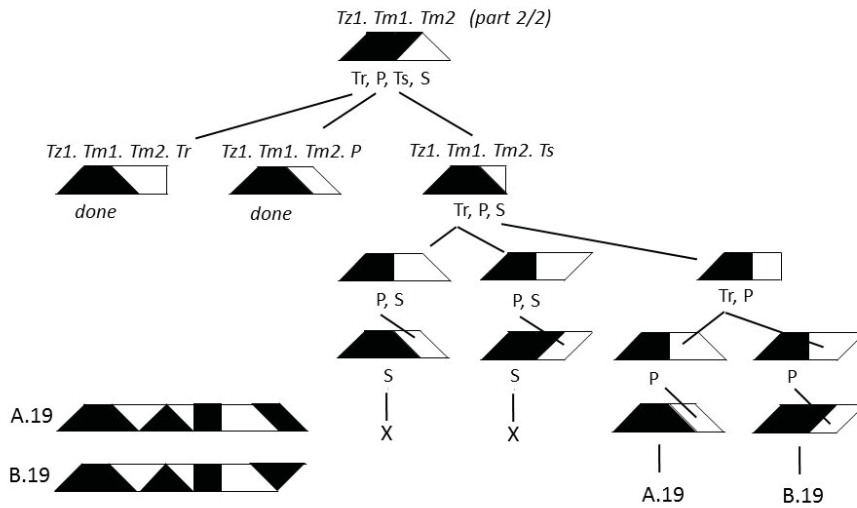


Figure 88: The tree  $Tz1.Tm1.Tm2$  (part 2/2).

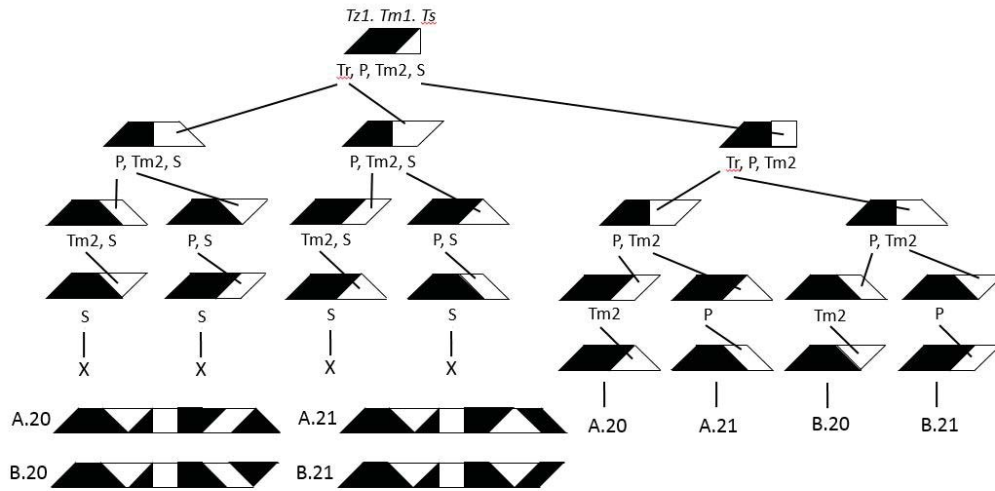


Figure 89: The tree  $Tz1.Tm1.Ts$ .

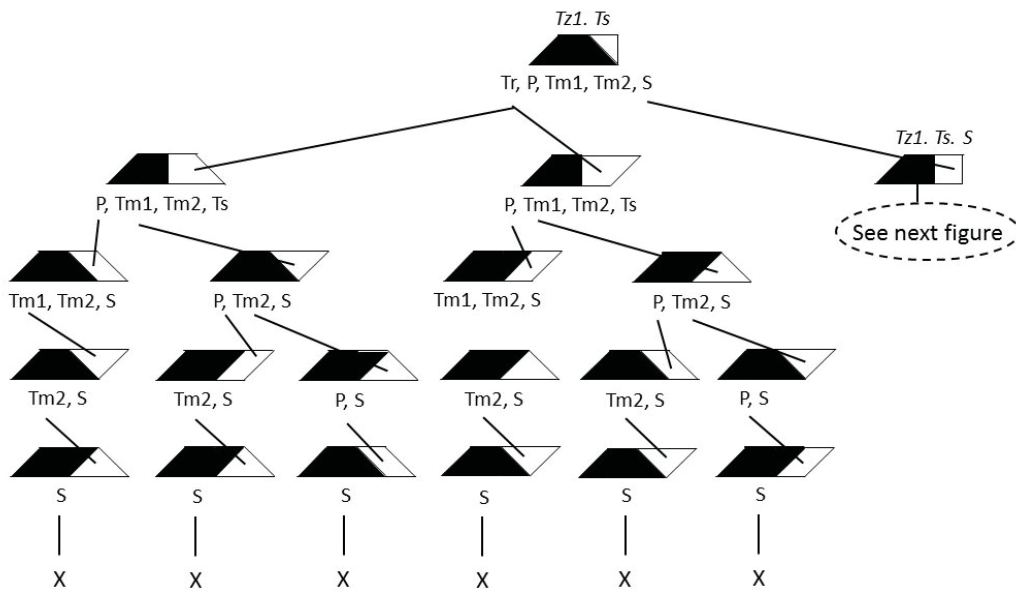


Figure 90: The tree  $Tz1.Ts$ . See also Fig. 91.

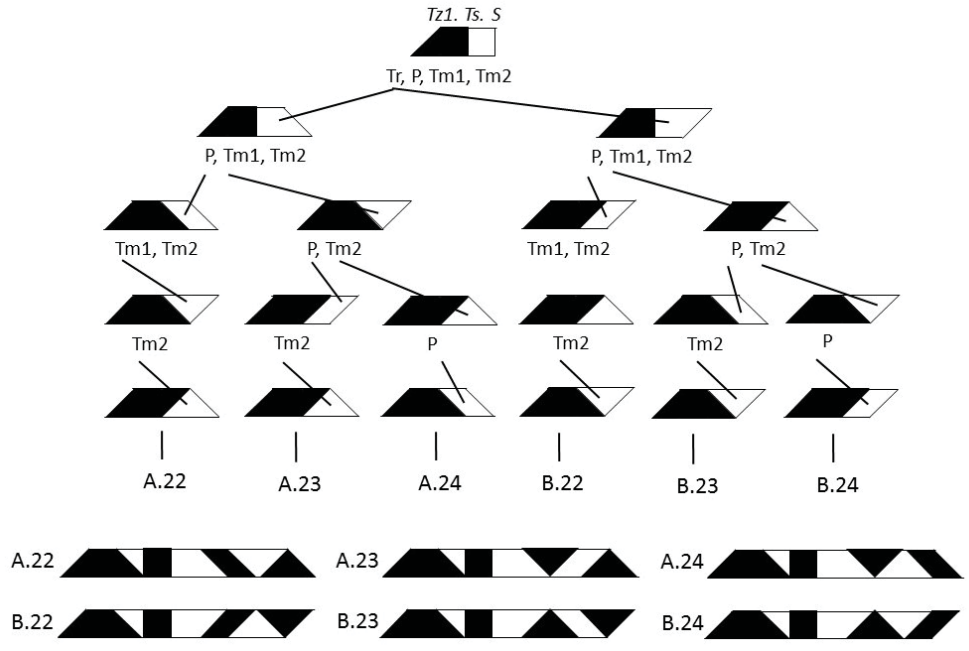


Figure 91: The tree  $Tz1.Ts.S$ .

**Conclusion:**

(13)

Now we have found all (= 24) different layouts for  $J15$  and  $J16$  with  $Tz1$ , see layouts A/B.1 up to A/B.24.

### A.5 The case $Tz2$

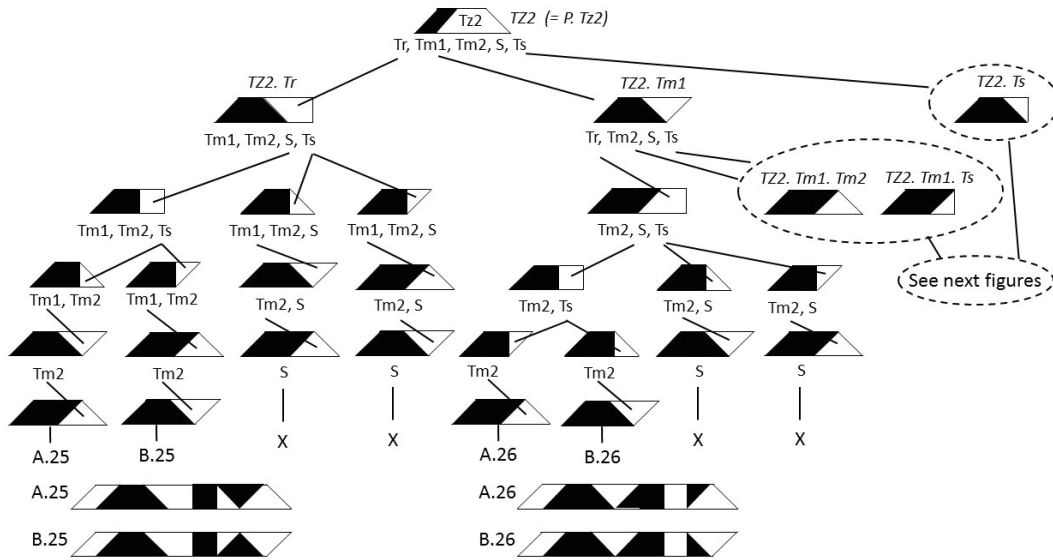


Figure 92: The tree  $J15.Tz2$ . See also Figs. 93 and 94.

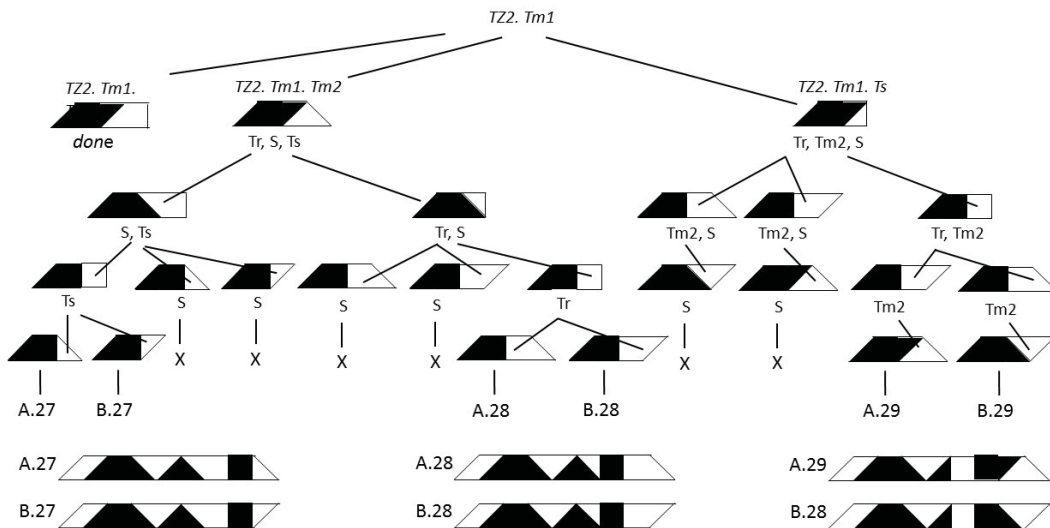


Figure 93: The tree  $J15.Tz2.Tm1$ .

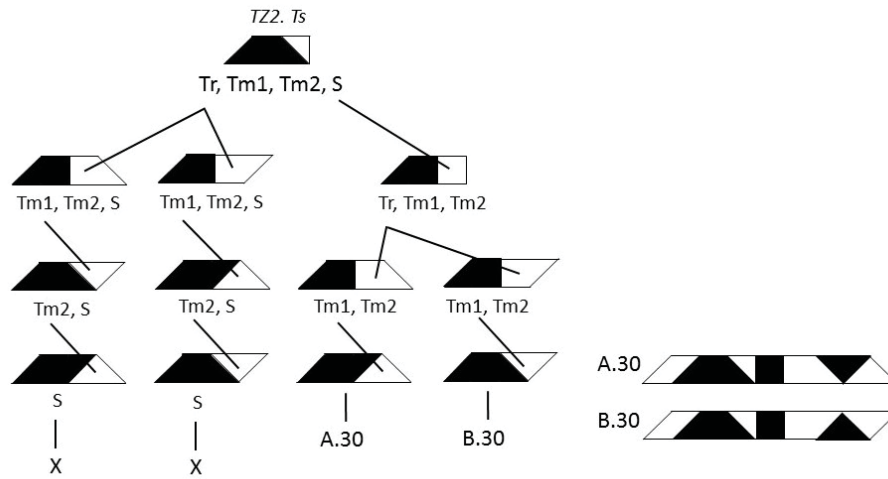


Figure 94: The tree  $J15.Tz2.Ts$ .

**Conclusion:**

(14)

Now we have found all (= 6) different layouts for  $J15$  and  $J16$  with  $Tz2$ , see layouts  $A/B.25$  up to  $A/B.30$ .



## A.6 The case $Tz3$

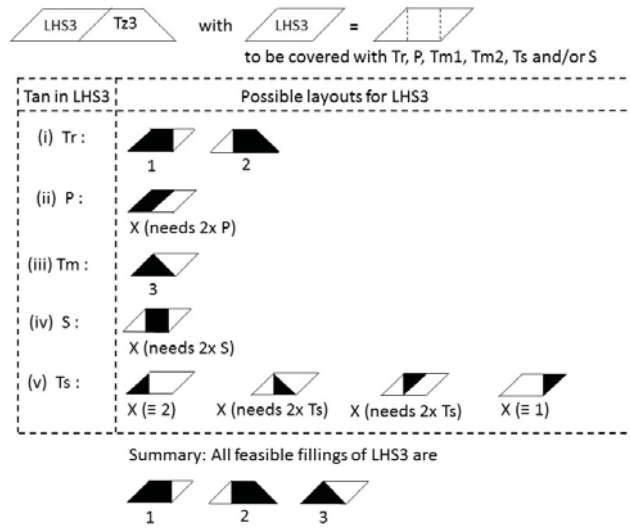


Figure 95: The possible fillings for LHS3 for the strips  $J15$  and  $J16$ .

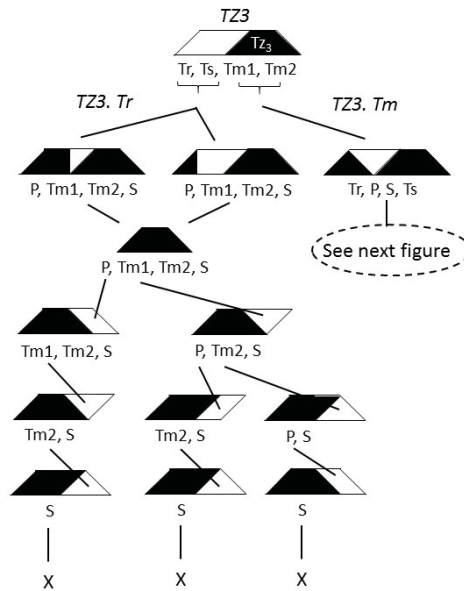


Figure 96: The tree  $Tz3.Tr$ . See also Fig. 97.

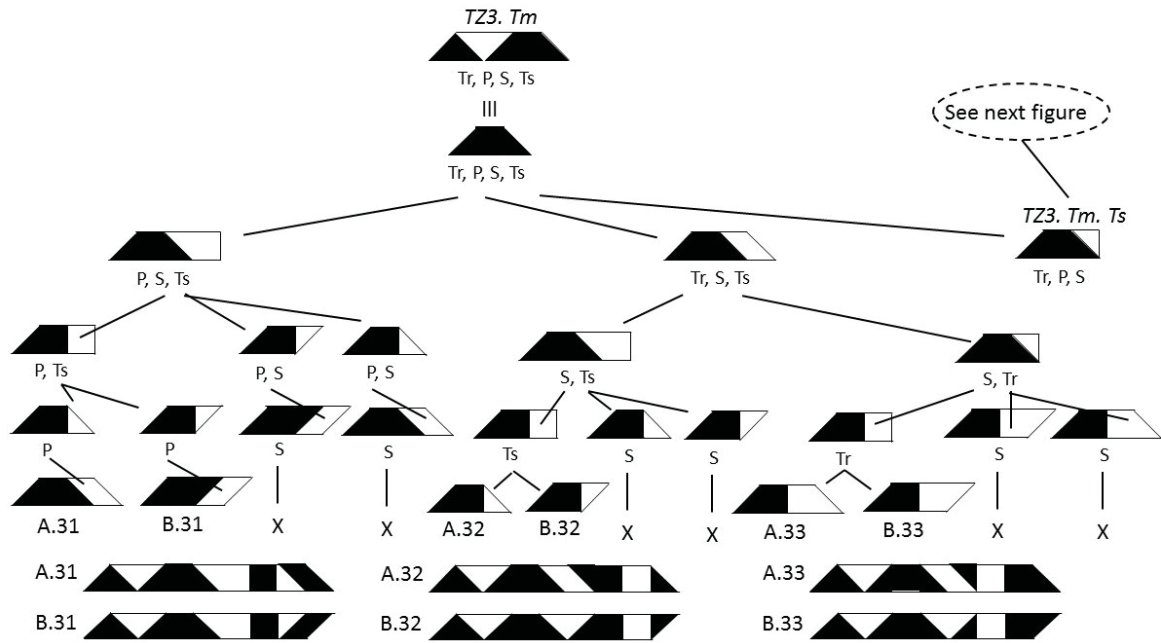


Figure 97: The tree  $Tz3.Tm$ . See also Fig. 98.

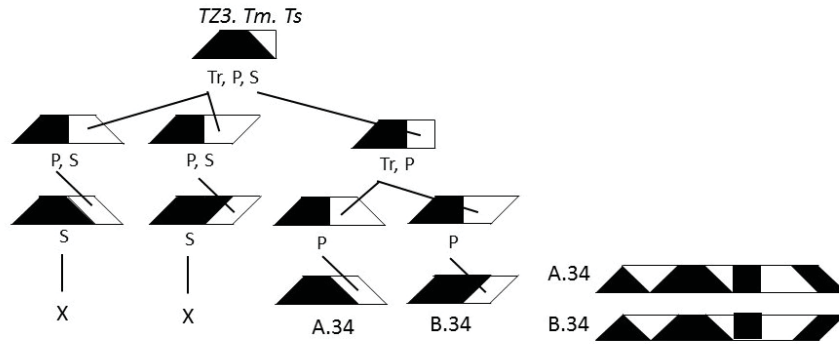


Figure 98: The tree  $Tz3.Tm.Ts$  for the strips  $J15$  and  $J16$ .

**Conclusion:**

Now we have found all (= 4) different layouts for  $J15$  and  $J16$  with  $Tz3$ , see layouts A/B.31 up to A/B.34.

(15)

## A.7 The case $Tz4$

### A.7.1 Finding all possible fillings for LHS4 with one single tan inside

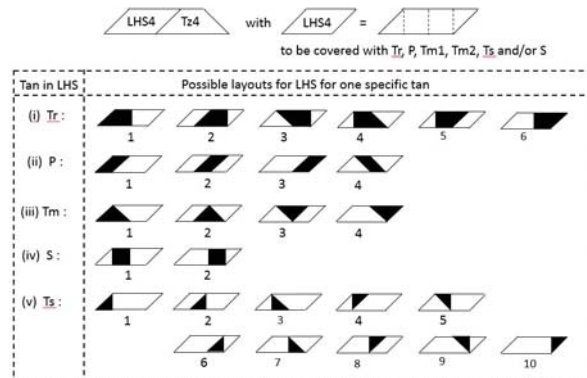
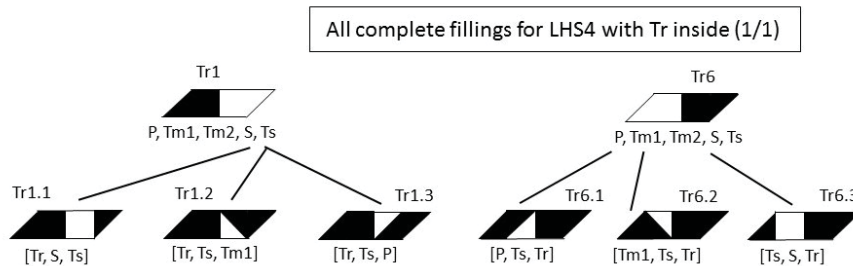


Figure 99: The possible fillings for LHS4 with one single tan inside.

### A.7.2 Finding all complete fillings for LHS4

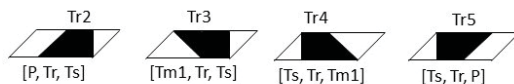


Notation: [a, b, c] = the composition of LHS with the tans a, b and c.

Conclusion:

We have in total 6 fillings for the tans Tr1 and Tr6.

Furthermore, we have one unique filling for each of the 4 tans Tr2 up to Tr5 (see previous figure and below).



Thus, LHS4 with Tr inside has 10 different fillings in total.

Figure 100: All fillings for LHS4 with Tr inside.

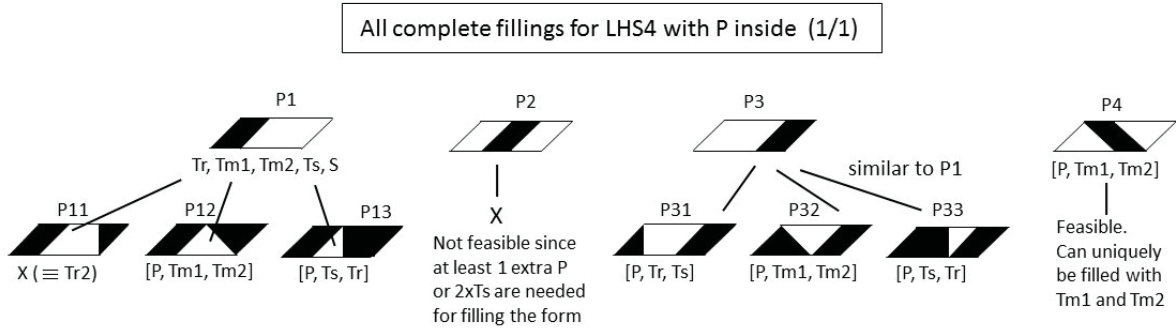


Figure 101: All fillings for LHS4 with P inside.

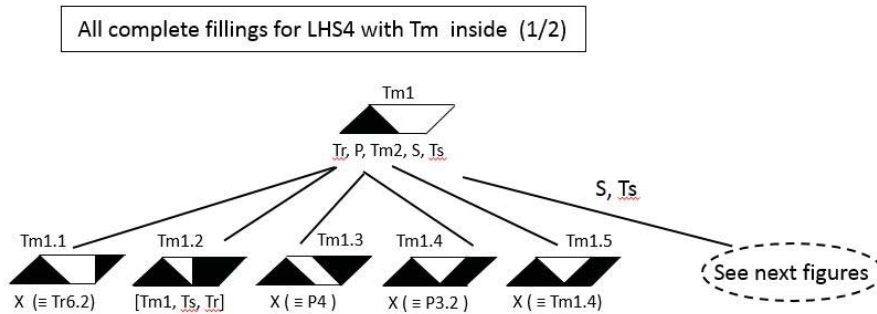
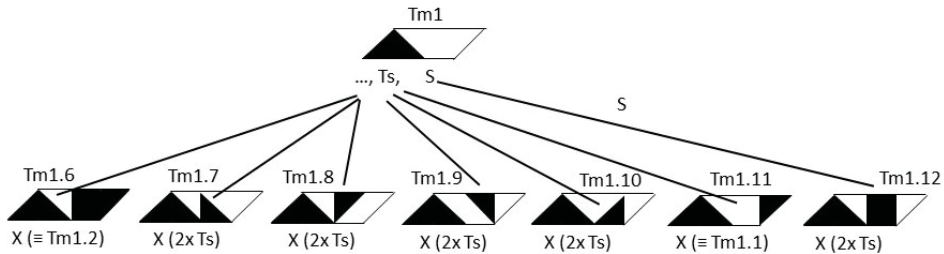


Figure 102: All fillings for LHS4 with Tm inside (part 1/2). See also Figs. 104 and 105.

All complete fillings for LHS4 with Tm inside (2/2)



Conclusion:

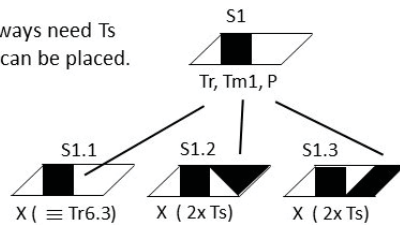
Adding Ts or S to LHS4 with Tm1 inside does not result into a new filling. So,

LHS4 with Tm1 inside has one feasible filling:

Figure 103: All fillings for LHS4 with Tm inside (part 2/2).

All complete fillings for LHS4 with S inside (1/1)

In S1 and S2 we always need Ts and at most 1xTm can be placed.



X

Not feasible since S2 ≡ S1 by reflection in vertical line at left bottom corner of S2.

Conclusion:

LHS4 with S inside has only one feasible filling, shown earlier in Tr6.3.

Figure 104: All fillings for LHS4 with S inside.

All complete fillings for LHS4 with Ts inside (1/1)

We have established all complete fillings for LHS4 with the tans Tr, P, Tm, and S.

So, we need not to investigate fillings for LHS4 with Ts inside (indeed, if we would start with LHS4 with Ts inside, then at least one of the tans Tr, P, Tm or S is needed for completing this LHS4, but all these tans have already been studied).

However, notice that we do have fillings for LHS4 with Ts inside.

Figure 105: All fillings for LHS4 with Ts inside for the strips  $J15$  and  $J16$ .

### A.7.3 Finding all complete layouts of $J15$ and $J16$ with $Tz4$ and LHS4

(i) LHS4 with P inside (1/2)

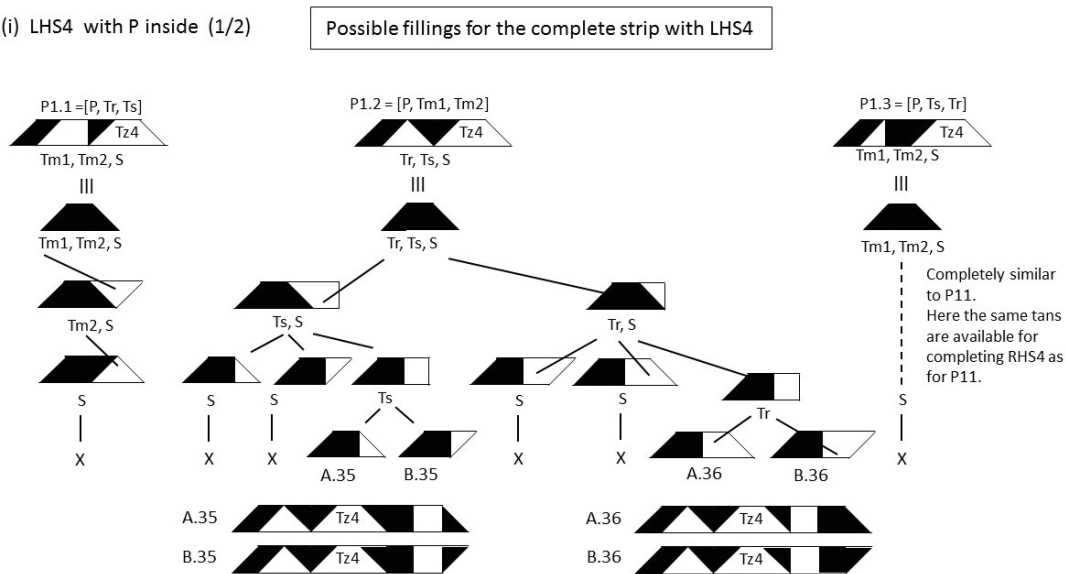


Figure 106: All fillings for LHS4 with P inside (part 1/2).

(i) LHS4 with P inside (2/2)

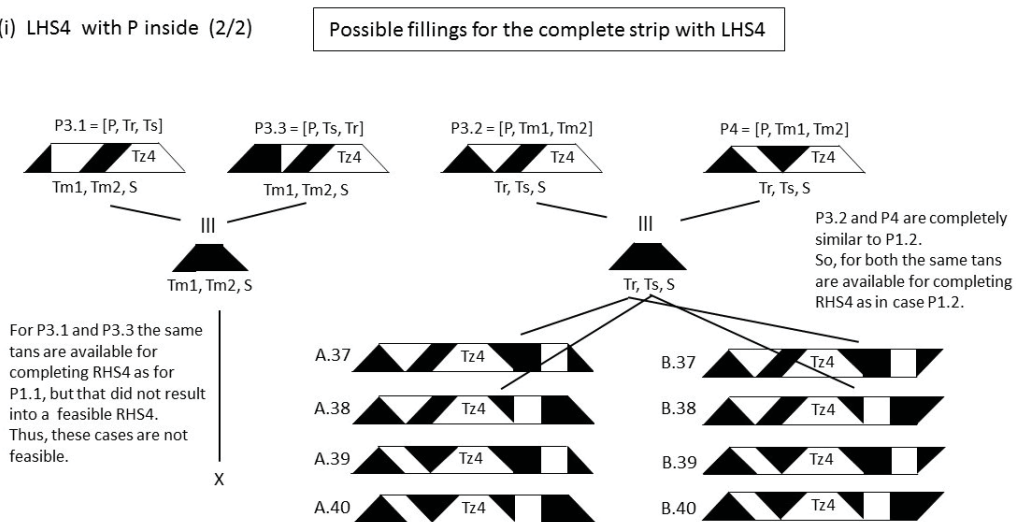


Figure 107: All fillings for LHS4 with P inside (part 2/2).

(ii) LHS4 with Tr inside (part 1/3)

Possible fillings for the complete strip with LHS4

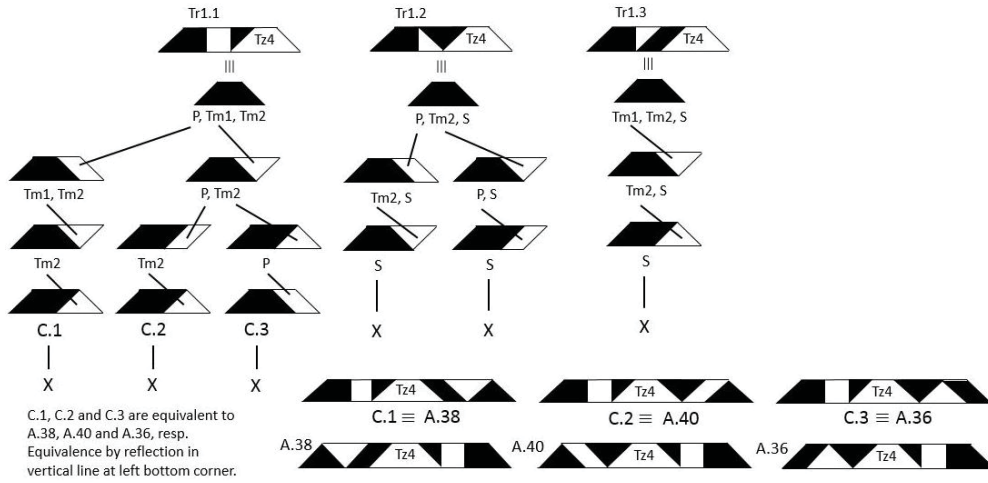


Figure 108: All fillings for LHS4 with Tr inside (part 1/3): No new layouts found.

(ii) LHS4 with Tr inside (part 2/3)

Possible fillings for the complete strip with LHS4

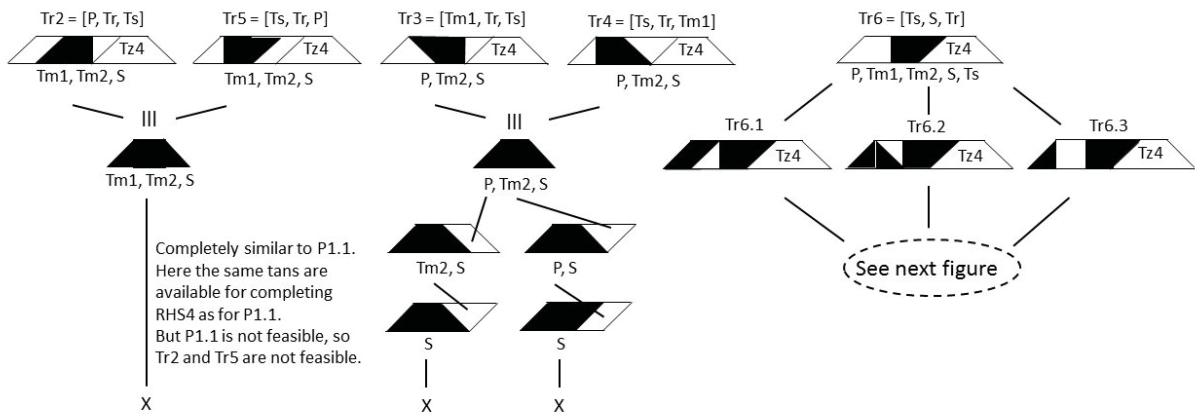


Figure 109: All fillings for LHS4 with Tr inside (part 2/3). See also Fig. 110.



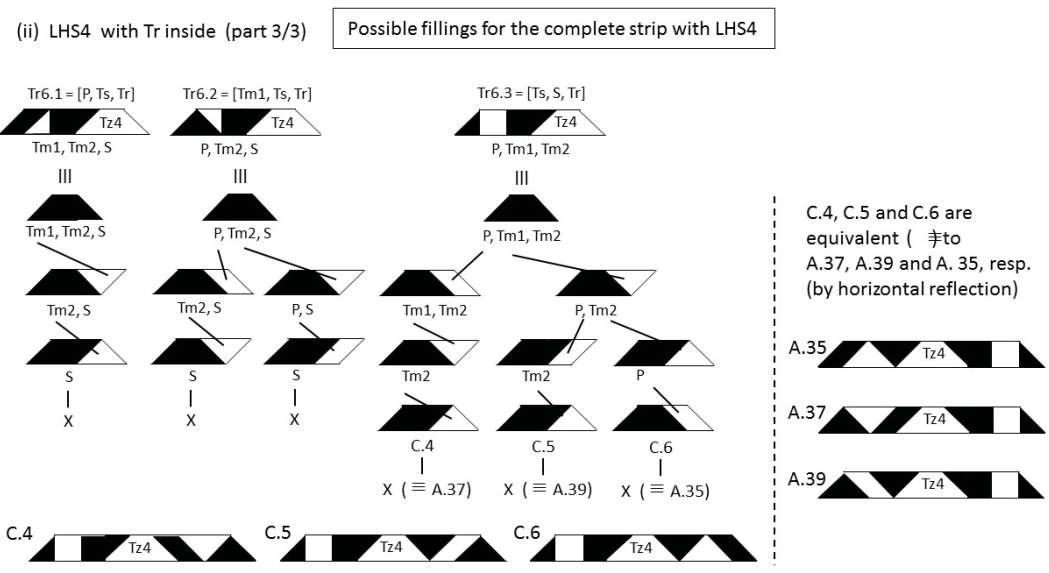


Figure 110: All fillings for LHS4 with Tr (part 3/3) for  $J15$  and  $J16$ : No new layouts found.

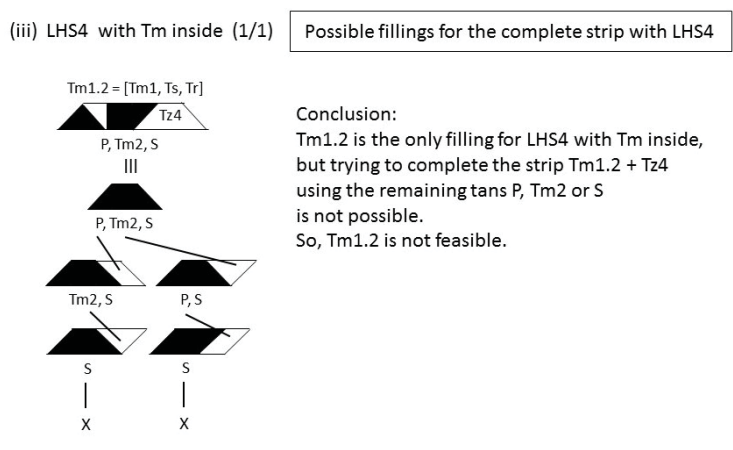



Figure 111: All fillings for LHS4 with Tm inside for the strips  $J15$  and  $J16$ .

**Conclusion:** (16)  
Now we have found all (= 6) different layouts for  $J15$  and  $J16$  with  $Tz4$ ,  
see layouts A/B.35 up to A/B.40.

Summary

Up to here we have investigated the strips with the trapeziums  $Tz_1$ ,  $Tz_2$ ,  $Tz_3$  or  $Tz_4$  inside.

Recalling Conclusion 3 in section 3.3.1 we can conclude that these cases

with  $Tz$  having the form  are complete.

Next we have to investigate the cases with  $Tz$  **upside down** in the strip, i.e.,

then  $Tz$  has the form .

This will be discussed in the next section.

Figure 112: Summary sofar for the strips  $J15$  and  $J16$ .

**A.8 Finding all layouts for the strips  $J15$  and  $J16$  with  $Tz$  upside down**

For convenience, we recall some results presented in sections A.1 and A.2. Below we will use the notation  $Ty_k$  instead of  $Tz_k^*$  for  $Tz$  upside down.

We have

- We do not need to study the cases  $J16$  with  $Ty$  since each of these cases are equivalent to one case of  $J15$ . See Conclusion 12, section A.1;
- The strip  $J15$  has 5 possible positions for  $Ty$ . See Fig. 17;
- We only need to study the cases for  $Ty_1$  up to  $Ty_3$ . Recall Conclusion 11 in section A.1;
- The case  $Ty_1$  is studied in Figs. 113 up to 118;
- The case  $Ty_2$  is studied in Figs. 119 up to 121;
- The case  $Ty_3$  is investigated in the figures after Fig. 121.

**Notational conventions**

In the next figures we will denote the layouts found for the trapezium-shaped strip  $J15$  by  $A.k$  and the corresponding parallelogram-shaped strip  $J16$  by  $B.k$ , where  $k$  is an integer  $\geq 1$ .

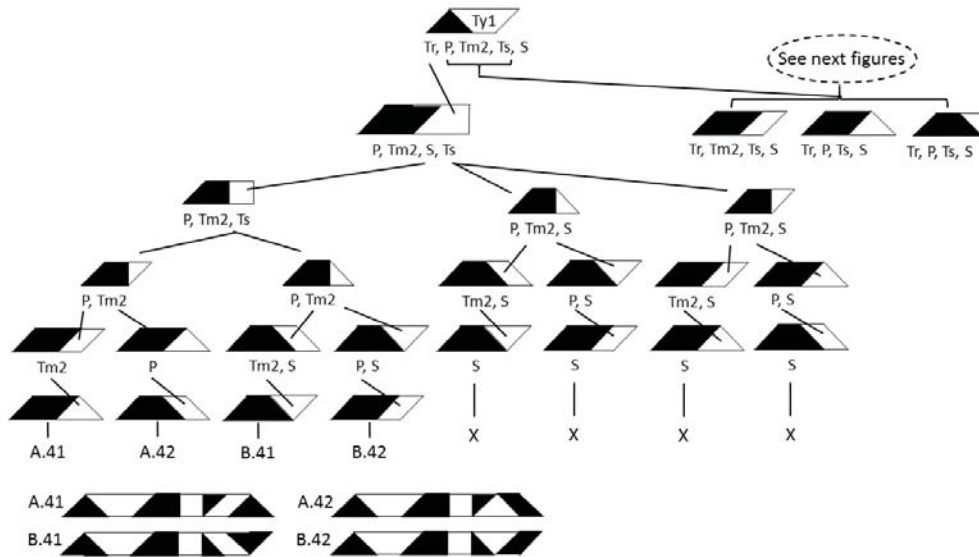


Figure 113: The tree *Ty1* with layouts 41 and 42. See also Figs. 114, 116 and 118.

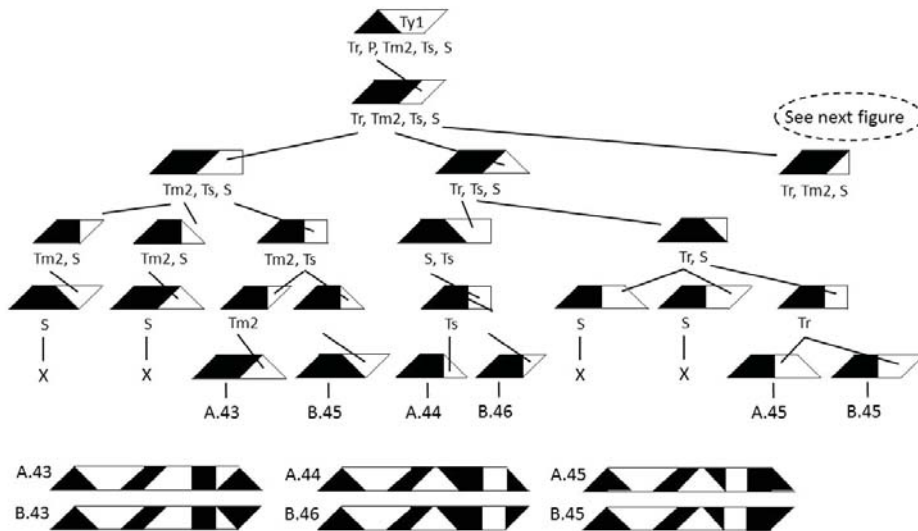


Figure 114: The tree *Ty1* with layouts 43 up to 45. See also Fig. 115 .

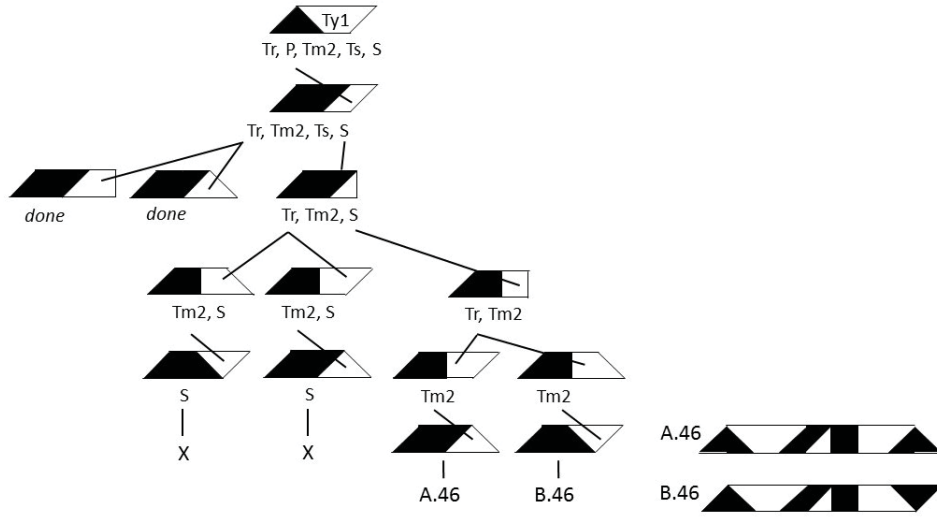


Figure 115: The tree *Ty1* with layout 46 for the strips *J15* and *J16*.

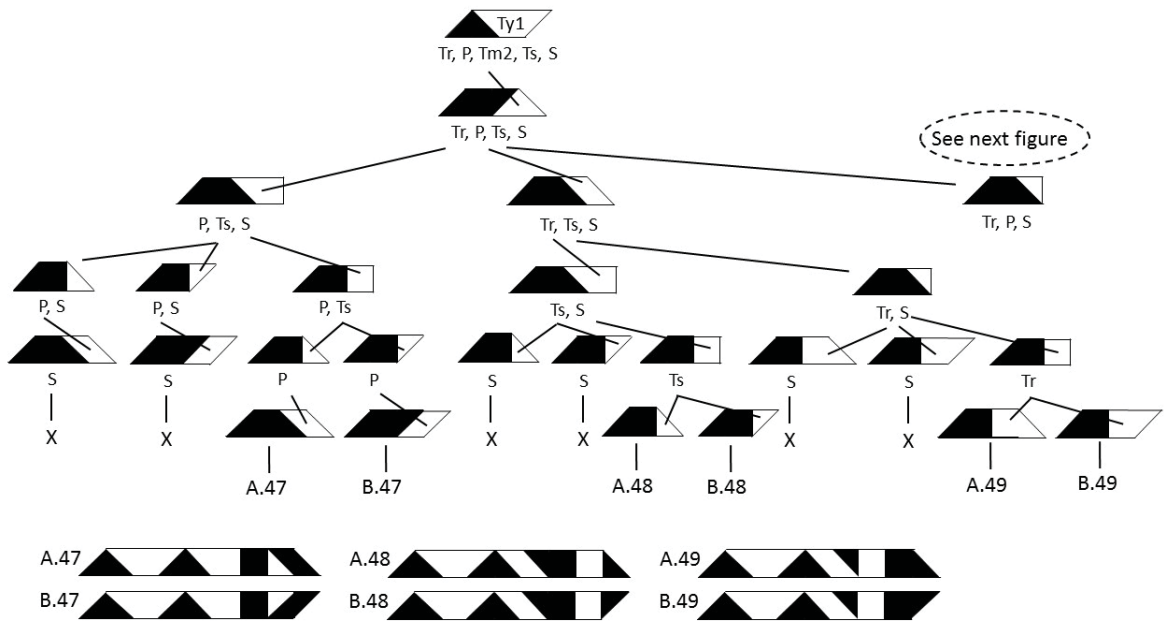


Figure 116: The tree *Ty1* with layouts 47 up to 49. See also Fig. 117.

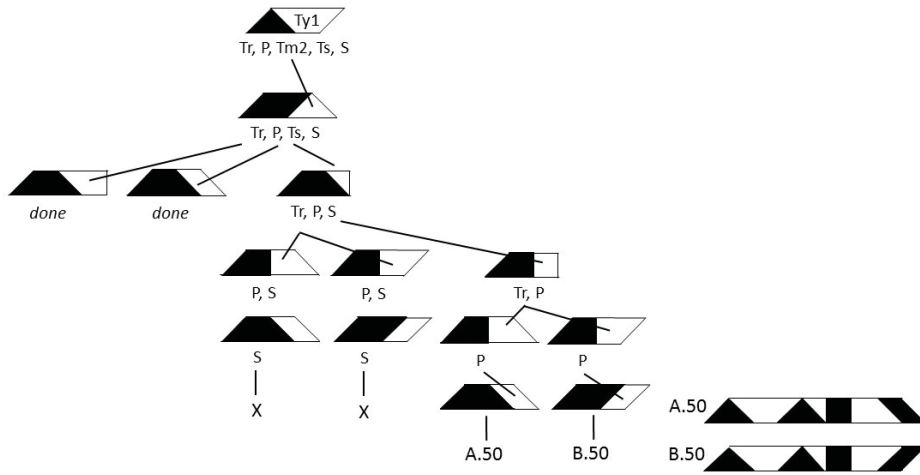


Figure 117: The tree  $Ty_1$  with layout 50 for the strips  $J_{15}$  and  $J_{16}$ .

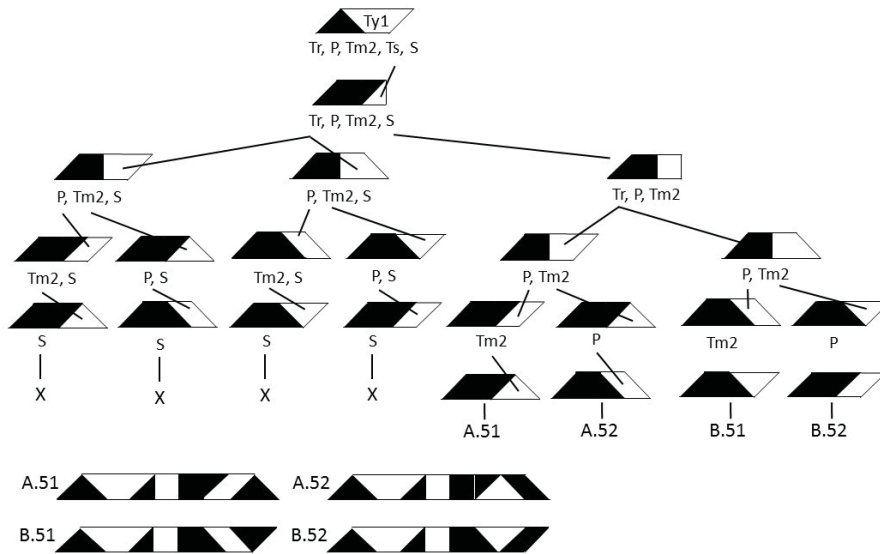


Figure 118: The tree  $Ty_1$  with layouts 51 up to 52 for the strips  $J_{15}$  and  $J_{16}$ .

**Conclusion:**

We have found all different layouts for  $J_{15}$  and  $J_{16}$  with  $Ty_1$  inside, see layouts A/B.41 up to A/B.52.

(17)

### A.9 Investigating the possible layouts for $J15$ and $J16$ with $Ty2$



Tan in LHS	Possible layouts for $LHS_2$ for one specific tan
(i) $Tr$ :	1 = $[Tr, Ts]$ 2 = $[Ts, Tr]$
(ii) $P$ :	3 = $[P, Tm1]$ 4 = $[Tm1, P]$
(iii) $Tm$ :	Not feasible: $Tm+Tr$ (see 1, 2), $Tm+S$ , $Tm+Ts$ (2xTs needed), $Tm + P$ (see 3, 4)
(iv) $S$ :	Not feasible: 2xTs needed
(v) $Ts$ :	Layouts with $Ts$ are already included in those above

Conclusion: We have 4 different fillings for  $LHS_2$  associated to  $Ty_2$

Remark: By  $LHS_{1,2}$  we will denote the layout 1 or 2 with  $Tr$  and  $Ts$ , by  $LHS_{3,4}$  the layout 3 or 4 with  $P$  and  $Tm1$

Figure 119: The possible layouts for  $LHS_2$  for the strips  $J15$  and  $J16$ .

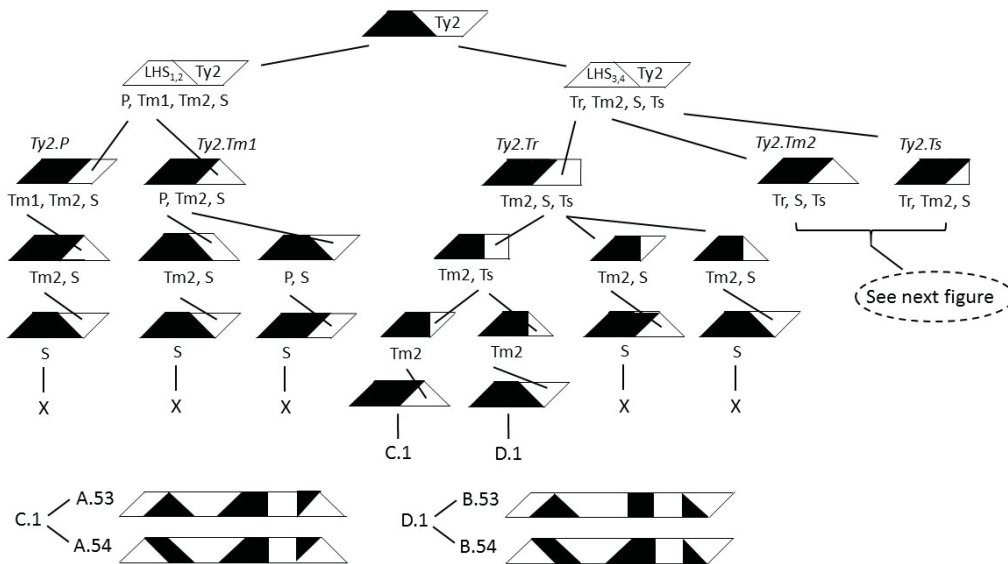


Figure 120: The tree  $Ty_2$  with layouts 53 up to 54 for the strips  $J15$  and  $J16$ . See also Fig. 121.

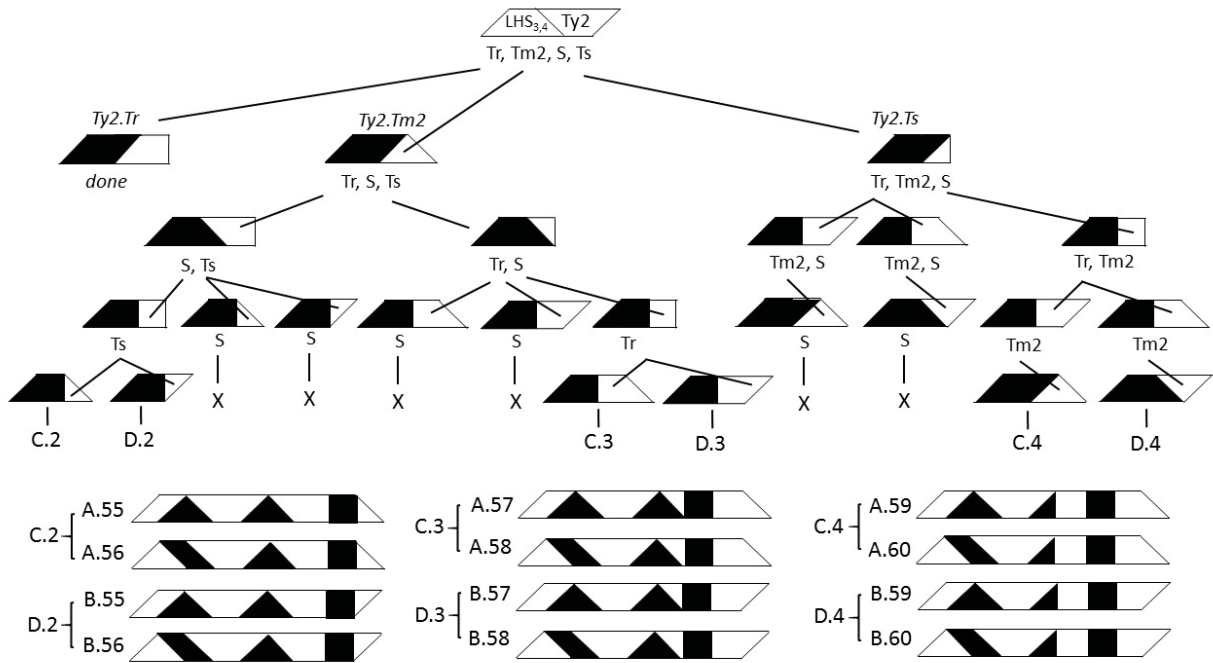


Figure 121: The tree  $Ty_2$  with layouts 55 up to 60 for the strips  $J_{15}$  and  $J_{16}$ .

**Conclusion:** (18)

We have found all different layouts for  $J_{15}$  and  $J_{16}$  with  $Ty_2$  inside, see layouts A/B.53 up to A/B.60.

**Conclusion:** (19)

So, up to here we have found 60 different layouts for  $J_{15}$  and  $J_{16}$ , with  $Tz_1$  up to  $Tz_4$ ,  $Ty_1$  and  $Ty_2$  inside.

### A.10 Investigating the possible layouts for $J15$ and $J16$ with $Ty3$

In this section we will prove the following statement

**Statement:** (20)

**There are no layouts for  $J15$  with  $Ty3$  that are different from the 60 layouts found sofar.**

For convenience, we recall the global layout for  $J15$  with  $Ty3$  in Fig. 122.

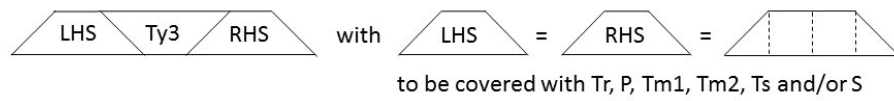


Figure 122: Global layout for  $J15$  with  $Ty3$

Clearly, tan  $Tr$  is either in LHS or in RHS. We will investigate both cases below.

#### A.10.1 The layouts with $Ty3$ and $Tr$ in LHS

In Fig. 123 all possible fillings in LHS with  $Tr$  inside are shown.

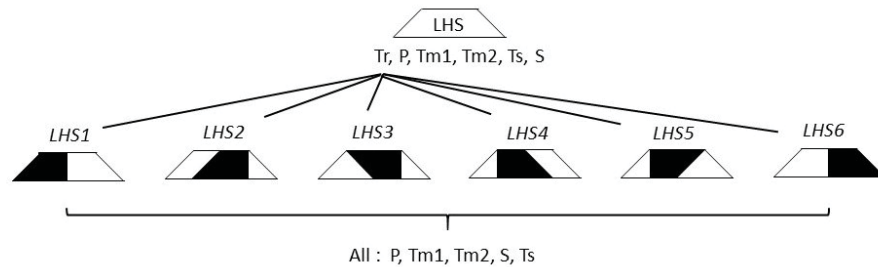


Figure 123:  $J15$  with  $Ty3$ : all possible fillings of LHS (with  $Tr$  inside).

We will now prove that all fillings shown in Fig. 123 are not feasible.

It can easily be seen from Fig. 123 that there is precisely one filling for each of LHS2, LHS3, LHS4 and LHS5, given the position of  $Tr$ . Furthermore, LHS2 and LHS4 consist of the same set of tans  $Tr, P, Ts$ . Hence, the corresponding RHS2 and RHS4 must be filled with  $Tm1, Tm2, S$ . However, this is not possible, see Fig. 124. So, we have

**Conclusion:** (21)

**LHS2 and LHS4 are not feasible.**



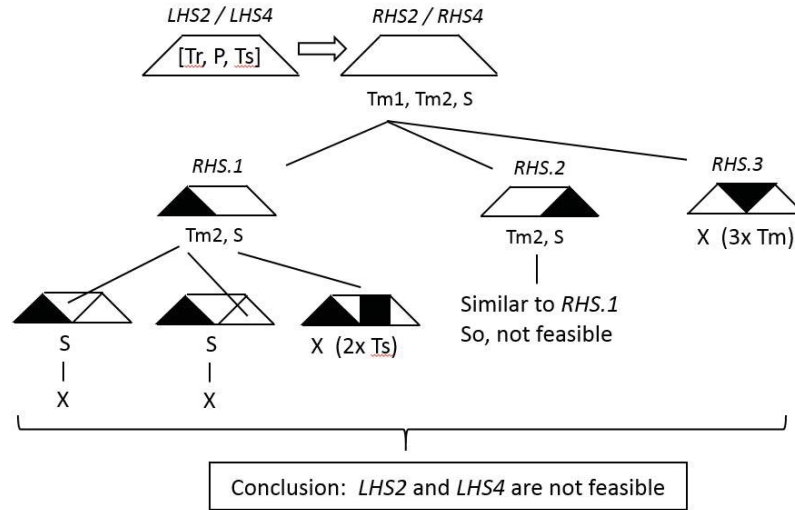


Figure 124:  $J15$  with  $Ty3$  and  $LHS2$  or  $LHS4$  is not feasible.

Notice that  $LHS3$  and  $LHS5$  consist of the same set of tans  $Tr, Tm1, Ts$ . Hence, the corresponding  $RHS3$  and  $RHS5$  must be filled with  $P, Tm2, S$ . However, this is not possible, see Fig. 125. So, we have

**Conclusion:** (22)  
 **$LHS3$  and  $LHS5$  are not feasible.**

Now consider  $LHS6$ . It is easily seen that we have

**Conclusion:** (23)  
 **$LHS6$  is equivalent to  $LHS1$  by horizontal reflection.**

So, we only need to investigate all fillings for  $LHS1$ . See Fig. 126.

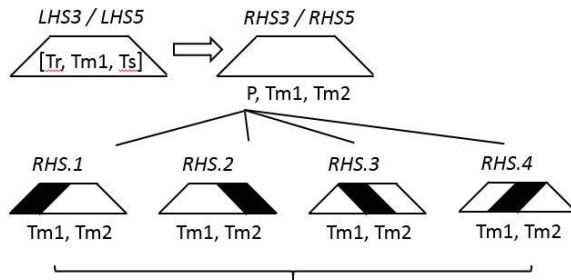
It is clear from this figure that  $LHS1$  has only 3 different feasible fillings ( $LHS1.P$ ,  $LHS1.Tm1$  and  $LHS1.S$ ).

Indeed, we see from Fig. 126 that we have 4 different fillings of  $LHS1$  with  $Ts$ , being  $LHS1.Ts1$  up to  $LHS1.Ts4$ . However, in  $LHS1.Ts1$  and  $LHS1.Ts2$  we need 2 more  $Ts$  for a full filling, but this is not possible. In  $LHS1.Ts3$  and  $.Ts4$  we can find a full filling, but these are equivalent to  $LHS1.P$  and  $LHS1.Tm1$ , respectively.

Summarizing, all layouts of  $LHS1$  with  $Ts$  are not feasible.

Now we will investigate the corresponding  $RHS$  for each of these 3 feasible  $LHS$ . We start with  $RHS1.P$  corresponding to  $LHS1.P$ , see Fig. 127.

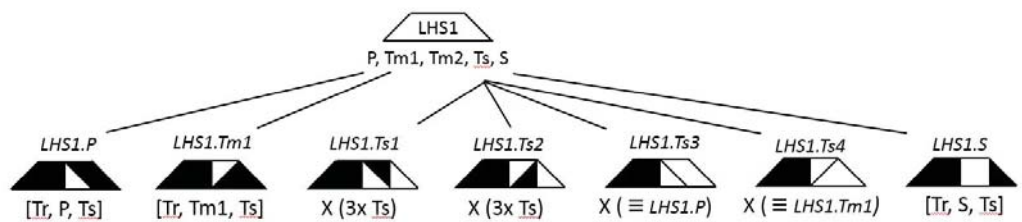
As shown in this figure,  $RHS1.P$  is not feasible.



Clearly, for each of the 4 forms we see that the empty spaces cannot be covered by both  $Tm1$  and  $Tm2$ .

Conclusion: *LHS3* and *LHS5* are not feasible

Figure 125: *J15* with  $Ty3$  and *LHS3* or *LHS5* is not feasible.



Conclusion: *LHS1* has 3 different feasible layouts (*LHS1.P*, *LHS1.Tm1* and *LHS1.S*).

Figure 126: *J15* with all possible *LHS1*.

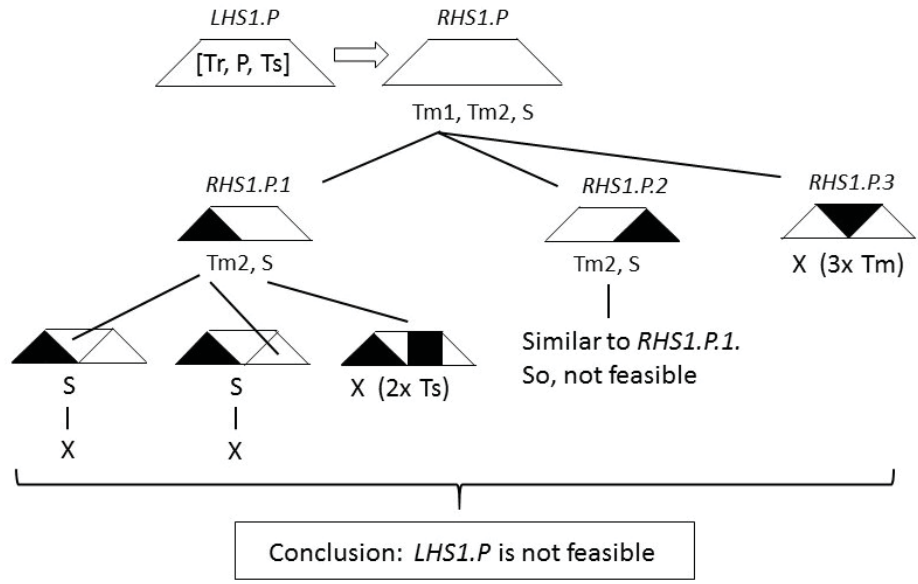


Figure 127: *J15* with all possible fillings for *RHS1.P*

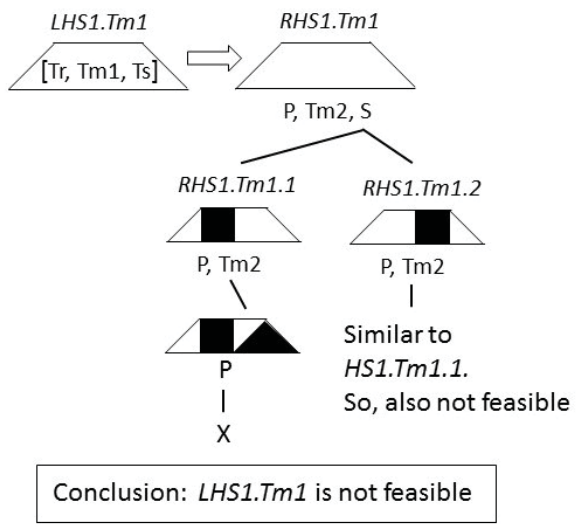


Figure 128: *J15* with all possible fillings for *RHS1.Tm1*

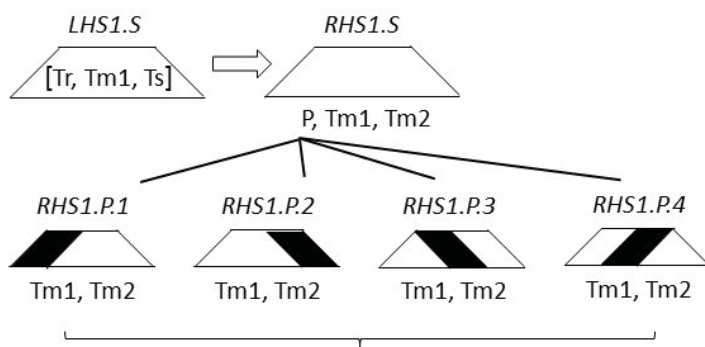
It follows from Fig. 127

**Conclusion:** (24)  
**LHS1.P is not feasible.**

Next we consider LHS1.Tm1. See Fig. 128. It follows from Fig. 128

**Conclusion:** (25)  
**LHS1.Tm1 is not feasible.**

Finally, we have to investigate case LHS1.S. See Fig. 129.



Clearly, for each of the 4 forms we see that the empty spaces cannot be covered by both  $Tm1$  and  $Tm2$ .

**Conclusion:  $LHS1.S$  is not feasible**

Figure 129:  $J15$  with all possible fillings for  $RHS1.S$

Then we can conclude from Fig. 129

**Conclusion:** (26)  
**LHS1.S is not feasible.**

Combination of the Conclusions (24), (25) and (26) we have

**Conclusion:** (27)  
**LHS1 is not feasible.**

Combining the Conclusions (23) and (27) we find

**Conclusion:** (28)  
**LHS6 is not feasible.**

Then by combining Conclusions (21), (22), (27) and (28) we find

**Conclusion for  $J15$ :** (29)  
**LHS1 up to LHS6 are not feasible. Thus,**  
 **$J15$  with  $Ty3 = Tz_3^*$  is not feasible.**

By recalling Conclusion (11) in section A.1 we know that for  $J15$  we only had to investigate the layouts with  $Ty1$  up to  $Ty3$ . Thus, by combining Conclusion (11) and (29) we see that  $J15$  only has feasible layouts with  $Ty1$  and  $Ty2$ .

Indeed, all these layouts with  $Ty1$  and  $Ty2$  have been found (for both  $J15$  and  $J16$ ) in the previous sections, see Conclusions 17 and 18. Recall that  $Ty1 = Tz_1^*$  and  $Ty2 = Tz_2^*$ . Therefore, we now have

**Final Conclusion for  $J15$ :** (30)  
 **$J15$  has 60 feasible layouts (A.1 up to A.60), as found in the previous sections.**  
**These layouts have precisely one trapezoidal tan out of the set  $Tz1, \dots, Tz4, Tz_1^*, Tz_2^*$ .**

Recall that we also have found 60 feasible layouts for  $J16$ , also with precisely one trapezoidal tan out of the set  $Tz1, \dots, Tz4, Tz_1^*, Tz_2^*$ .

Furthermore, it was stated in Conclusion 12 that we only needed to investigate layouts for  $J16$  with  $Tz1$  up to  $Tz6$ .

So far, we have found 60 feasible  $J16$ -layouts with trapezoidal tans  $Tz1$  up to  $Tz4$ . So, in fact we still have to investigate  $J16$ -layouts with  $Tz5$  or  $Tz6$ . However, this is not needed anymore.

Indeed, suppose there exists a  $J16$ -layout with  $Tz5$  or  $Tz6$  (say  $Tz5$  without loss of generality) that is essentially different from those already found. Then its dual  $J15$ -layout with  $Tz5$  would also be found by our backtracking algorithm and this  $J15$ -layout would also be essentially different from all  $J15$ -layouts found sofar.

But this contradicts Conclusion 30.

Thus, the assumption above on  $J16$  is not valid and we have

**Final Conclusion for  $J16$ :** (31)  
 **$J16$  has 60 feasible layouts (B.1 up to B.60), as found in the previous sections.**  
**These layouts have precisely one trapezoidal tan out of the set  $Tz1, \dots, Tz4, Tz_1^*, Tz_2^*$ .**

## B Acknowledgments and References

### Acknowledgments

The author wishes to thank co-author Tom Verhoeff for his stimulating discussions and for providing and running his dedicated software to generate all solutions we were looking for. Without his help the results as presented in this report would not have been found.

Last but not least I would like to express my appreciation to Mrs. Hui Jun Chang who read this report carefully and gave several valuable suggestions for improvement.

### References

- [1] Fu Traing Wang, Chuan-Chih Hsiung, *A Theorem on the Tangram*, The American Mathematical Monthly, Vol. 49, No. 9, 1942, pp. 596-599, available at <http://www.jstor.org/stable/2303340>.
- [2] Joost Elffers, *Tangram, Das alte chinesische Formenspiel / Het oude Chinese vormenspel*, M. DuMont Schauberg, Cologne, 1976, 3rd edition.
- [3] T.G.J. Beelen, *Finding all convex tangrams*, Eindhoven University of Technology, CASA-report 17-02, 2017.
- [4] T.G.J. Beelen, *Determining the essentially different partitons of all Chinese convex tangrams*, Eindhoven University of Technology, CASA-report 18-02, 2018.
- [5] <http://www.pentoma.de/>, Tangram Figuren Uebersicht, Konvexe Figuren, 2017.
- [6] Erik van der Tol and Tom Verhoeff, *The Puzzle Processor Project: Towards an Implementation*, Nat. Lab. Unclassified Report NL-UR 2000/828, Koninklijke Philips Electronics N.V., 2001.
- [7] <https://en.wikipedia.org/wiki/Backtracking/>, Description of the (backtracking) method, 2017.
- [8] <https://www.geeksforgeeks.org/backtracking>, 2017.
- [9] Eli Fox-Epstein, Ryuhei Uehara, *The Convex Configurations of “Sei Shonagon Chie no Ita”*, and Other Dissection Puzzles, arXiv:1407.1923v1, July 2014.

## PREVIOUS PUBLICATIONS IN THIS SERIES:

Number	Author(s)	Title	Month
18-03	N.K. Yadav J.H.M. ten Thije Boonkkamp W.L. IJzerman	Computation of double freeform optical surfaces using a Monge-Ampère solver: application to beam shaping	August '18
18-04	J. de Graaf	Some Mathematical Comments on Thermostatistics	August '18
18-05	B.S. van Lith J.H.M. ten Thije Boonkkamp W.L. IJzerman	Active flux schemes on moving meshes with applications to geometric optics	September '18
18-06	A.J. Vromans A.A.F. van de Ven A. Muntean	Periodic homogenization of a pseudo-parabolic equation via a spatial-temporal decomposition	October '18
18-07	T.G.J. Beelen T. Verhoeff	Determining the essentially different partitions of all Japanese convex tangrams	October '18